

AD 493441

⑥ BARIUM TITANATE AND BARIUM-STRONTIUM TITANATE
as
NONLINEAR DIELECTRICS

⑩ SHEPARD ROBERTS ⑪ 1946

S.B. Massachusetts Institute of Technology
(1938)

S.M. Massachusetts Institute of Technology
(1939)

⑨ Technical rept.

SUBMITTED IN PARTIAL FULFILLMENT OF THE

REQUIREMENTS FOR THE DEGREE OF

DOCTOR OF SCIENCE

at the

⑭ TR-1

MASSACHUSETTS INSTITUTE OF TECHNOLOGY
(1946)

⑮ W5 vol - 79(2)

⑫ Historical thesis.

Signature of Author..... *Shepard Roberts*.....
Department of Electrical Engineering
September 9, 1946

Certified by..... *Chas. W. Fippel*.....
Thesis Supervisor

..... *Harold R. Nelson*.....
Chairman, Department Committee on Graduate Students

201 400

474

ACKNOWLEDGMENT

This work was carried out in the Laboratory for Insulation Research at M.I.T. under the direction of Professor A. von Hippel. Financial support was received from the Office of Research and Invention of the Navy Department under Task Contract I.

The author is especially indebted to Professor von Hippel for encouragement and helpful advice during the course of the work. He also wishes to thank Mr. J. M. Brownlow for assistance and advice in the preparation of the ceramic samples, and Mr. J. Maccarone for drawing many of the figures.

In addition, the author gratefully acknowledges the substantial help of his wife, who did the typing.

ABSTRACT

Nonlinear inductors and resistors have been used for many years for a number of important applications, and yet nonlinear condensers have never been used commercially. In fact the nonlinear dielectrics suitable for circuit applications have not been known. In recent years, however, certain high-dielectric-constant ceramics consisting of barium titanate and mixtures of barium and strontium titanates have been developed. These ceramics are nonlinear ferroelectric dielectrics similar in many respects to Rochelle salt. They have a Curie point, corresponding to the temperature at which the dielectric constant reaches a maximum value. Below this temperature electrical hysteresis is found and above it the reciprocal of dielectric constant increases linearly with temperature.

an investigation was made of
We have investigated the nonlinear dielectric properties of barium titanate and barium-strontium titanate with special emphasis on those properties that are pertinent to the design of nonlinear condensers for circuit applications. In order to carry the investigation to the highest possible field strengths, *it was* ~~we found~~ it necessary to use samples in the form of thin sheets, *which we prepared.* ~~Our~~ *The* measuring circuit makes use of a General Radio type 916-A impedance bridge, which measures the high-frequency impedance of a sample condenser containing the dielectric in question.

In addition to the high frequency measuring voltage a relatively large "biasing" voltage is applied, which may be d-c for the first type of measurement or low frequency a-c for the second type of measurement. The impedance of the condenser is measured versus the d-c or instantaneous value of a-c biasing voltage. For measurements of the second type, an oscilloscope is necessary as a bridge balance indicator. ~~We have measured~~ the dielectric constant versus field strength, temperature and frequency, ^{was measured} ~~our~~ results are given in the figures included in this report.

The second type of measurement is necessary in order to predict the operation of a nonlinear condenser as a modulator. We find that at temperatures above the Curie point the results of this method agree well with measurements by the first method, but below this temperature the two methods give different results, especially with respect to loss. In fact the losses are so much greater when measured by the second method than by the first method at temperatures below the Curie point, that the usefulness of these nonlinear dielectrics for circuit elements is severely restricted in this range.

At temperatures above the Curie point we find a definite relation between dielectric constant and biasing voltage, which we have expressed in the form of an equation. This equation makes use of a new parameter, namely the

critical field strength which reduces the dielectric constant to half its initial value at low field strength.

The critical field strength increases rapidly at temperatures above the Curie point. Therefore, if the dielectric is to be used at temperatures higher than the Curie point, but not so high that the critical field strength exceeds the maximum allowable operating value, the useful temperature range is thereby limited. We find that on this basis the barium-strontium titanate has a useful temperature range which is almost six times that of Rochelle salt. Furthermore, the range of barium-strontium titanate can be centered at any desired temperature by adjusting the composition. Although both the critical field strength and the initial dielectric constant change very rapidly with temperature in the above operating range, they can partially compensate for each other's changes so that the dielectric constant at a given field strength does not change nearly so rapidly versus temperature.

In measuring the dielectric constant and loss versus frequency we found a surprising series of resonance phenomena which occurred only during or after application of a moderately strong d-c field. Upon application of a weaker field of reversed polarity the resonances could be "erased". The resonance frequencies were found to be relatively independent of field strength and temperature except that they disappeared above the Curie point. The resonance frequencies

were finally shown to correspond to the mechanical modes of vibration, a fact which proves the existence of a new electrostriction or piezoelectric phenomenon in barium titanate.

We have considered several circuit applications, which seem feasible, using barium-strontium titanate as a nonlinear dielectric. These include: Harmonic generation, frequency control and modulation, amplitude modulation and amplification. In addition, we have worked out the details for the design of an original phase-modulator circuit suitable for use in a frequency-modulation transmitter. This method allows the direct modulation of phase over a range of several cycles without vacuum tubes, thus permitting a substantial simplification in the circuits now used in frequency modulation transmitters.

CONTENTS

	<u>Page</u>
Acknowledgment	11
Abstract	111
I Introduction	1
1. Outline of the Problem	1
2. History of Barium Titanate as a Dielectric	3
II Preparation of Samples	10
III Measuring Techniques	16
1. Outline of Methods	16
2. Description of Apparatus	17
3. Determination of Dielectric Constant & Loss	22
IV Experimental Results	26
1. Dielectric Constant & Loss Versus Field Strength	26
2. Nonlinear Dielectric Properties Versus Temperature	42
3. Dielectric Constant & Loss Versus Frequency	50
4. D-C Conductivity and Breakdown Strength	59
V Theory of Ferroelectric Dielectrics	63
1. Introduction	63
2. Some Dielectric Properties of Rochelle Salt	63
3. Domain Theory	68
4. Extrapolation of the Curie-Weiss Law Below the Upper Curie Point	69
VI Conclusions and Proposed Applications	72
1. General Conclusions	72
2. Miscellaneous Circuit Applications	76

	<u>Page</u>
3. Application as a Phase Modulator	82
4. Summary of Our Results	89
Appendix A: Calculation of Edge Correction	92
Appendix B: Dependence of ϵ on Field Strength in a Nonlinear Dielectric	97
Appendix C: Vibrational Modes of a Circular Plate	100
Bibliography	102
Biography of the Author	108
Publications by the Author	109

LIST OF ILLUSTRATIONS

<u>Figure</u>	<u>Page</u>
1. Dielectric Properties of Ticon B, BaTiO ₃	4
2. Dielectric Properties of Ticon B-S #249 75% BaTiO ₃ + 25% SrTiO ₃	4
3. D-C Field Strength Dependence of B-S #249	6
4. Polarization Curves for Barium Titanate	7
5. Ceramic Disc Samples with Painted Silver and Platinum Foil Electrodes	15
6. Mounting Arrangement Showing Connections to Impedance Bridge	15
7. Broad Band Preamplifier for Oscilloscope	18
8. Dielectric Constant of BaTiO ₃ Measured at 400 Kc Versus D-C Field Strength	27
9. Loss Factor of BaTiO ₃ Measured at 400 Kc Versus D-C Field Strength	28
10. Dielectric Constant of BaTiO ₃ Measured at 10 Mc Versus D-C Field Strength	29
11. Loss Factor of BaTiO ₃ Measured at 10 Mc Versus D-C Field Strength	31
12. Dielectric Constant of BaTiO ₃ Measured at 400 Kc Versus Phase of A-C Field	32
13. Dielectric Constant of BaTiO ₃ Measured at 400 Kc Versus Instantaneous Strength of A-C Field	33

14. Loss Factor of BaTiO ₃ Measured at 400 Kc Versus Instantaneous Strength of A-C Field	34
15. Dielectric Constant of BaTiO ₃ Measured at 400 Kc Versus Peak Strength of A-C Field	36
16. Loss Factor of BaTiO ₃ Measured at 400 Kc Versus Peak Strength of A-C Field	37
17. Dielectric Constant of (Ba-Sr)TiO ₃ Measured at 400 Kc Versus D-C Field Strength	39
18. Theoretical Curve for Dielectric Constant Versus Field Strength	41
19. Dielectric Constant and Loss Factor of BaTiO ₃ Measured at 400 Kc Versus Temperature	43
20. Critical Field Strength E ₀ of BaTiO ₃ Versus Temperature, from Measurements at 400 Kc	44
21. Increase in Loss Factor of BaTiO ₃ Measured at 400 Kc Versus Temperature	46
22. Dielectric Constant and Loss Factor of (Ba-Sr)TiO ₃ Measured at 400Kc Versus Temperature.	47
23. Reciprocal of Dielectric Constant of (Ba-Sr)TiO ₃ Measured at 400 Kc Versus Temperature	48
24. Critical Field Strength E ₀ of (Ba-Sr)TiO ₃ Versus Temperature, from Measurements at 400 Kc	49
25. E ₀ ^{2/3} of (Ba-Sr)TiO ₃ Versus Temperature, from Measurements at 400 Kc	51.
26. Increase in Loss Factor of (Ba-Sr)TiO ₃ Measured at 400 Kc Versus Temperature	52

27.	Real Component of Capacitance of BaTiO ₃ Condenser Versus Frequency	53
28.	Loss Component of Capacitance of BaTiO ₃ Condenser Versus Frequency	53
29.	Loss Component of Capacitance of BaTiO ₃ Condenser Versus Frequency and Temperature	55
30.	Loss Component of Capacitance of (Ba-Sr)TiO ₃ Condenser Versus Frequency and Temperature	57
31.	Loss Component of Capacitance Versus Frequency of a BaTiO ₃ Condenser Before and After Chipping Edge	58
32.	D-C Conductivity of BaTiO ₃ Versus Temperature	62
33.	Remanent Polarization P ₀ , Coercive Force E _c , and Dielectric Constant for Small Fields, of Rochelle Salt	64
34.	Polarization Curves for Rochelle Salt	64
35.	The Reversible Dielectric Constant of Rochelle Salt	66
36.	Verification of the Law $EX^{-\frac{1}{2}} = M(t - t_c) + NX$	66
37.	Dielectric Constant of (Ba-Sr)TiO ₃ Versus Field Strength at Different Temperatures	74
38.	Frequency Control by Nonlinear Condensers	77
39.	Nonlinear Condenser as a Harmonic Generator	77
40.	Amplitude Modulator Circuit	80
41.	Dielectric Amplifier	80
42.	Electrically Variable Phase Shifter	83
43.	Phase Shift Per Section of Ladder Network Versus Field Strength, at Different Temperatures	85

I. INTRODUCTION

1. Outline of the Problem--

For many years the nonlinear properties of iron have been known and utilized in communication and power circuits. The principal applications are: voltage regulation and control,¹² frequency multiplication,¹⁵ modulation and amplification.^{1,20} Nonlinear resistors, such as copper-oxide and crystal rectifiers and thyrite have likewise been used successfully in some of the above applications^{4,14} and in new ones.¹² However, there has been no commercial application of nonlinear condensers. There is no lack of uses to which a nonlinear condenser could be put, but the required nonlinear dielectrics have not been known.

Until recently the only materials known to have significant nonlinear dielectric properties were certain piezoelectric crystals known as "Seignette-electrics", the prototype of this class being Rochelle salt (sel de Seignette). Rochelle salt is extremely interesting from a theoretical point of view and its properties will be considered in greater detail later. However the usefulness of Rochelle salt as a nonlinear circuit element is strictly limited because the dielectric properties depend very critically upon temperature.⁴² Furthermore the piezoelectric nature of Rochelle salt permits mechanical resonances to be excited which further limit the use of this material in

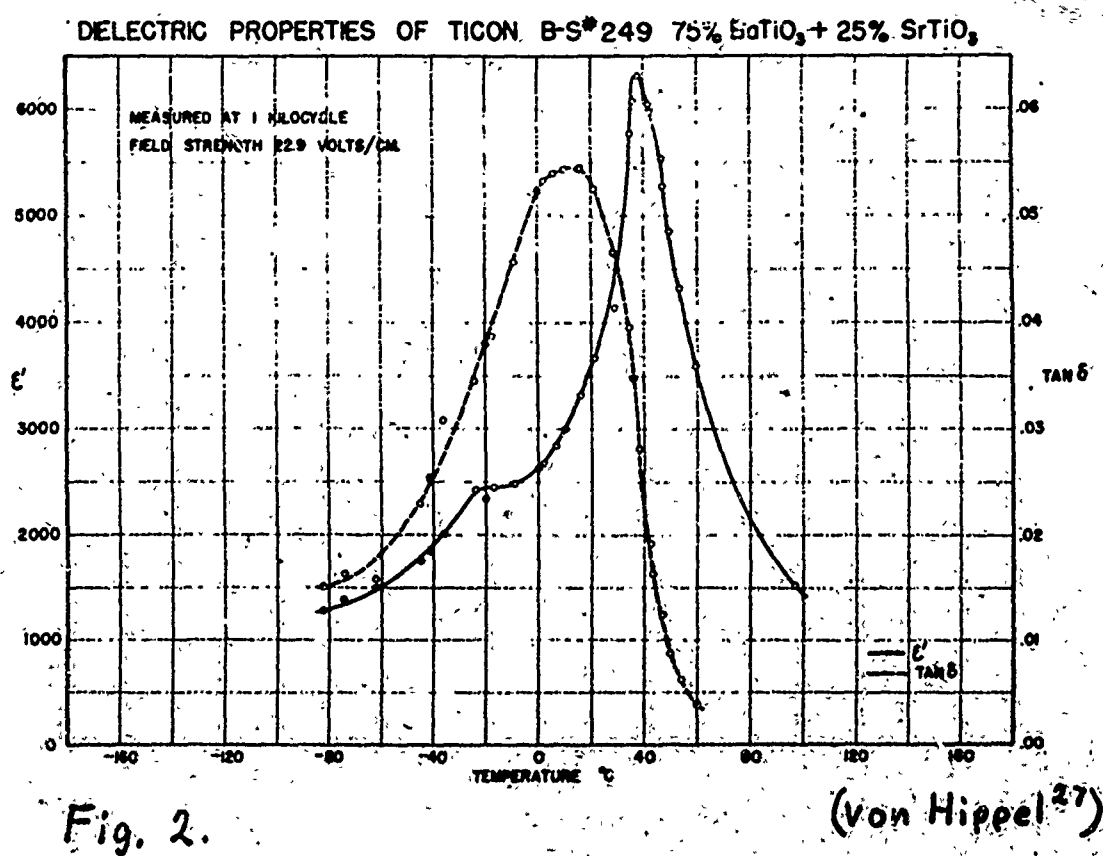
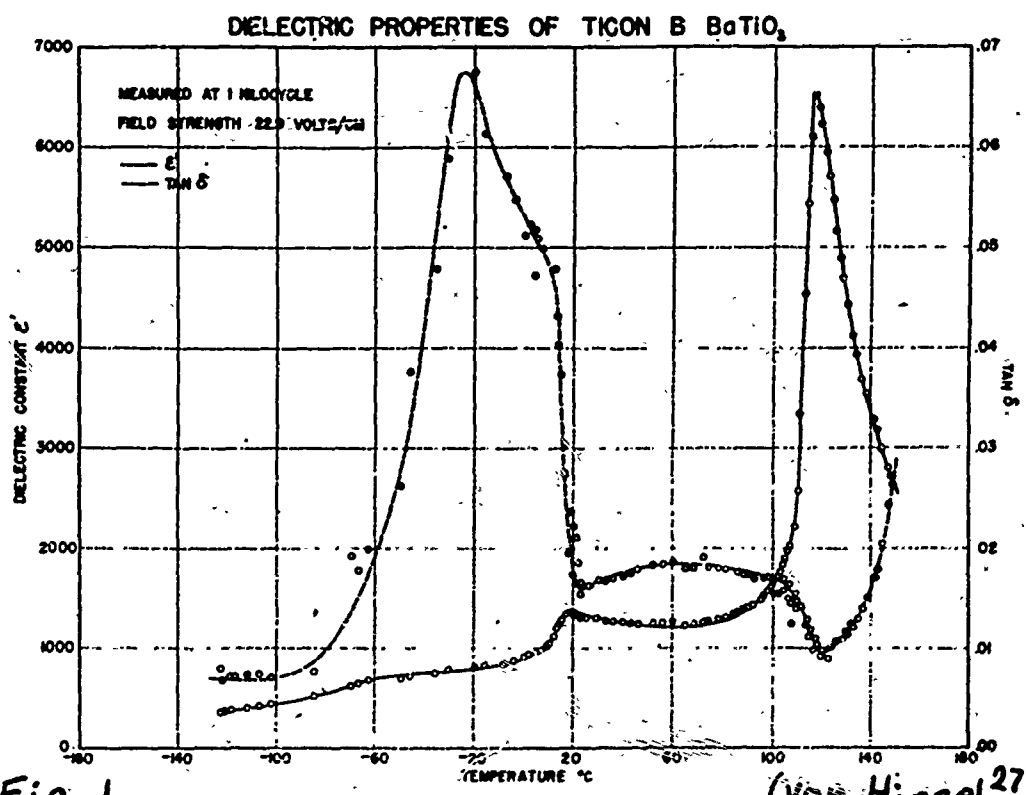
high frequency circuits.

Several years ago certain high-dielectric-constant ceramics consisting of barium titanate and mixtures of barium and strontium titanates were developed.²⁶ Since that time there has been considerable effort directed toward the study of these materials, especially in the Laboratory for Insulation Research at M.I.T. under the direction of Prof. A.R. von Hippel.^{27,28} Many interesting properties of these materials have been discovered in this laboratory including some nonlinear characteristics which will be described below. On the basis of these results the author was encouraged to undertake a continuation of this research. The object of this work was to investigate the applicability of barium titanate condensers as nonlinear circuit elements. It was at first supposed that after some preliminary "routine" measurements, nonlinear condensers could be designed and circuits demonstrated. However, the results of the "routine" measurements were quite unexpected and indicated that much more complicated phenomena were involved than anticipated earlier. As a result of these findings it was decided to redirect the course of the work stressing the fundamental dielectric properties of the materials rather than the circuit applications. Thus instead of making only a few "routine" measurements it has been necessary to devote the entire program to a study of the nonlinear properties of these materials.

2. History of Barium Titanate as a Dielectric--

The earliest reference to the high dielectric constant of barium titanate, that we know of, is found in a report of the Titanium Alloy Mfg. Co., dated September, 1942.²⁶ Subsequent work indicated that the dielectric constant of barium titanate and mixtures of barium and strontium titanates depends critically on the temperature (but not so much so as Rochelle salt) and has a sharp maximum with a value of 5000 or more at a temperature depending more or less linearly on the percentage composition.²⁹ For pure barium titanate the maximum dielectric constant comes at about 120°C, while for a mixture containing 25% strontium titanate, it occurs at a temperature of about 37°C. The dielectric constants and loss tangents measured at low field strength for these materials are shown in figs. 1 and 2.

The Laboratory for Insulation Research began an active study of these materials at an early date and has discovered many new and interesting properties.^{27,28} Of particular interest here are the nonlinear dielectric properties studied by various techniques. In one method the ceramic condenser is allowed to charge at the specified voltage for one second and then is discharged through a ballistic galvanometer. The results by this method for a ceramic containing 75% barium titanate and 25% strontium



titanate are shown in fig. 3. The initial dielectric constant, measured at low field strengths, is relatively small but rises rapidly as the field increases up to about 0.1 Mv/m. At still higher field strengths the dielectric constant diminishes indicating a saturation effect. These measurements also show that at higher field strengths the maximum dielectric constant is shifted to lower temperatures. These conclusions are supported by bridge measurements at high a-c voltages using a detector which is sensitive only to the fundamental frequency.

The "ferroelectric" nature of barium titanate, indicated by the nonlinear dielectric properties described above, was confirmed using the oscillographic method of Sawyer and Tower.⁴² In this method the horizontal deflection of the oscilloscope is proportional to the electric field strength, while the vertical deflection is proportional to the dielectric polarization. A number of hysteresis diagrams obtained in this way for barium titanate are shown in fig. 4. In these diagrams the electric field has the same peak value of 0.48 Mv/m (4800 V/cm) and a frequency of 60 cycles per second. An interesting result is obtained by plotting the slope of these hysteresis curves, measured at the intersection with the vertical axis, versus temperature. This curve has a maximum, as one would expect, in the vicinity of +120°C.

D.C. FIELD STRENGTH DEPENDENCE OF $BaTiO_3$ - $SrTiO_3$ #249

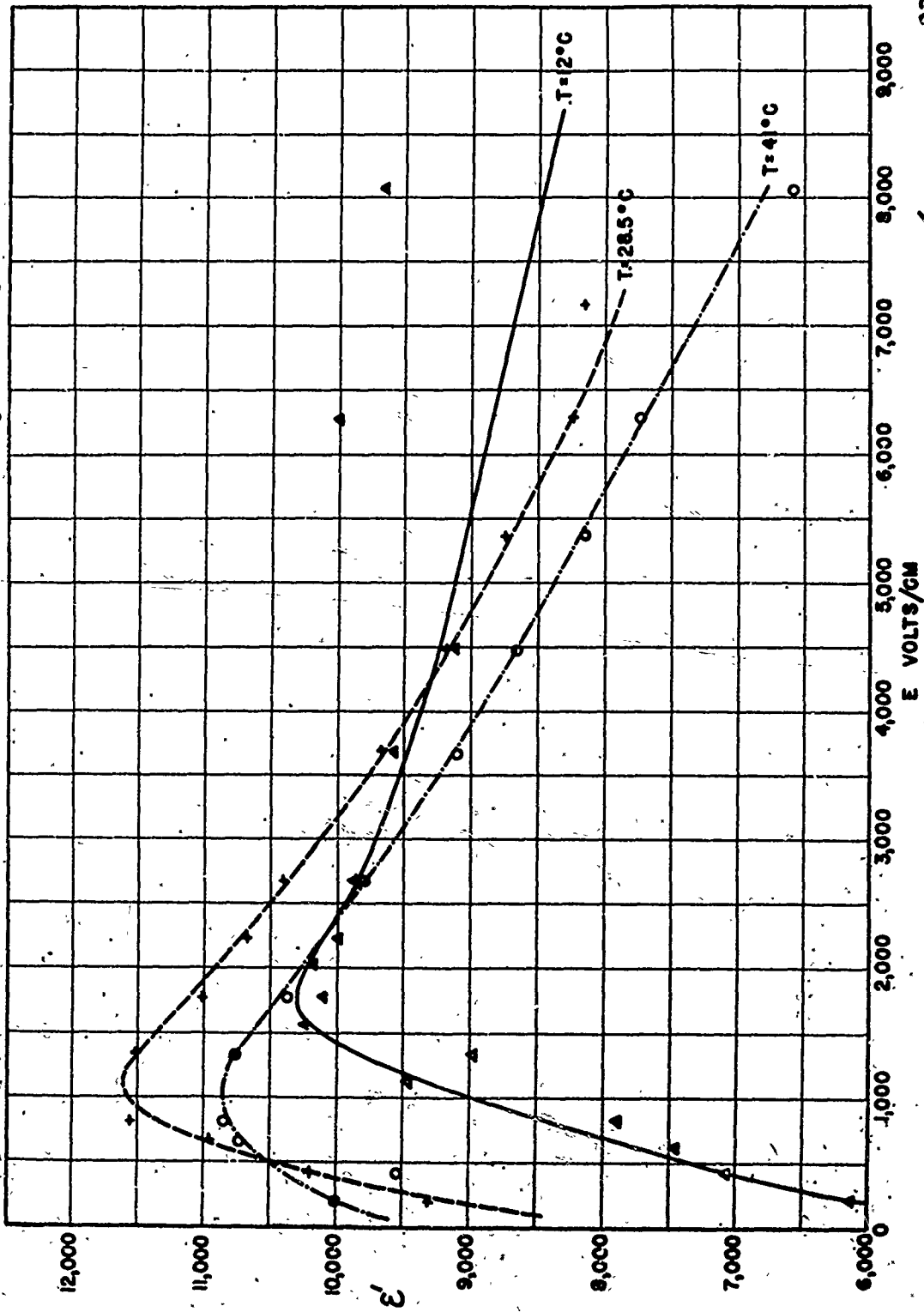


Fig. 3

(von Hippel²⁷)

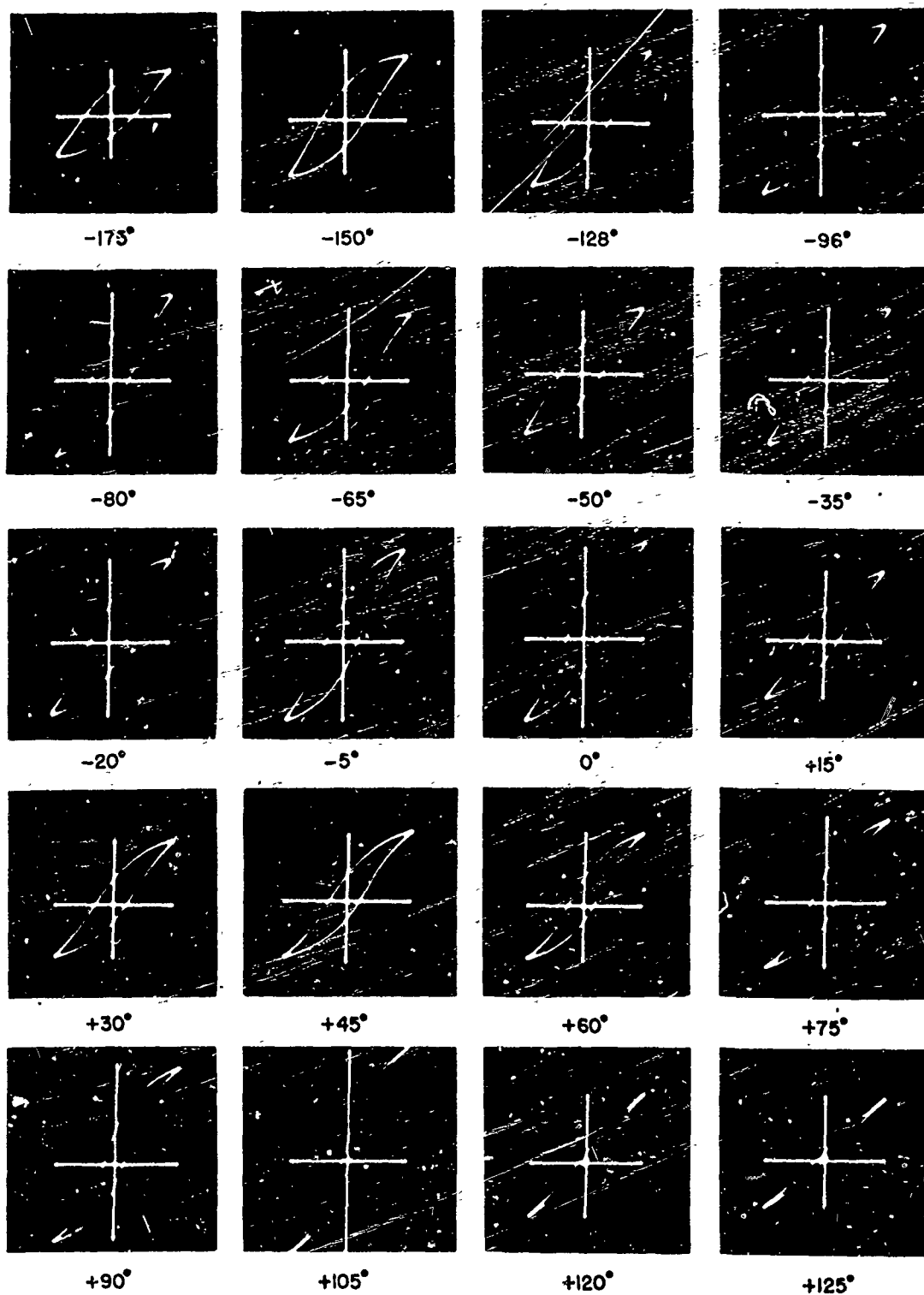


Fig. 4. Polarization Curves for BaTiO_3
(von Hippel²⁸)

But it also has maxima at about $+10^{\circ}\text{C}$ and -90°C , at which temperatures there are no corresponding maxima in $\frac{\epsilon'}{\epsilon_0}$ when ϵ' is measured at low field strengths.

Two discontinuities are likewise found in the thermal expansion versus temperature in the range -75°C to $+180^{\circ}\text{C}$. The upper limits of these discontinuities are about $+10^{\circ}\text{C}$ and $+120^{\circ}\text{C}$. X-ray powder diffraction data indicate a change in the crystal lattice from pseudo-cubic into cubic above 120°C .

The maximum in the dielectric constant at $+120^{\circ}\text{C}$ is identified as a Curie point. The evidence for this is, first of all, the practical disappearance of hysteresis above this temperature, and secondly, the fact that above this temperature the dielectric constant is given by the Curie-Weiss law.⁵⁰

$$\frac{\epsilon'}{\epsilon_0} = \frac{C}{T - T_c} \quad (I-1)$$

where T is the absolute temperature and T_c and C are constants. The temperatures $+10^{\circ}\text{C}$ and -90°C might be called "secondary" Curie points because they have some of the anomalous properties commonly associated with the transition at the Curie point but not all these properties. Von Hippel has postulated that these two secondary Curie points may be the temperatures at which thermal agitation overcomes the spontaneous polarization in the directions of two of the crystal coordinate axes respectively, while

at the Curie point, $+120^{\circ}\text{C}$ the spontaneous polarization in the third and remaining axis direction is finally overcome.

The fact that there is a pronounced peak in the dielectric constant at the Curie point but not at the secondary Curie points for weak fields is explained by the fact that the only transition from an unpolarized state to a spontaneously polarized state occurs at the Curie point. Above the secondary Curie points the material is already spontaneously polarized and energy is required to shift the polarization into a different axis direction. This energy is supplied by the external electric field.

We are now beginning to receive reports of work done on barium titanate in other countries during the war. This material is listed in the bibliography.^{21-25 and 30-33 incl.}

II. PREPARATION OF SAMPLES

Samples in the form of thin sheets were chosen for this investigation for several reasons. It was clear from the beginning that operation at very high field strengths would be required in order to take full advantage of the nonlinear dielectric properties. On the other hand, the applied voltages should not exceed several hundred volts if the ceramic condensers are to be useful in ordinary electronic circuits. Furthermore the insulation of our bridge circuit is limited to about 500 volts and thin dielectric samples generally have a greater breakdown field strength than thick ones, if the electrodes have sharp edges. Ceramic condensers are no exception to this rule.²⁷ As a result of these considerations, we were led to the use of thin samples which could be conveniently prepared in the form of sheets.

The barium titanate sheets were made on the equipment and by the methods described by von Hippel.²⁸ The barium-strontium titanate sheets were made by similar methods but with simpler equipment which we will describe later. The general principles of the method are as follows.

The ceramic powder is suspended in a toluene "slip" with a resin binder and, after proper de-airing, is extruded on a flat base-plate that has been previously coated with a thin film of ethyl cellulose. The extruded sheet, when nearly dry, may be readily stripped from the base, cut in

the form of discs about $\frac{1}{4}$ " in diameter and fired in a ceramic kiln. If desired, the discs can be fired on a sheet of platinum foil, in which case the ceramic fuses to the platinum which can be used as one electrode. After additional silver electrodes are fired on, the ceramic condensers are ready for use.

The following formula is copied from von Hippel's report,²⁸ with slight modifications.

1. Staybelite resin	30 g.	Hercules Powder Co.
2. Abalyn	30 "	" " "
3. Ethyl cellulose	6 "	
4. Toluene	140 "	(nitration grade)
5. V-495 resin	2 "	E.I. Du Pont de Nemours & Co.
6. Diethyl oxalate	5 "	
7. Barium titanate	790 "	Titanium Alloy Mfg. Co.,
or		Niagara Falls, N.Y.
(75%Ba/25%Sr)TiO ₃	750 "	"

In preparing a batch, the staybelite is melted and the abalyn added. The ethyl cellulose is then mixed in, followed by half the toluene. This batch is stirred until solution is complete. The V-495 and diethyl oxalate are added to the remaining toluene and the two portions combined. Finally the ceramic powder is added to the hot liquid with constant stirring.

To insure completely homogeneous fired samples, the slip is ball-milled for at least twenty-four hours. After milling,

the slip is passed through a 325 mesh screen. The screened slip is then evacuated at the vapor pressure of toluene for 15 minutes in order to remove air bubbles. The formation of scum during this operation may be prevented by slow stirring. The consistency of the slip obtainable by the procedure outlined above is of importance to the success of the extrusion operation.

Before the sheets are extruded, a "parting layer" is applied to the base surface. This is a thin film of ethyl cellulose, applied as a 0.5% solution in ethyl alcohol. The solution is either flowed on or painted on with a very clean paint brush, care being taken to obtain an even coat. The film is then air dried and is ready for the extrusion operation.

The extrusion machine used for the barium titanate sheets has an endless stainless steel belt thirty feet long and seven inches wide which passes over rollers about twelve inches in diameter at opposite ends of the machine and is driven at a speed of about 5 feet per minute. The ceramic slip is extruded on to the belt from a hopper having an open bottom five inches wide and mounted above the belt near one end of the machine. The distance the hopper is held above the belt determines the thickness of the extruded layer and is accurately adjustable.

The $(\text{Ba-Sr})\text{TiO}_3$ sheets were extruded on glass plates from a U-shaped yoke closed by a straight knife blade. In operation the yoke is placed flat on the glass plate and

the knife blade is adjusted with its edge almost touching the glass. The ceramic slip is poured into the yoke and the yoke is pulled slowly across the glass plate leaving behind it a layer two inches wide which is extruded under the knife blade. This method was found more satisfactory for making sheets of the required thickness.

The extruded sheet is stripped from the base surface by means of a thin straight blade. If the sheet is thin, it has to be stripped almost immediately after extrusion. If it is allowed to become too dry, it tends to stick; on the other hand, if it is not dry enough it does not have the necessary mechanical strength.

After being stripped, the sheet is laid flat and allowed to dry some more. When dry, it is cut into discs. A $\frac{1}{4}$ inch paper punch was found to be quite well suited for this operation.

Some of the samples of barium titanate were fired on a flat surface of powder of the same material, while other samples were fired directly on platinum foil. At higher temperatures, the samples tend to fuse to the platinum which then makes a very good electrode. The second electrode is a spot of silver paint (du Pont Paste 4351) applied to the top surface with a brush. For samples without platinum electrodes on the bottom, the latter surface is covered with silver paint instead. After the silver paint is dry the samples are refired at a temperature

of 600°C for $\frac{1}{2}$ hour in order to burn on the silver electrodes.

Table 1 shows the composition and firing conditions for the samples we have measured. These samples are shown in fig. 5 arranged in numerical order starting in the upper left hand corner. The diameter of the circular piece of platinum foil under sample 16 is $\frac{1}{2}$ inch, which determines the scale of this figure.

Table 1 — Composition and Firing Conditions

Sample No.	Composition	Temp.	Time	Surface fired on	Thickness inches
4	BaTiO ₃	1300	3 hr.	Powder	.0085
5	"	"	" "	"	.0077
9	"	1350	4 "	Platinum (not fused)	.0080
16	(75%BaTiO ₃) (25%SrTiO ₃)	1400	$\frac{1}{2}$ "	Platinum	.0042
18	BaTiO ₃	1500	" "	"	.0036
23	"	"	" "	"	.0041

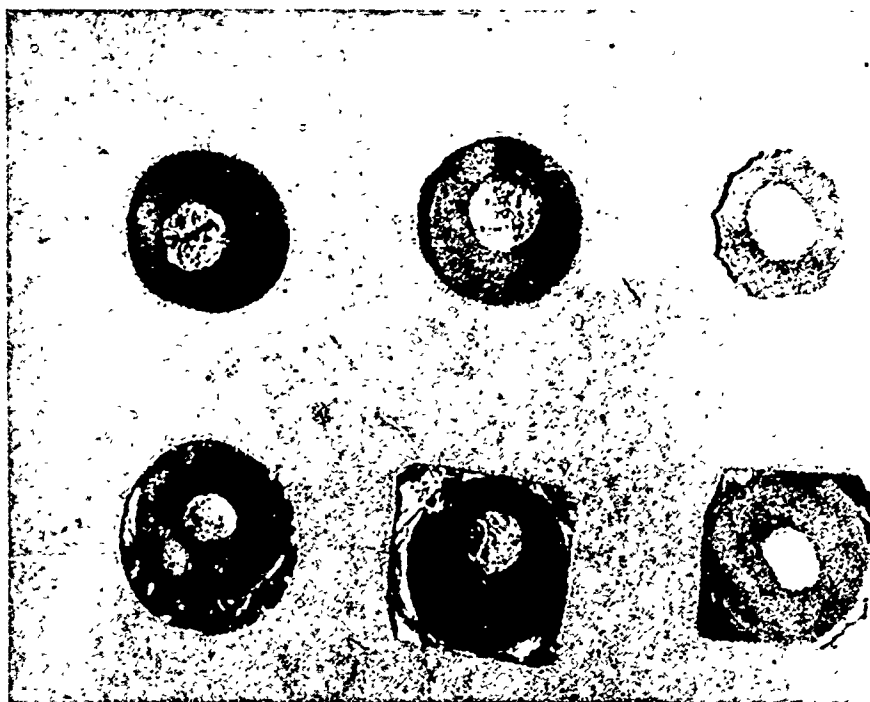


Fig. 5. Ceramic disc samples with painted silver and platinum foil electrodes.

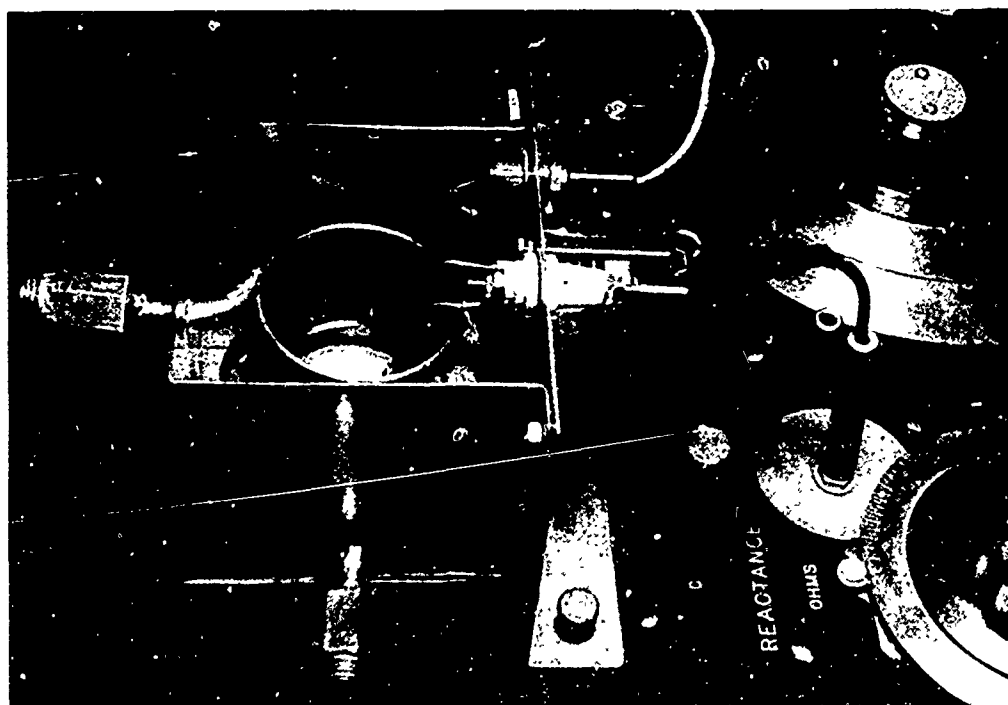


Fig. 6. Mounting arrangement showing connections to impedance bridge.

III. MEASURING TECHNIQUES

1. Outline of Methods--

In attempting to evaluate the potential usefulness of barium titanate as a nonlinear circuit element, we have found the existing data inadequate. Most of the circuit applications which we have to consider, especially those involving modulation, have one thing in common. They depend for their operation on the variation in impedance of the nonlinear element as a function of a "biasing" voltage.

The significance of the biasing voltage can best be explained in reference to a hypothetical nonlinear condenser for which the charge Q is a given function of the voltage V .

$$Q = F(V) \quad (\text{III-1})$$

If the dielectric is an isotropic medium, the charge must be of the same magnitude and opposite in sign when the voltage is reversed, thus Q must be an odd function of V .

$$F(-V) = -F(V) \quad (\text{III-2})$$

The capacitance C at a voltage V is defined as the derivative of eq. III-1.

$$C = \frac{dQ}{dV} = F'(V) \quad (\text{III-3})$$

Since the derivative of an odd function is an even function, the capacitance must be an even function of voltage. The voltage V is called the biasing voltage and it may be constant (d-c) or a function of time (low frequency a-c). The same

considerations apply to the dielectric constant versus biasing field strength in a nonlinear dielectric.

Mueller has measured the capacitance of nonlinear Rochelle salt condensers in an a-c bridge while simultaneously applying a d-c biasing voltage.⁴⁰ In this way the dielectric constant is determined versus biasing field strength. This method is found to be satisfactory in predicting the operation of the nonlinear condensers in circuit applications where the bias really is d-c. However, in circuits where modulation is to be obtained by superimposing low frequency a-c on the biasing voltage, the capacitance and loss as a function of time can not be correctly predicted from the measurements with d-c bias. To obtain the necessary information we have devised a method of applying a low frequency a-c biasing voltage instead of (or in addition to) d-c, and of measuring the capacitance and loss versus the phase of this a-c voltage.

2. Description of Apparatus—

The apparatus used for most of the measurements at frequencies from one tenth to three megacycles consists of a General Radio type 916-A impedance bridge with a type 700-A beat-frequency oscillator as a generator and a Dumont type 224 oscilloscope as an indicator. A wide band amplifier, shown in fig. 7, is used between the bridge and the oscilloscope. The amplifier has a voltage gain of about 70. At

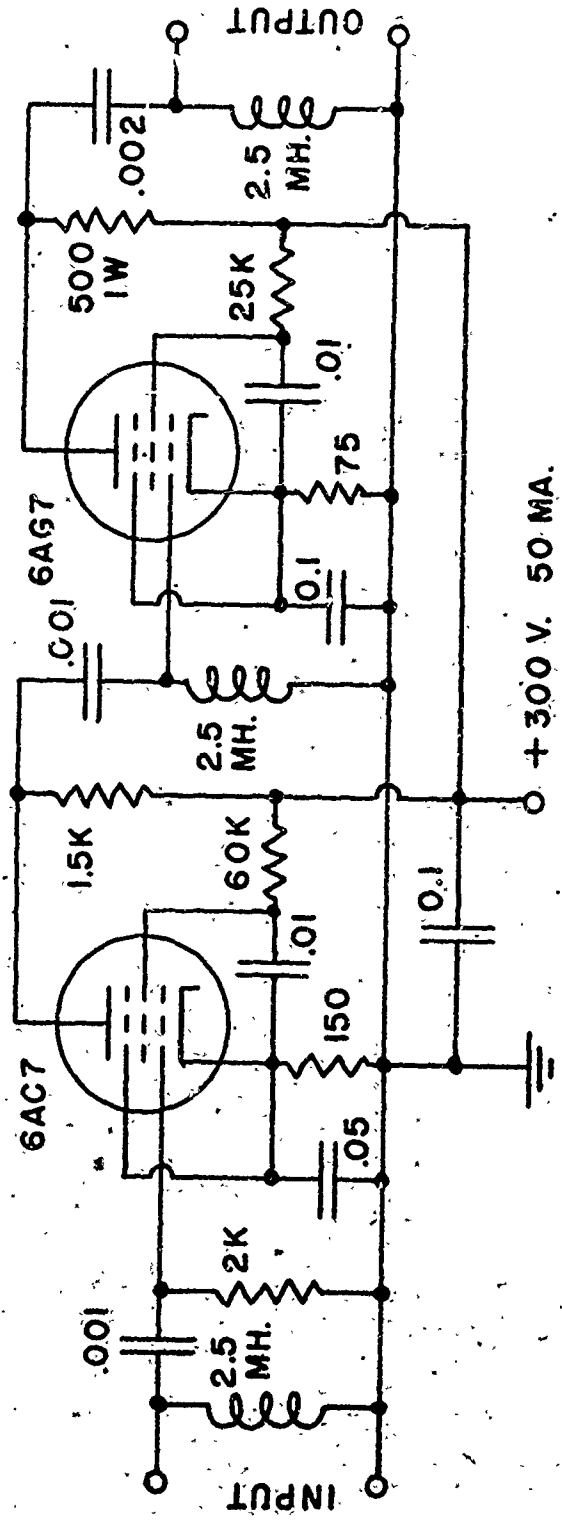
considerations apply to the dielectric constant versus biasing field strength in a nonlinear dielectric.

Mueller has measured the capacitance of nonlinear Rochelle salt condensers in an a-c bridge while simultaneously applying a d-c biasing voltage.⁴⁰ In this way the dielectric constant is determined versus biasing field strength. This method is found to be satisfactory in predicting the operation of the nonlinear condensers in circuit applications where the bias really is d-c. However, in circuits where modulation is to be obtained by superimposing low frequency a-c on the biasing voltage, the capacitance and loss as a function of time can not be correctly predicted from the measurements with d-c bias. To obtain the necessary information we have devised a method of applying a low frequency a-c biasing voltage instead of (or in addition to) d-c, and of measuring the capacitance and loss versus the phase of this a-c voltage.

2. Description of Apparatus—

The apparatus used for most of the measurements at frequencies from one tenth to three megacycles consists of a General Radio type 916-A impedance bridge with a type 700-A beat-frequency oscillator as a generator and a Dumont type 224 oscilloscope as an indicator. A wide band amplifier, shown in fig. 7, is used between the bridge and the oscilloscope. The amplifier has a voltage gain of about 70. At

NOTE: CAPACITANCES ARE EXPRESSED IN MICROFARADS AND RESISTANCES IN OHMS. RESISTORS ARE RATED AT 1/2 WATT EXCEPT WHERE NOTED.



7. FIG. 10. BROAD BAND PREAMPLIFIER FOR OSCILLOSCOPE

higher frequencies than three megacycles a General Radio type 605-B signal generator and a National type HRO receiver are used as generator and detector respectively.

The method of mounting the sample is shown in fig. 6. The sample, not visible in this picture, is held in a spring clip which makes contact with both electrodes and is supported by its lead wires, one of which connects to the ceramic bushing in the center of the picture, and the other to a ground terminal close by on the vertical panel. The ceramic sample is immersed in an oil bath in a cup about two inches in diameter. The cup is supported by a coiled copper tube soldered to it, through which a refrigerant can be circulated for cooling the oil bath.

The biasing voltage connects to the pin jack visible on the vertical panel and is by-passed to ground by a .008 mfd. condenser at this point. The jack also connects through a 30 mh. choke, visible behind the right end of the ceramic bushing, to the terminal which the bushing supports.

The unbalance voltage from the bridge, after amplification, is applied directly to the vertical deflection plates of the oscilloscope, i.e. without detection, so that the cathode ray beam is deflected at the measuring frequency. The pattern on the screen of the oscilloscope thus takes the form of a horizontal band, which is straight if d-c bias is used on the nonlinear condenser. When the bridge is brought into balance, this band contracts to a straight line.

The use of the oscilloscope as an indicator is especially valuable in measuring the capacitance when an a-c biasing voltage of low frequency compared to the measuring frequency is used instead of d-c. In this case the sweep pattern, when synchronized to the biasing voltage, dilates during those portions of the sweep cycle where the capacitance of the specimen is poorly balanced in the bridge circuit and contracts during those portions where the capacitance is near the correct value for balance. If balance occurs at any point during the sweep cycle, then the oscilloscope pattern closes at this point. Using this method it is possible to measure the capacitance of the specimen versus the instantaneous phase of the biasing voltage.

It is interesting to note that in these tests the output of the bridge really is an amplitude modulated wave. By applying d-c in addition to a relatively small a-c biasing voltage and by slightly unbalancing the bridge, the envelope of the output as seen on the oscilloscope can be made to reproduce more or less faithfully the low frequency biasing voltage. In this case the bridge circuit with the nonlinear condenser functions as a linear amplitude modulator. Not only can the operation of the nonlinear condenser as an amplitude modulator be observed directly on the oscilloscope, but it can also be measured accurately by the method we have devised. It is to be stressed that we have undertaken to

measure the fundamental properties of the dielectric which pertain to its use in any modulator circuit. But if one seeks in our work an experimental demonstration of an amplitude modulator circuit, one has to look no further than our measuring apparatus.

The dielectric constant of barium titanate is very sensitive to temperature. Consequently, we have to make measurements both above and below room temperature and we have to be able to hold the temperature constant over a period of time.

To raise the temperature above room temperature we use a small electric heater below the oil bath and to reduce the temperature below room temperature we pump some butyl alcohol first through a coiled copper tube in a dry ice bath and then through the copper tube around the oil bath holding the sample. The dry ice bath consists of a mixture of dry ice and butyl alcohol in a gallon size thermos jar. The coiled copper tube in the dry ice bath consists of two lengths of $\frac{1}{2}$ inch diameter copper tubing about ten feet long connected in parallel and wound in the form of a coil. The pump is a small centrifugal circulating pump. The pump, dry ice bath and oil bath are connected by rubber tubing which is insulated with hair felt. An adjustable thermostat (Fenwal) mounted in the cover (not shown) of the rectangular box shown in fig. 6 is used to control the heater or the circulating

pump. Some difficulty is encountered in controlling the bath at temperatures slightly below ambient. In this case the heater is turned on continuously, the flow of refrigerant is throttled down to a trickle and the pump is operated only intermittently by means of a switch which is connected in series with the thermostat and turns the power on for about two seconds during a cycle of about eight seconds. With these precautions, the temperature can be controlled automatically to within ± 1 degree at any temperature from -50 to $+135^{\circ}\text{C}$.

3. Determination of Dielectric Constant and Loss--

The fundamental properties of the dielectric, namely the dielectric constant and loss, are to be determined from impedance measurements of a sample condenser. If the condenser has a capacitance C , its impedance Z at a frequency $\omega/2\pi$ is normally written

$$Z = \frac{1}{j\omega C} \quad (\text{III-4})$$

The fact that Z is not a pure reactance can be attributed to a complex value of the capacitance.

$$C = C' - jC''$$

or

$$\frac{1}{Z} = j\omega C = \omega C'' + j\omega C' \quad (\text{III-5})$$

$\omega C''$ is thus equivalent to the conductance of the condenser and is responsible for its loss.

The complex capacitance of the condenser depends on the complex permittivity ϵ^* of the dielectric material which it contains.

$$C = \frac{\epsilon^*}{\epsilon_0} C_0 \quad (\text{III-6})$$

where C_0 is called the vacuum capacitance and ϵ_0 is the permittivity of free space. If $\epsilon^* = \epsilon' - j\epsilon''$, the relation between ϵ^* and C may be written

$$\frac{\epsilon'}{\epsilon_0} = \frac{C'}{C_0} \quad ; \quad \frac{\epsilon''}{\epsilon_0} = \frac{C''}{C_0} \quad (\text{III-7})$$

ϵ'/ϵ_0 is normally called the dielectric constant and ϵ''/ϵ_0 is called the loss factor. The ratio of ϵ'' to ϵ' is called the loss tangent.

The vacuum capacitance C_0 is determined by the electrode configuration and the permittivity of free space. For parallel plane electrodes of area A and separation d , the vacuum capacitance is

$$C_0 = \epsilon_0 \frac{A}{d} \quad (\text{III-8})$$

The vacuum capacitance can be determined either from measurements of the area of the electrodes and thickness of the dielectric (eq. III-8) or from the capacitance C' and the dielectric constant ϵ'/ϵ_0 , (eq. III-7) if the latter is known.

The thickness is measured by means of a dial indicator gage before the silver electrodes are applied. The diameter of the spot of silver paint is measured in several directions and averaged. An edge correction is necessary in order to find the effective area in eq. III-8. Since we did not find an appropriate formula for high-dielectric-constant materials, we have derived such a formula by a simple Schwarz-Christoffel transformation in Appendix A.

Our measurements of area are relatively inaccurate, while the capacitance can be measured with good accuracy. Therefore, values of ϵ'/ϵ_0 are determined initially for different samples of the same material by substituting eq. III-8 in eq. III-7.

$$\frac{\epsilon'}{\epsilon_0} = \frac{C'd}{\epsilon_0 A} \quad (\text{III-9})$$

The values of C_0 are finally determined from the measured values of C' by substituting the average of ϵ'/ϵ_0 in eq. III-7. The values of C_0 so obtained are at least consistent with the measured values of capacitance.

In interpreting the results of the bridge measurements, one has to be careful to make all the necessary corrections for stray capacitance and inductance in the lead wires and the choke coil. The stray capacitances and admittance of the choke coil are effectively in parallel with the sample and can be measured all at once by

opening the spring contact on the sample holder. The inductance and resistance of the lead wires can be measured by short circuiting the spring contact and amount to $0.1 + j4.9$ ~~ohms~~ ohms at a frequency of 10 megacycles. At 25 megacycles the series inductance is practically in resonance with the capacitance of the sample, making the accuracy very poor at and above this frequency.

IV. EXPERIMENTAL RESULTS

1. Dielectric Constant and Loss Versus Field Strength--

We have measured the dielectric constant and loss at room temperature versus d-c and a-c field strength for barium titanate and for the mixture of barium and strontium titanates. The room temperature is below the Curie point for the barium titanate and above the Curie point for the mixture. As a result the dielectric properties versus field strength are quite different for the two materials.

Fig. 8 shows the variation of ϵ'/ϵ_0 that is typical of barium titanate at ordinary temperatures with d-c bias. The field strength is expressed in megavolts per meter. This figure shows the values of dielectric constant at a frequency of 400 Kc for both increasing and decreasing fields. The fact that there is a difference is an indication of hysteresis, but there is not nearly as much difference here as that shown for Rochelle salt in fig. 35. The loss factor under the same conditions is shown in fig. 9 in which the effects of hysteresis are more noticeable, but still the loss tangent is quite small--less than three percent.

Fig. 10 shows the corresponding field strength dependence of ϵ'/ϵ_0 at a frequency of 10 Mc. At this frequency the value of ϵ'/ϵ_0 varies much more rapidly as a function of field strength and there is more indication of hysteresis

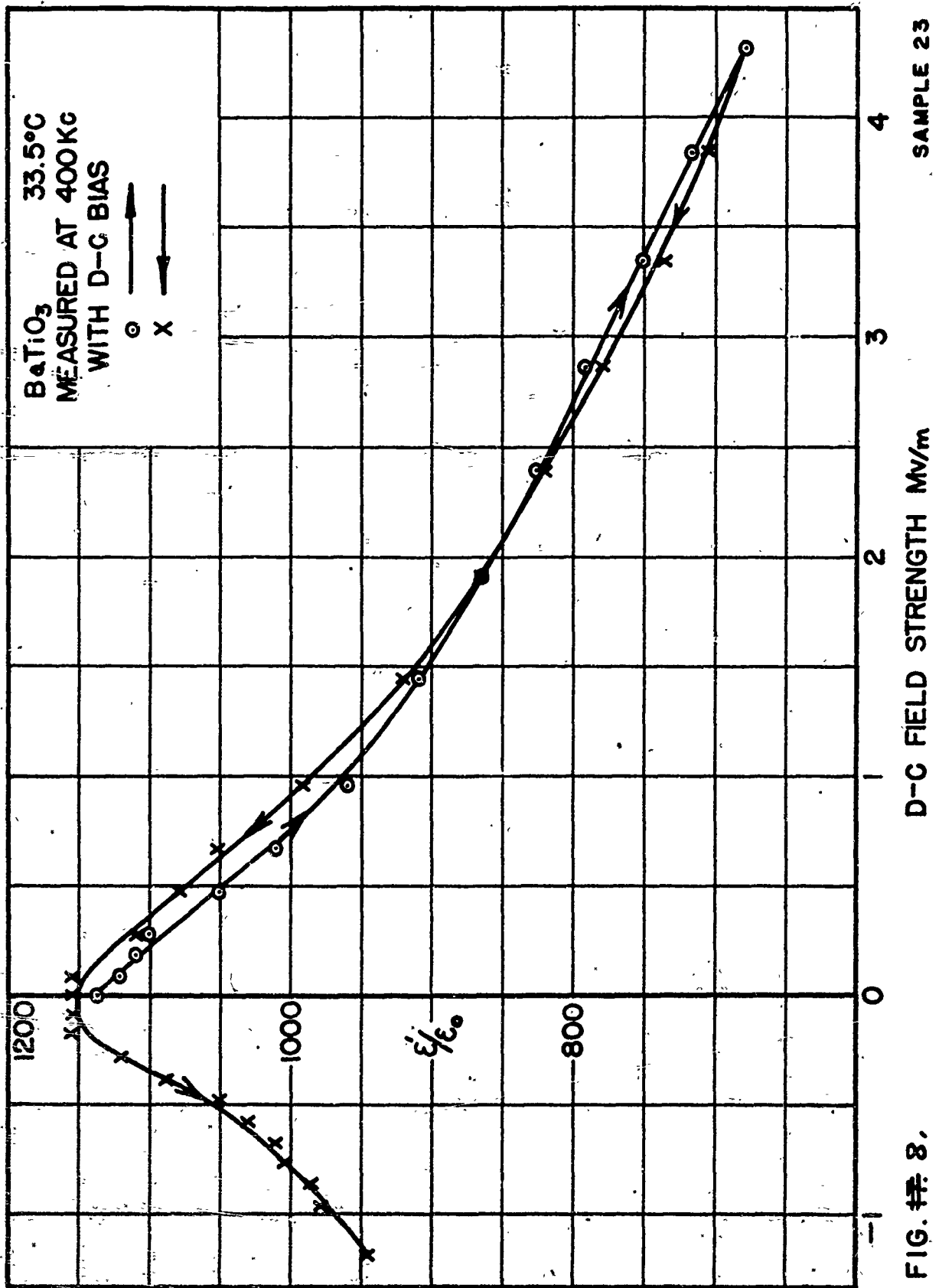
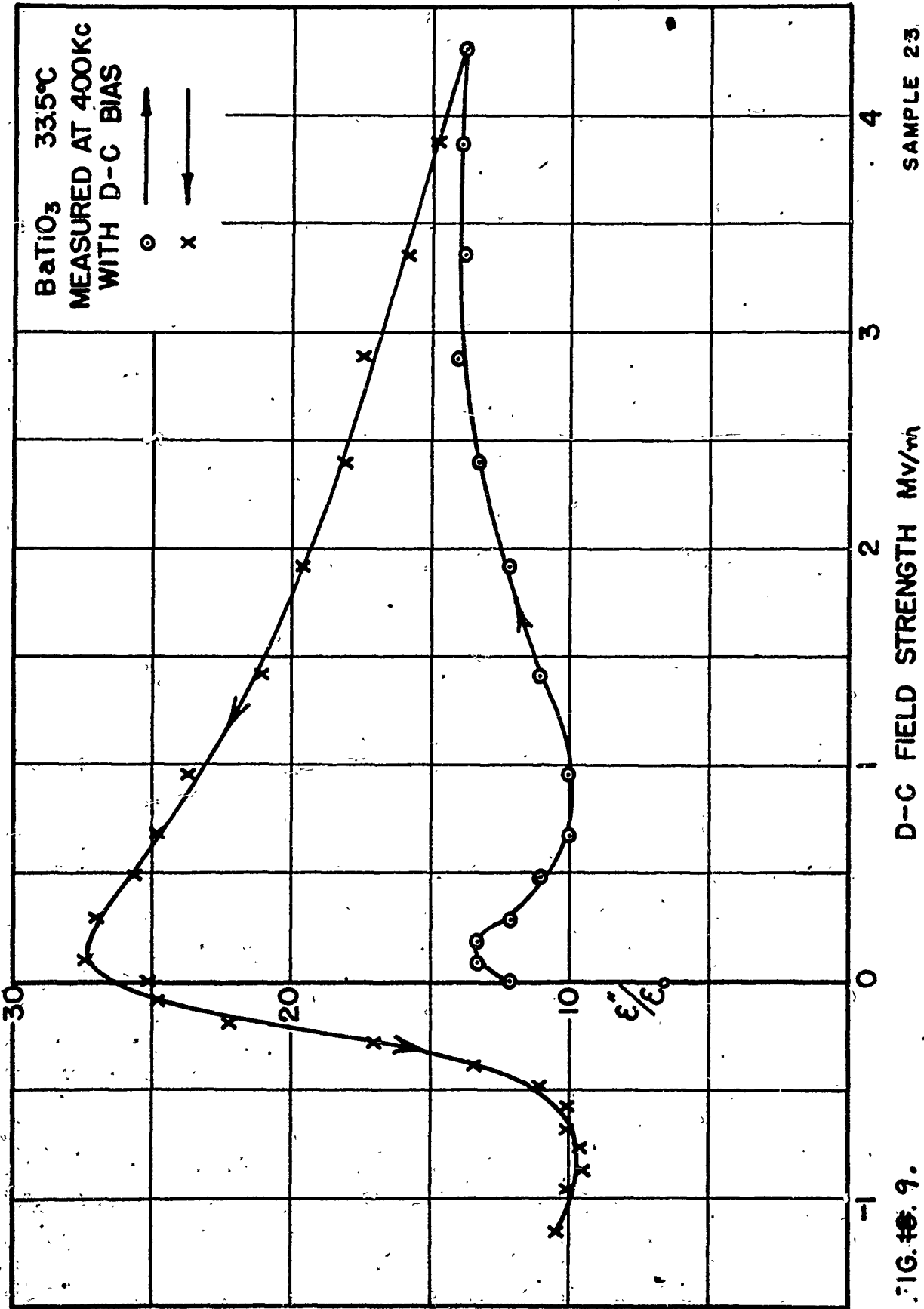


FIG. #8.



SAMPLE 23

FIG. 9.

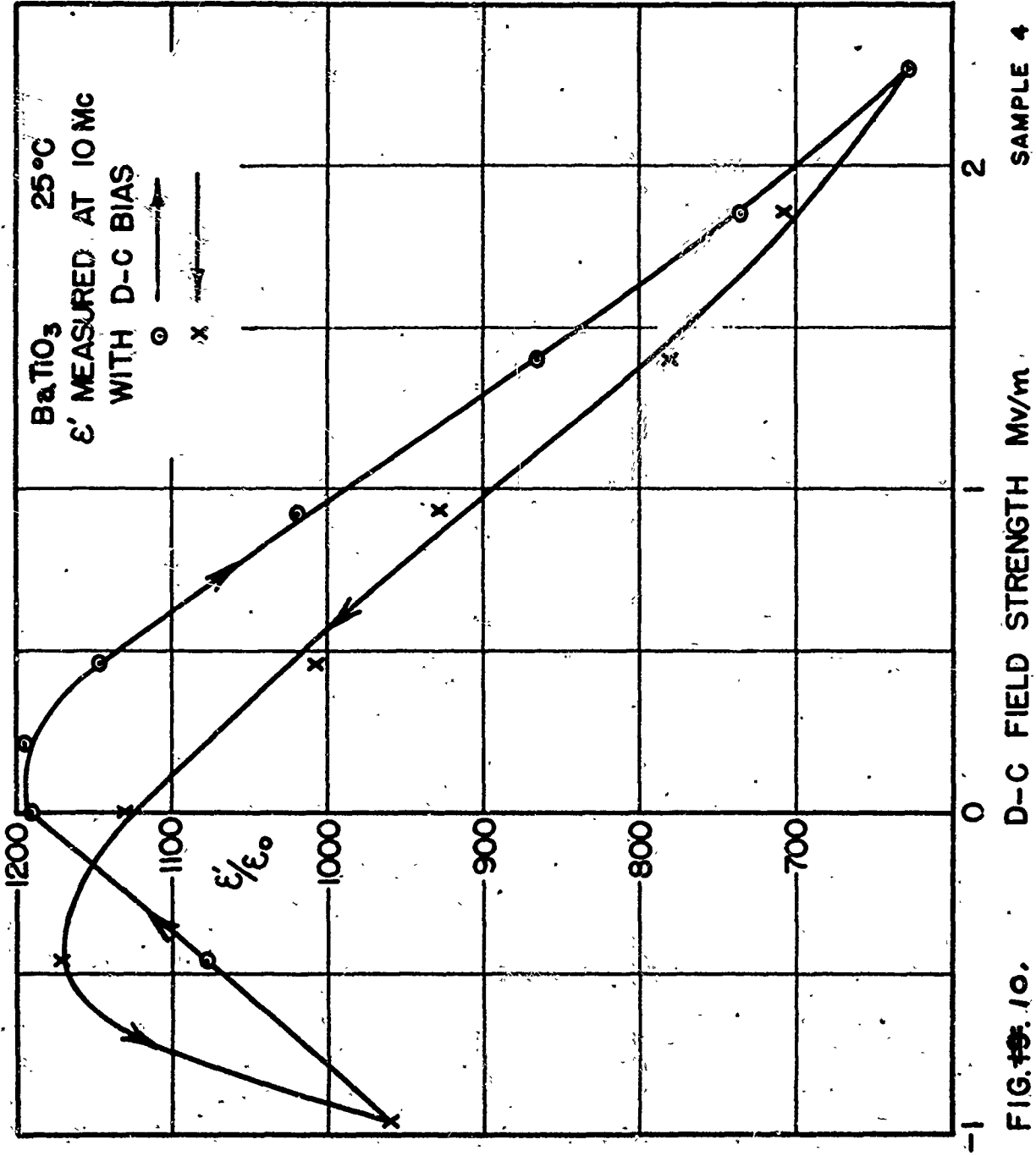


FIG. 10. D-C FIELD STRENGTH MV/m SAMPLE 4

than at 400 Kc. The loss factor under these conditions is shown in fig. 11 which indicates a very strong hysteresis effect. The intersection of the return curve at 400 on the vertical axis indicates a rather high remanent polarization, and the distance of the minimum to the left indicates a coercive field strength of about 0.5 Mv/m. This value may be subject to a rather large error because the curve is drawn with so few experimental points. In fig. 9 the corresponding value for the coercive field strength is 0.8 Mv/m.

The variation of ϵ'/ϵ_0 with 60 cycle a-c bias is indicated in fig. 12. Here ϵ'/ϵ_0 is plotted versus phase of the a-c biasing voltage. The same data are plotted in fig. 13 versus field strength. The latter figure shows substantially more hysteresis than does fig. 9. However the most striking difference between the results with d-c bias and with a-c bias is indicated in fig. 14, which shows the loss factor versus 60 cycle field strength. This figure shows that with 60 cycle bias voltage the loss rises to values more than ten times the highest values with d-c bias. This is not at all what one would expect and it is very important because it indicates that barium titanate is practically useless at normal temperatures for many of the applications we have in mind for a nonlinear condenser. This was a very disappointing discovery, but fortunately the investigation was not dropped at this point.

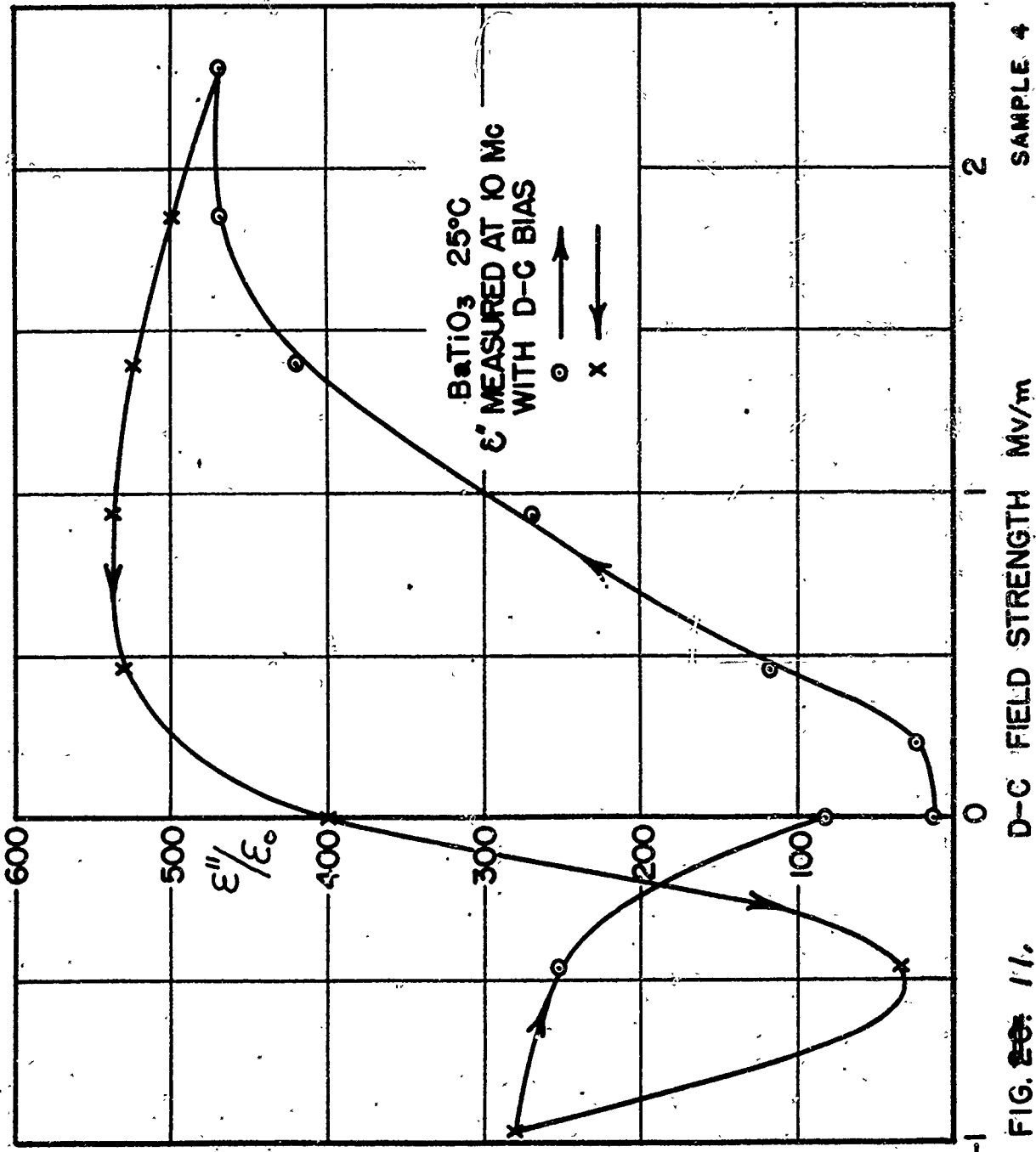


FIG. 11, D-C FIELD STRENGTH MV/m SAMPLE 4

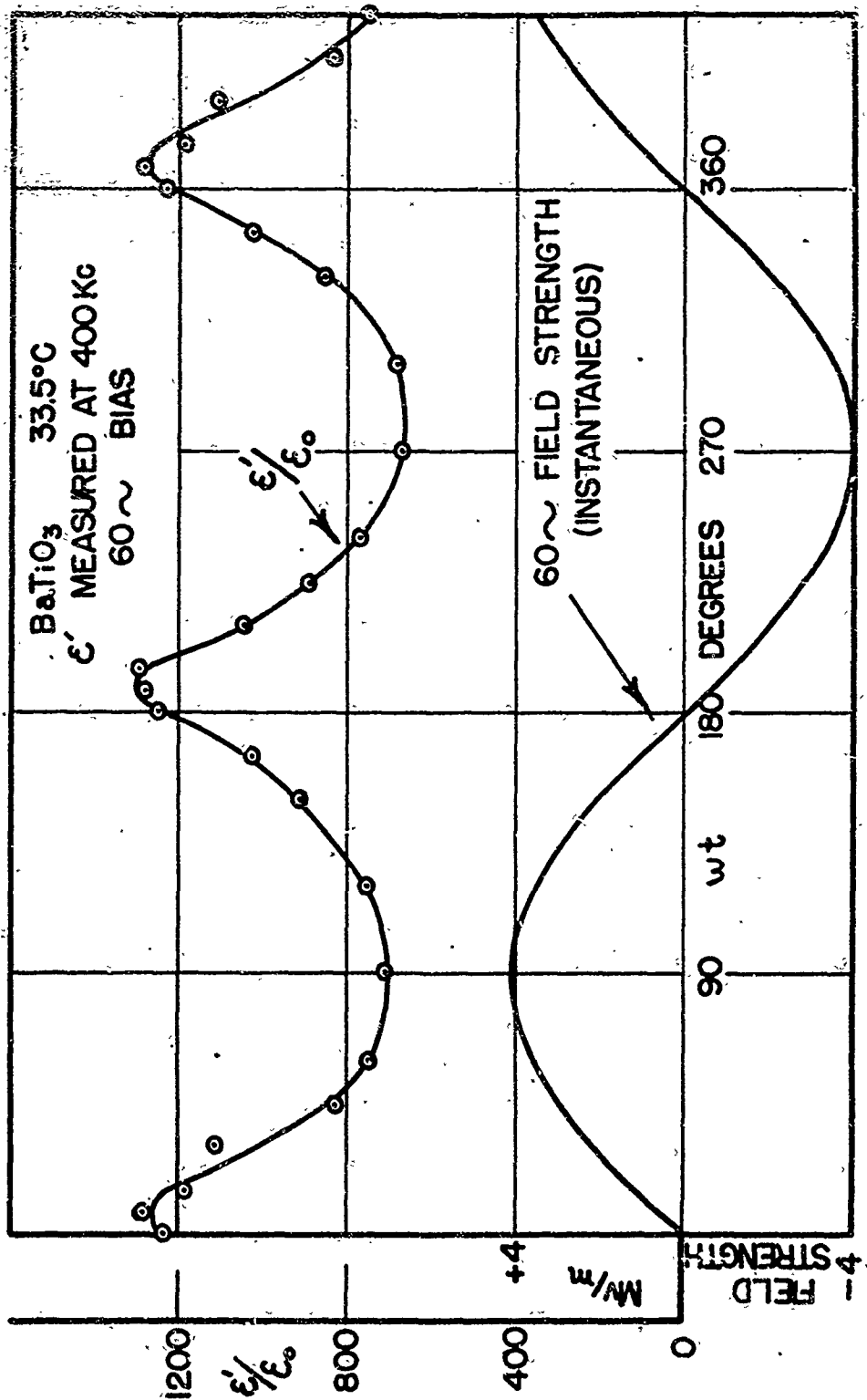


FIG. 12.

SAMPLE 23

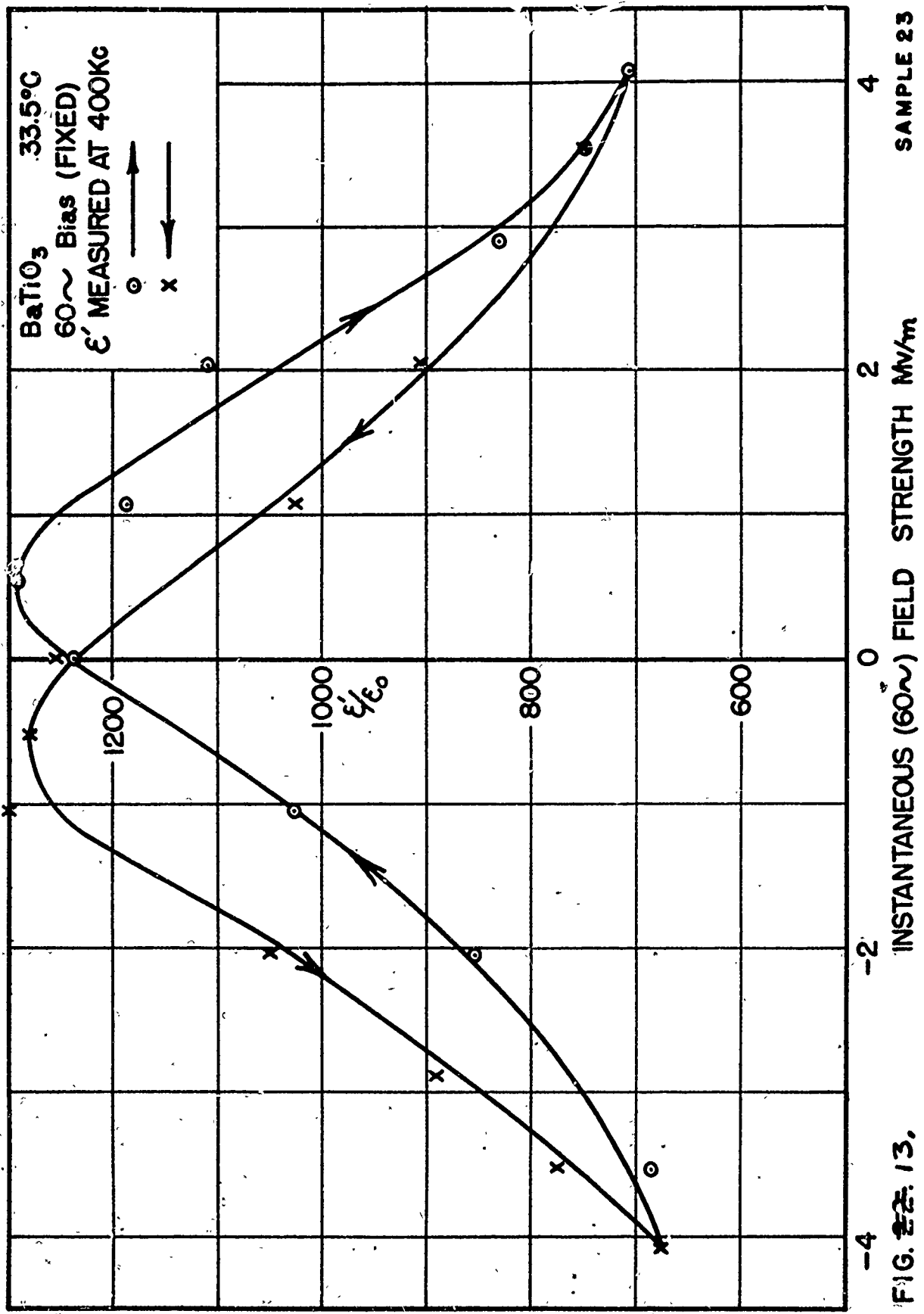


FIG. 22. 13.

SAMPLE 23

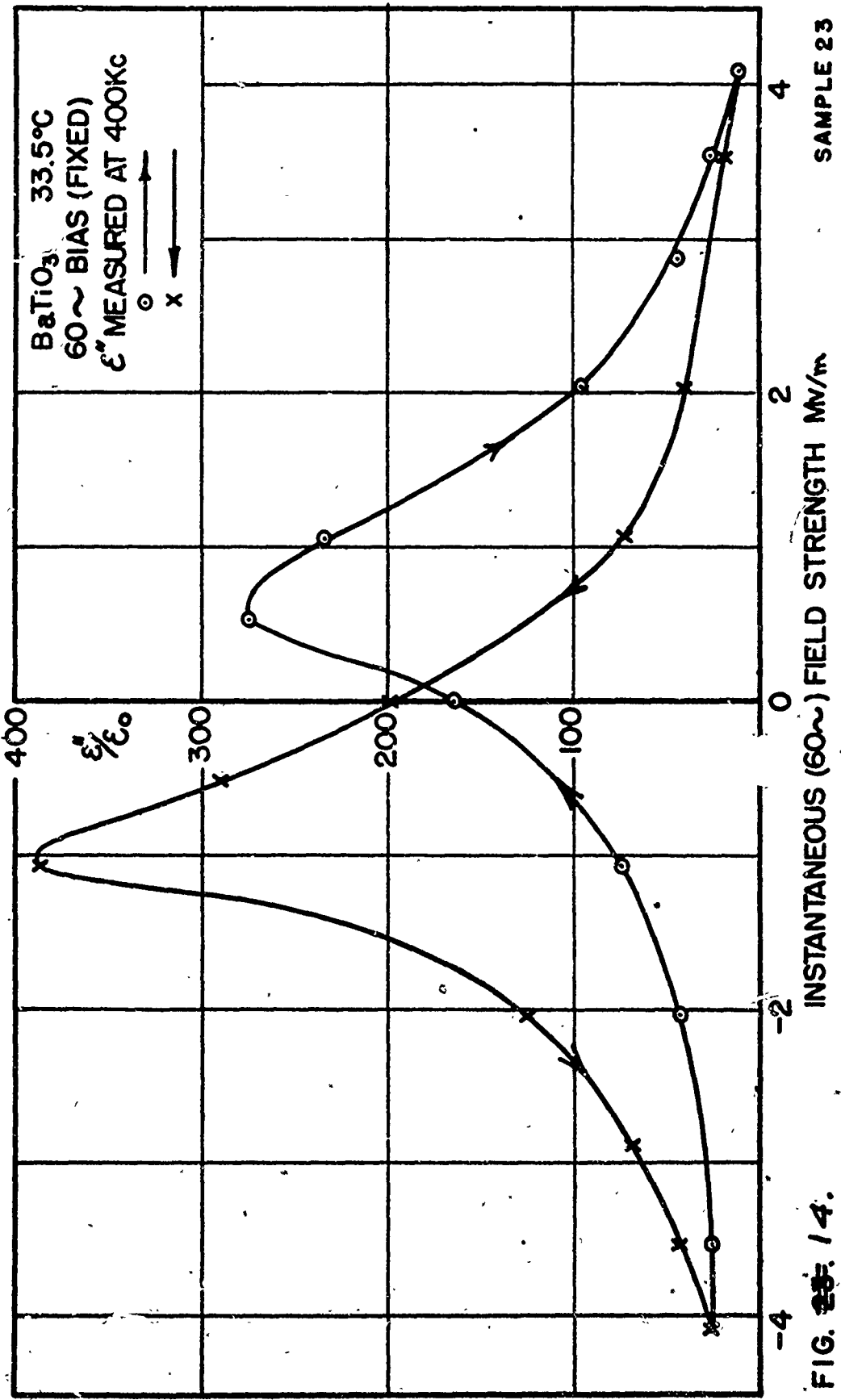


FIG. 28. 14.

As we have shown, the dielectric constant depends not only on the value of the d-c field strength, but also on its past history. In making a series of measurements it is sometimes very awkward to have to put the condenser through a prescribed cycle of voltages before each measurement. The situation is further complicated by a slow drift of the dielectric constant following application of any fixed voltage. For these reasons we greatly prefer to make measurements exclusively with an a-c biasing voltage. Accordingly we have adopted a method of measuring the dielectric constant and loss factor at the peak of the 60 cycle biasing voltage. If the values are different at the positive and negative peaks, as they are in figs. 13 and 14, then the two values are averaged. The results of such a series of measurements are shown in figs. 15 and 16, giving the dielectric constant and loss factor respectively. Each point on these curves corresponds to a different amplitude of the a-c biasing voltage.

So far we have measured the dielectric constant of barium titanate versus field strength by three different methods and each method gives a different result, as can be seen by comparing figs. 8, 13 and 15. The principal differences occur at low field strengths, however, and are not so important at the high field strengths.

In the case of the mixture of 75% barium titanate and 25% strontium titanate, the situation is quite different.

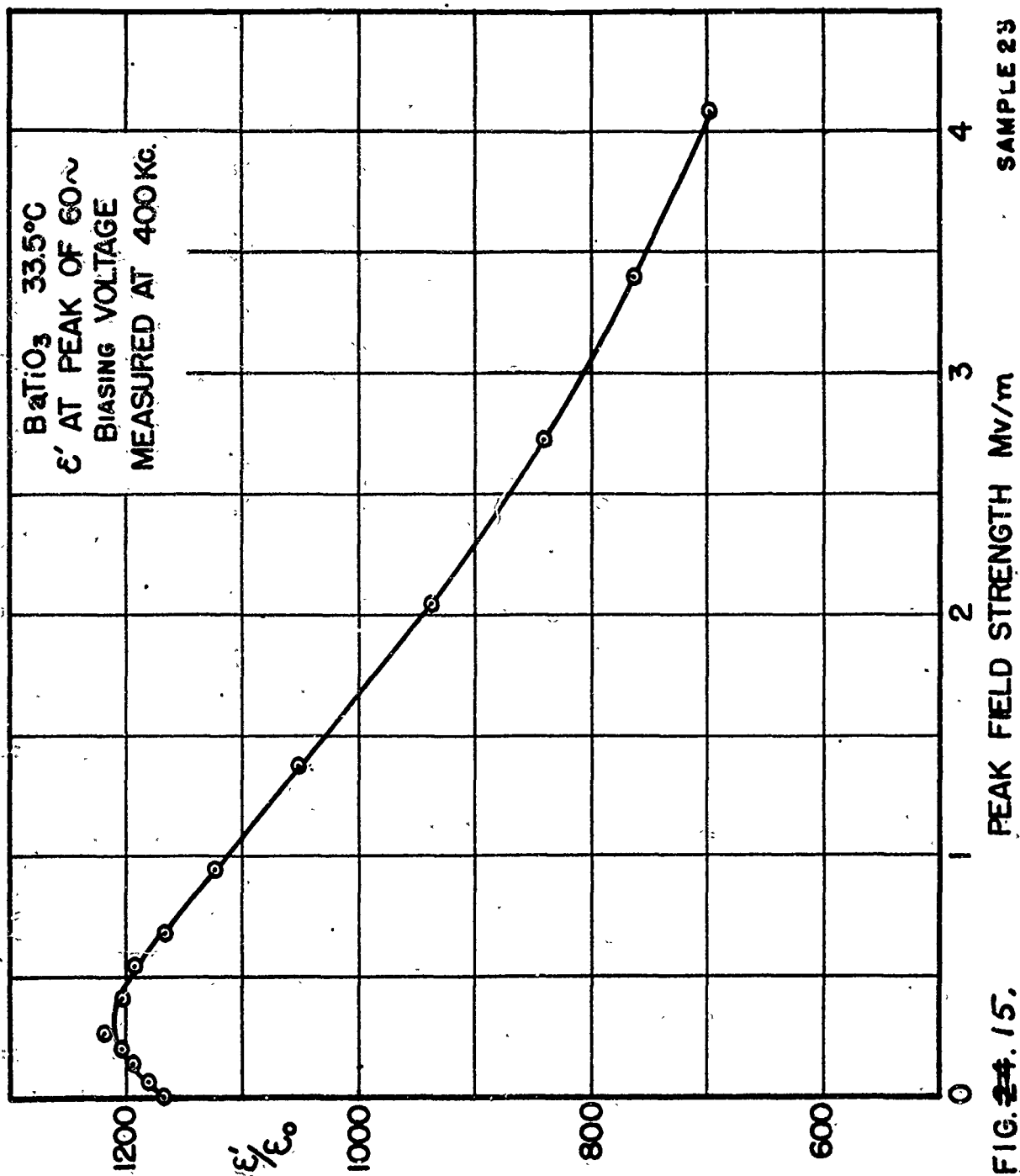
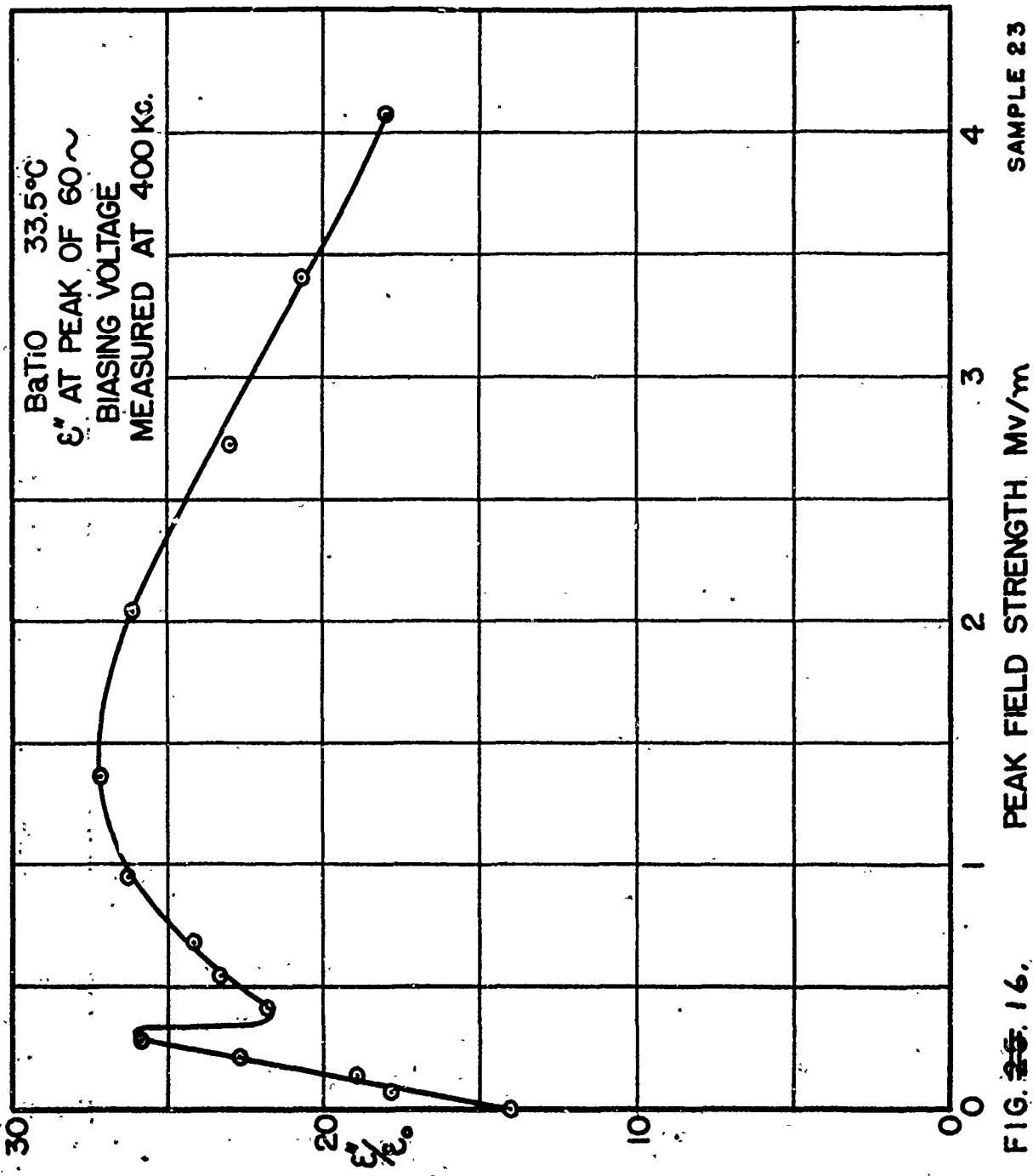


FIG. 24. 15.



The dielectric constant versus d-c field strength is shown in fig. 17. It turns out that the same curve is obtained by a-c measurements and there is no evidence of hysteresis. The corresponding loss is quite small even with a-c bias. The explanation of these phenomena is that in the case of barium titanate we are operating at a temperature below the Curie point, while in the case of the mixture we are operating at a temperature above the Curie point. This explanation receives further confirmation in the measurements of dielectric properties versus temperature.

The results obtained for the mixture of barium and strontium titanates indicate that above the Curie point the dielectric constant is a definite function of the biasing field strength. Therefore we are encouraged to look for a theoretical explanation for the nature of this function. Our derivation is based on a simple relation between electric displacement D and field strength E .

$$E = \alpha D + \beta D^3 \quad (\text{IV-1})$$

where α and β are constant at a given temperature. The derivation of the resulting equation for E versus ϵ ($\epsilon = dD/dE = \epsilon^* = \epsilon'$) is given in Appendix B.

$$\frac{E}{E_0} = \frac{1}{4} \sqrt{\frac{\epsilon_1}{\epsilon} - 1} \left(\frac{\epsilon_1}{\epsilon} + 2 \right) \quad (\text{IV-2})$$

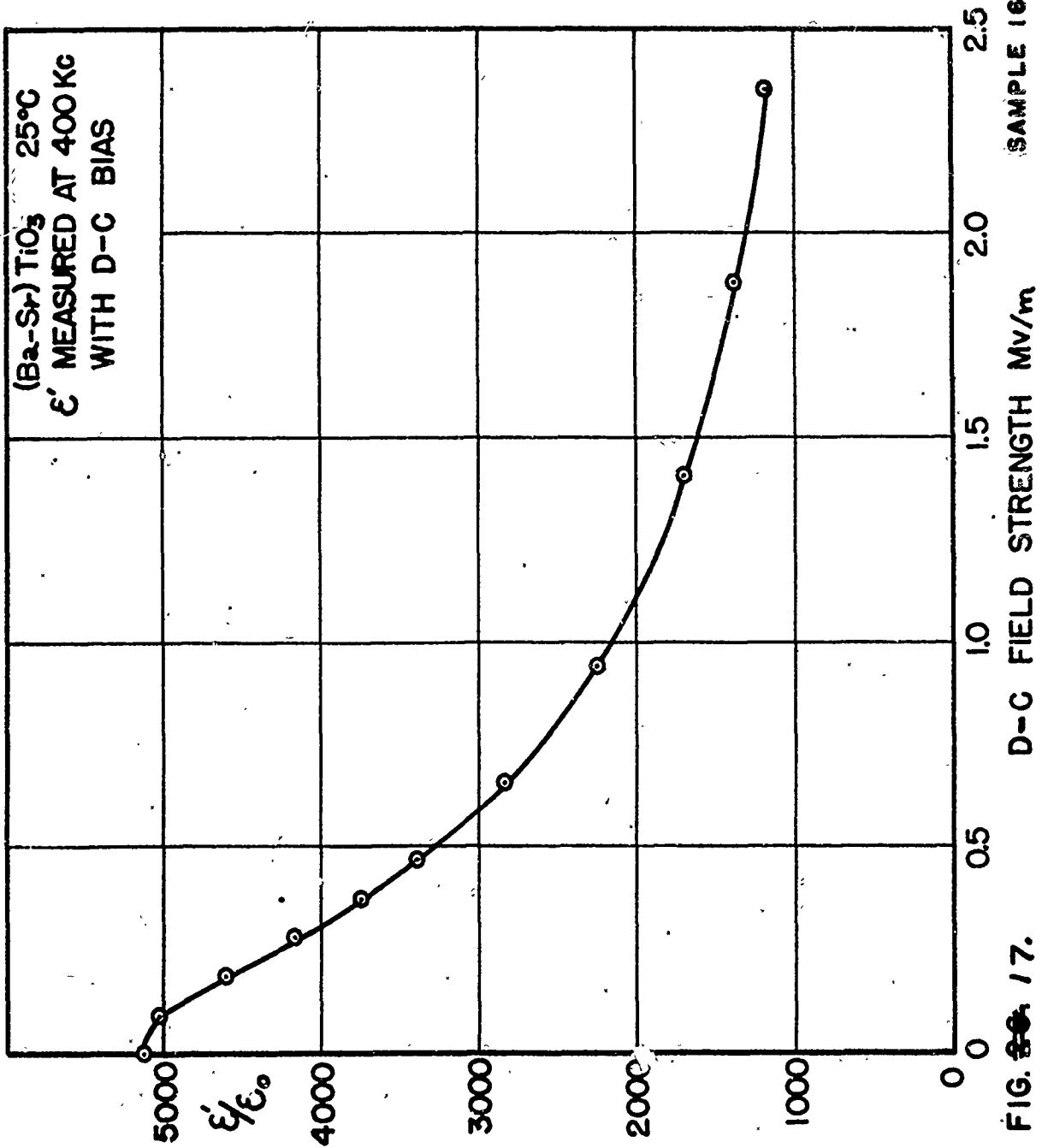


FIG. 17.

where

$$\epsilon_1 = \frac{1}{\alpha}$$

$$E_0 = 4 \left(\frac{\alpha}{3} \right)^{3/2} \beta^{-1/2}$$

Eq. IV-2 is plotted in fig. 18. If this figure is compared with the experimental curve of fig. 17, it is seen that the experimental values for barium-strontium titanate are given with good accuracy by eq. IV-2 putting $\epsilon_1/\epsilon_0 = 5130$ and $E_0 = 0.77$ Mv/cm. It is important to note that eq. IV-2 involves only these two parameters, the permittivity ϵ_1 at low field strengths and the field strength E_0 which reduces ϵ to one half its initial value ϵ_1 . This fact greatly simplifies the work involved in measuring the nonlinear dielectric properties as a function of temperature, etc. Instead of having to measure many points to determine a curve of ϵ versus field strength, only two points are required to establish the two parameters which describe the entire curve.

At temperatures below the Curie point, where hysteresis is encountered, the situation is not so simple, as our measurements have shown. Considerable divergence in ϵ' is possible at a given value of field strength. However even in this case it is instructive to determine the field strength E_0 at which ϵ' is reduced to half its initial value. It is also important to obtain some measure of the phenomenon indicated in fig. 14. This is done by averaging the maximum values of ϵ''/ϵ_0 and subtracting the value of ϵ''/ϵ_0 .

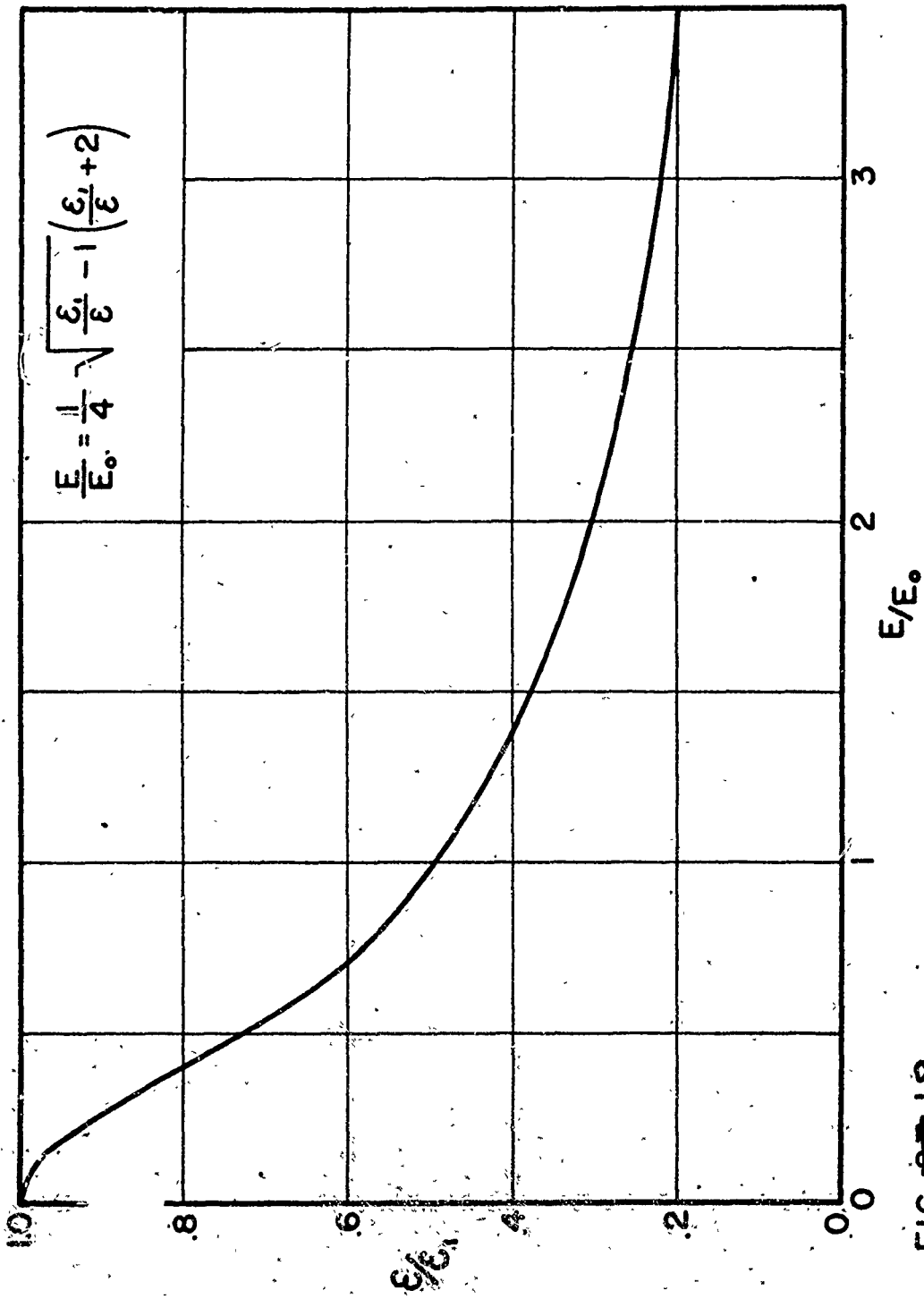


FIG. 18.

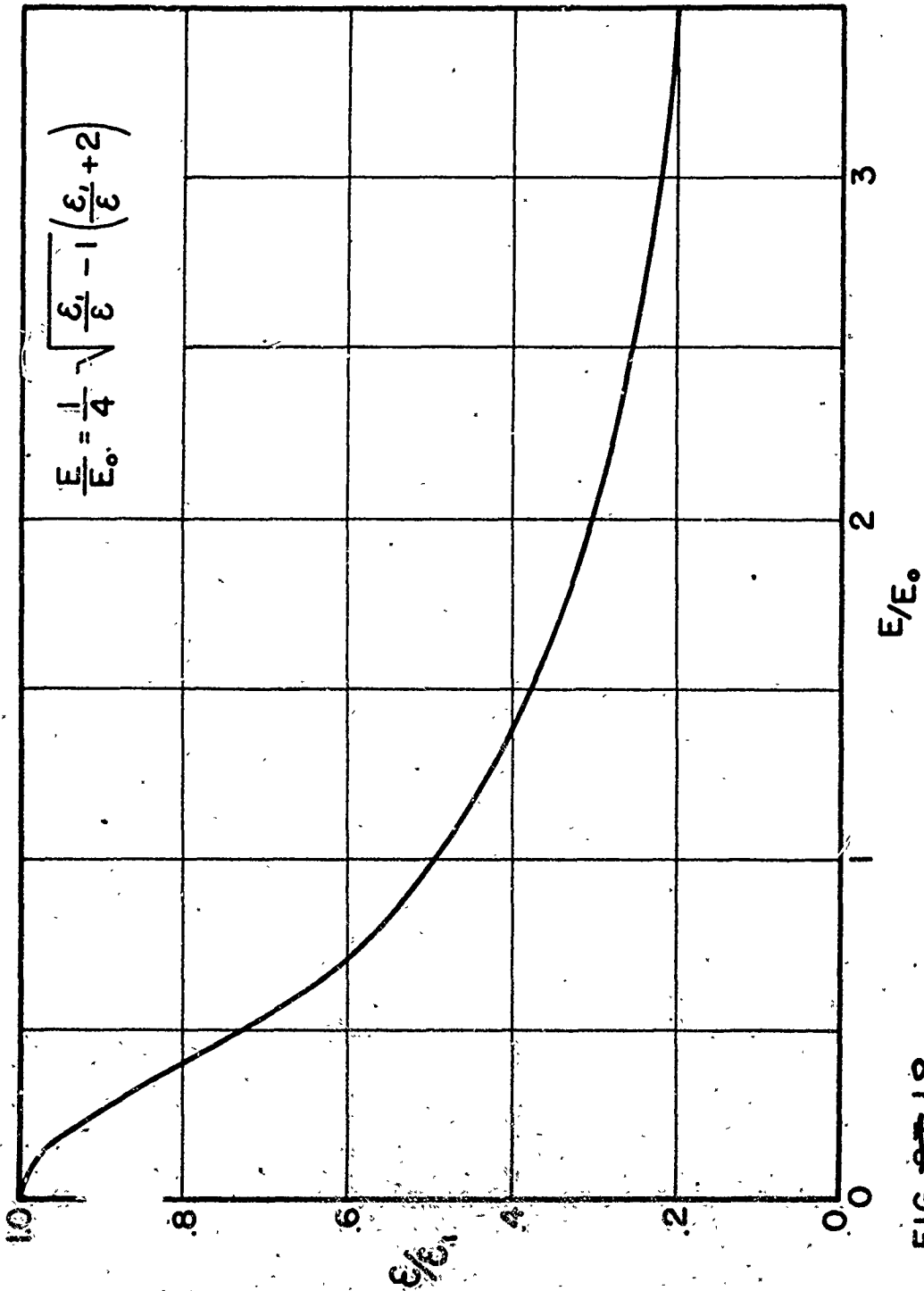


FIG. 18.

obtained with the bias voltage turned off. The peak value of the a-c field strength for this measurement is adjusted to the value E_0 . The parameter measured in this way is designated by the symbol $\Delta\epsilon''/\epsilon_0$.

2. Nonlinear Dielectric Properties Versus Temperature--

As one would expect, the dielectric constant and loss as functions of temperature are very similar to the data given in figs. 1 and 2, with the exceptions that the high losses at -20°C in fig. 1 disappear and the Curie point for the mixture comes at a lower temperature than that in fig. 2. The data that are of particular interest are the nonlinear parameters E_0 and $\Delta\epsilon''/\epsilon_0$. The results for barium titanate are of theoretical interest because they show anomalies at the secondary Curie point similar in some respects to those at the Curie point. The results for barium-strontium titanate are of practical interest because we find this material is preferable for use in nonlinear condensers.

Fig. 19 shows the dielectric constant and loss factor of barium titanate at low field strengths versus temperature from our measurements at 400 Kc. These curves can be compared with fig. 1, which shows the corresponding results at a frequency of 1 Kc. The Curie point is determined by the peak in the ϵ'/ϵ_0 curve, which occurs at about $+117^\circ\text{C}$. The nonlinear characteristics of barium titanate are represented by E_0 , shown versus temperature in fig. 20.

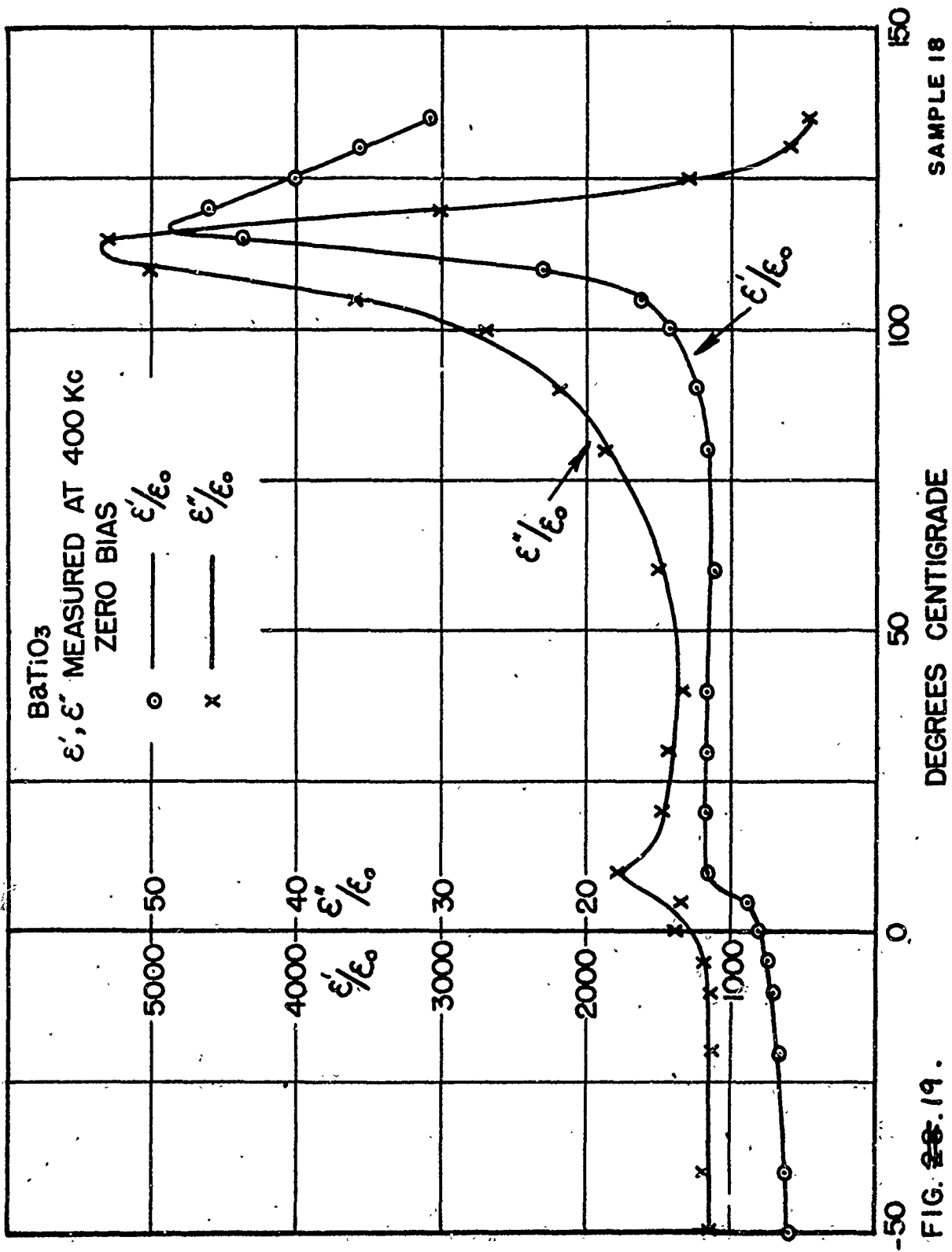


FIG. 19.

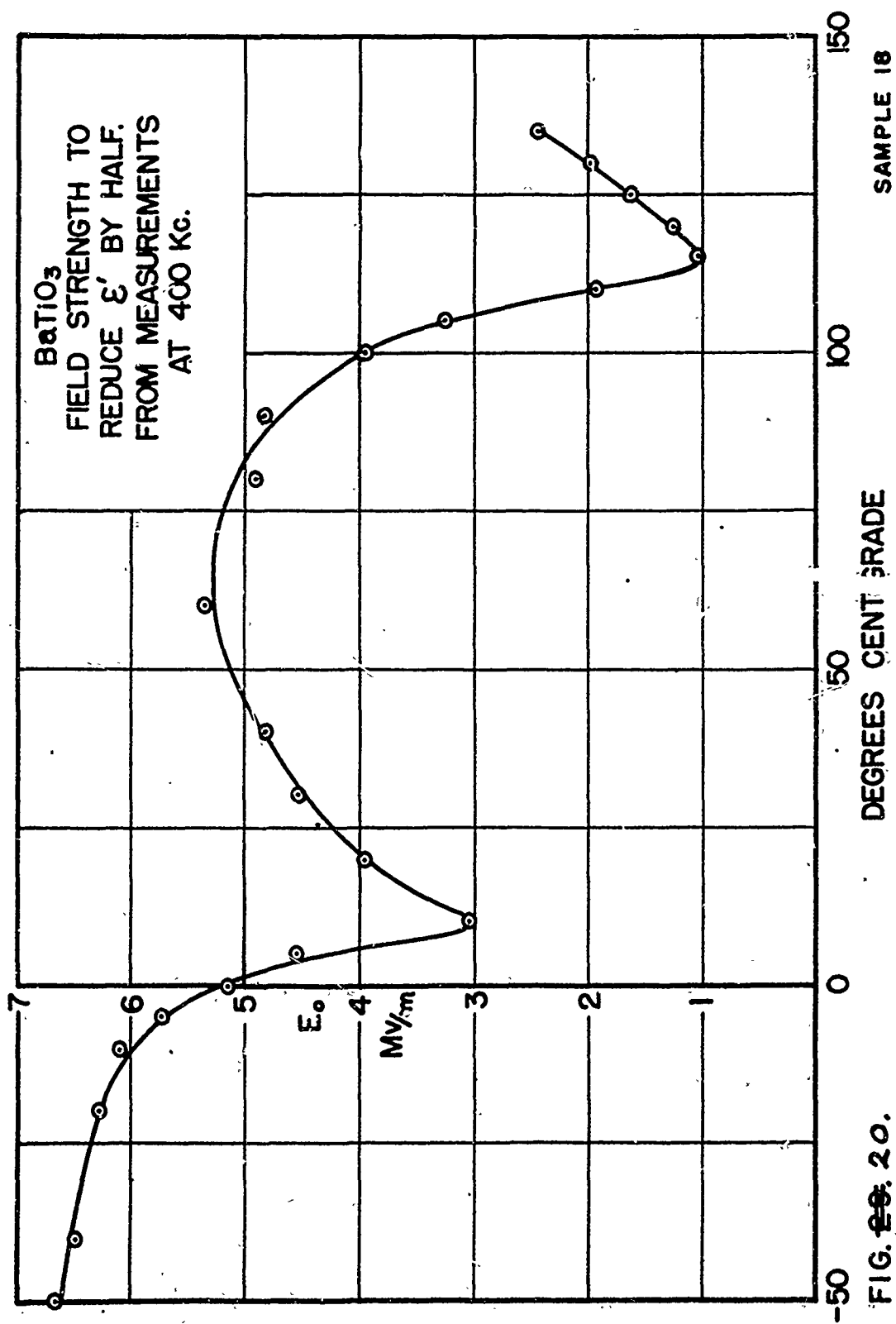


FIG. 20.

E_0 is the field strength required to reduce ϵ' to one half its initial value. These results are based on measurements with a-c bias. It is interesting to note the minimum which occurs at the Curie point and a second minimum occurring at 10°C , which corresponds to a secondary Curie point. Fig. 21 shows the increase in loss factor measuring the phenomenon shown in fig. 14. Values of $\Delta\epsilon''/\epsilon_0$ are plotted versus temperature. One notices the rapid disappearance of this phenomenon above the Curie point. The sudden rise at the secondary Curie point, 10°C , is also very striking. The high losses were maintained at lower temperatures than 0°C but the maximum field strength was less than E_0 for these temperatures.

Fig. 22 shows the dielectric constant and loss factor at low field strengths versus temperature for the mixture 75% barium and 25% strontium titanate. The curve for ϵ'/ϵ_0 indicates that the Curie point is 17°C . There is a discrepancy of 20°C between this value and the value indicated in fig. 2 for material of presumably the same composition. It is possible that there may have been enough actual difference in the composition of these materials to account for this. Fig. 23 shows the reciprocal of the dielectric constant versus temperature. This figure shows agreement with the Curie-Weiss laws, both above and below the Curie point, as indicated by the straight lines which have the correct relative slopes according to the theory derived in the next chapter. Fig. 24

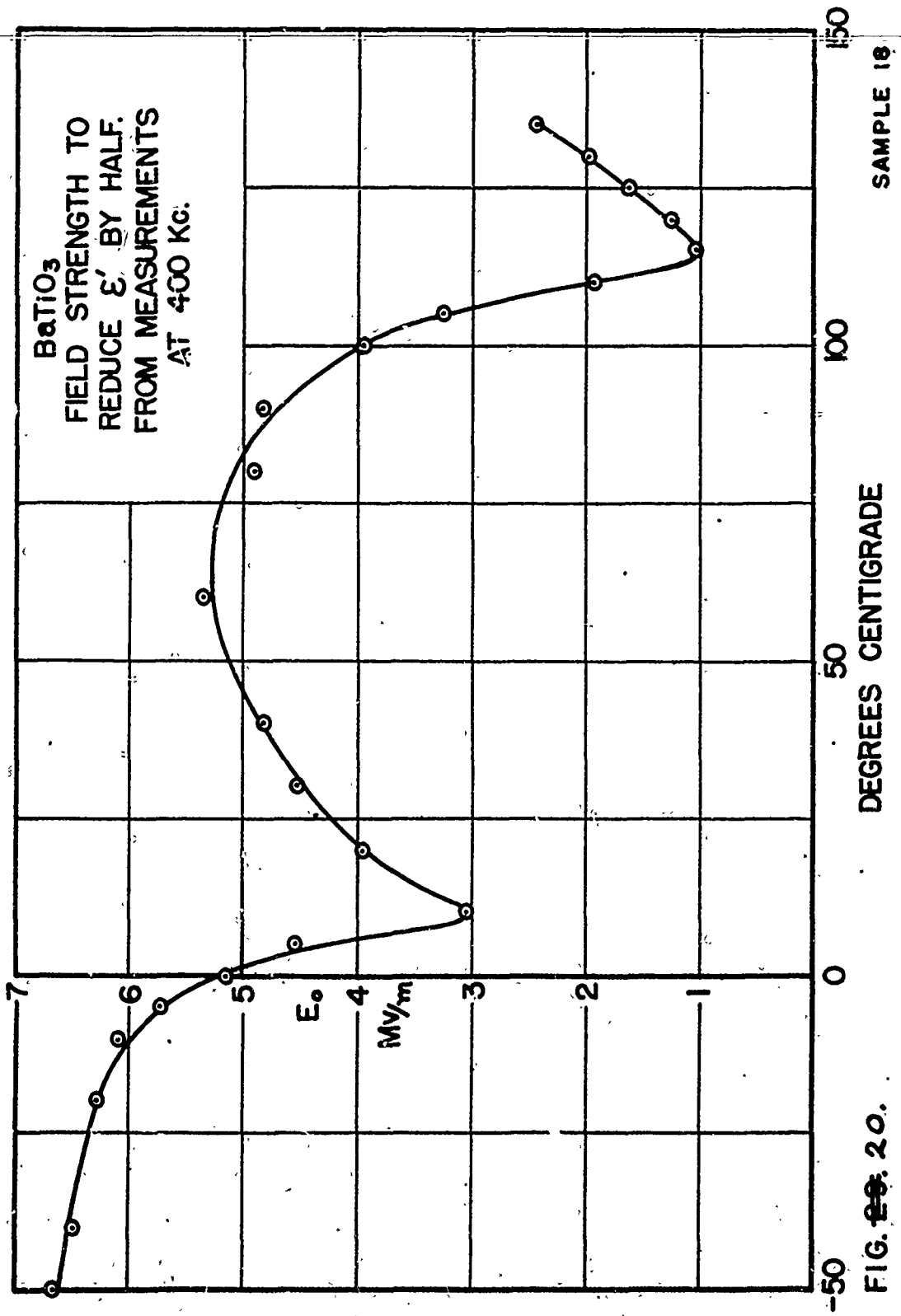


FIG. 20.

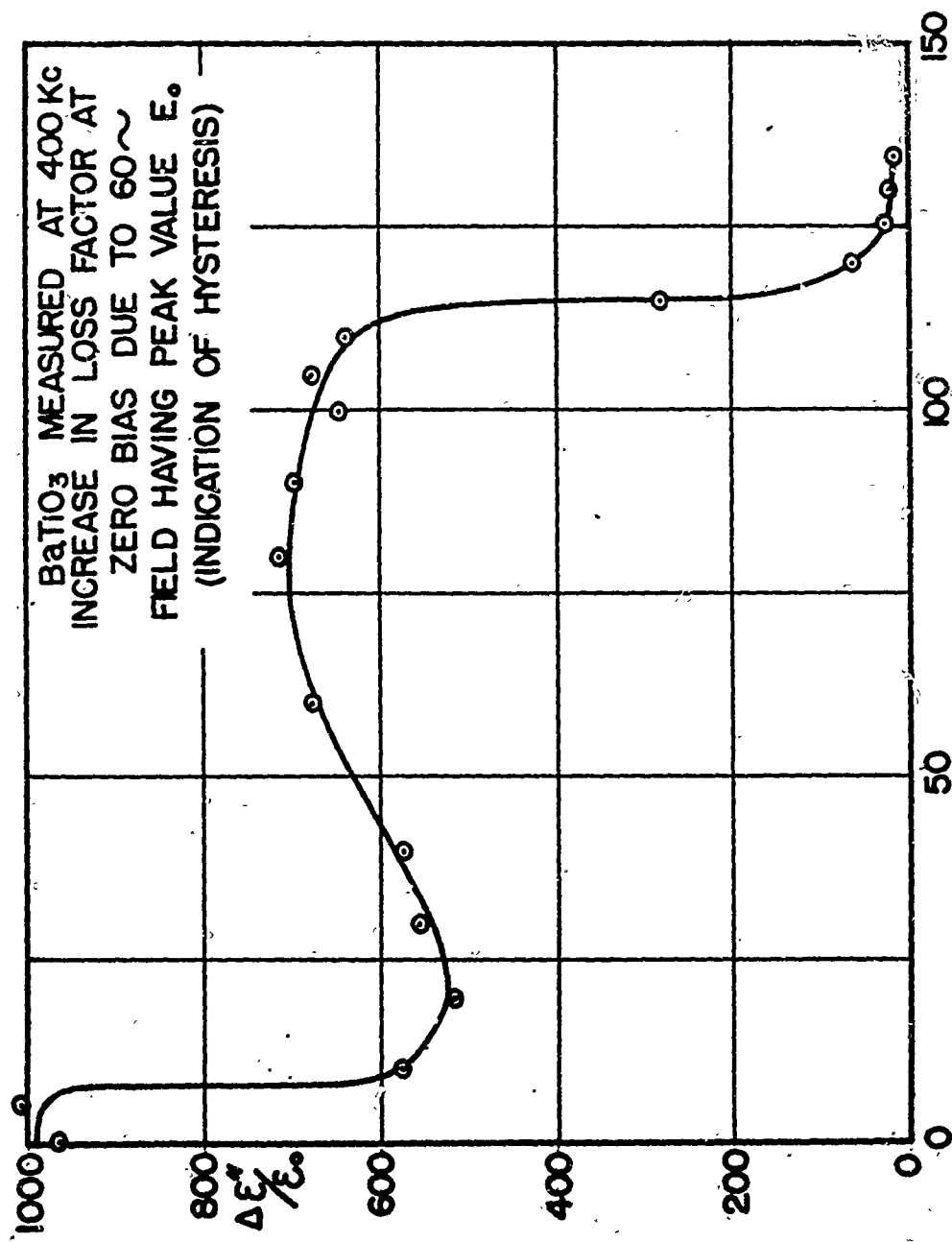


FIG. 21. SAMPLE 18

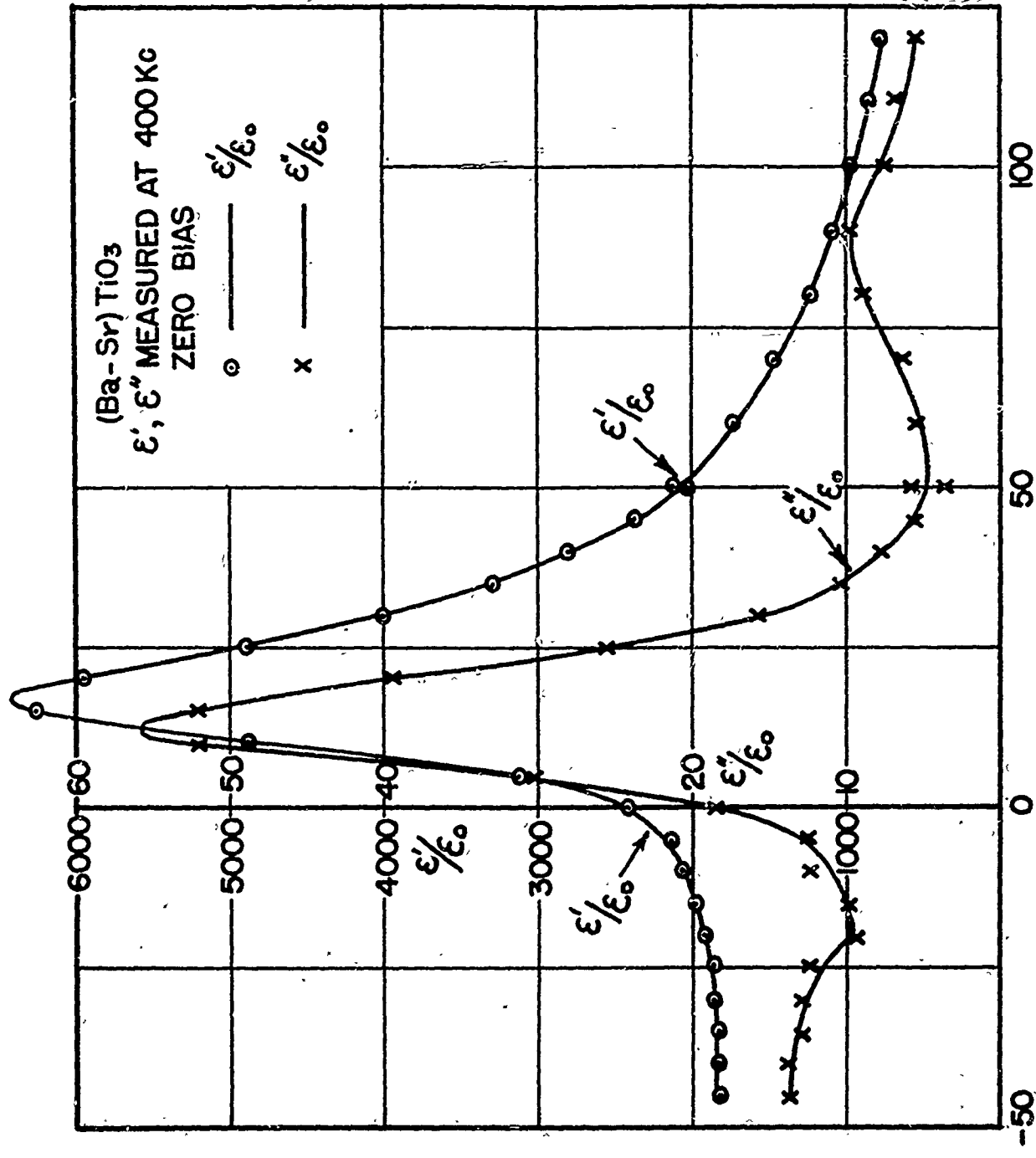


FIG. 22. SAMPLE 16

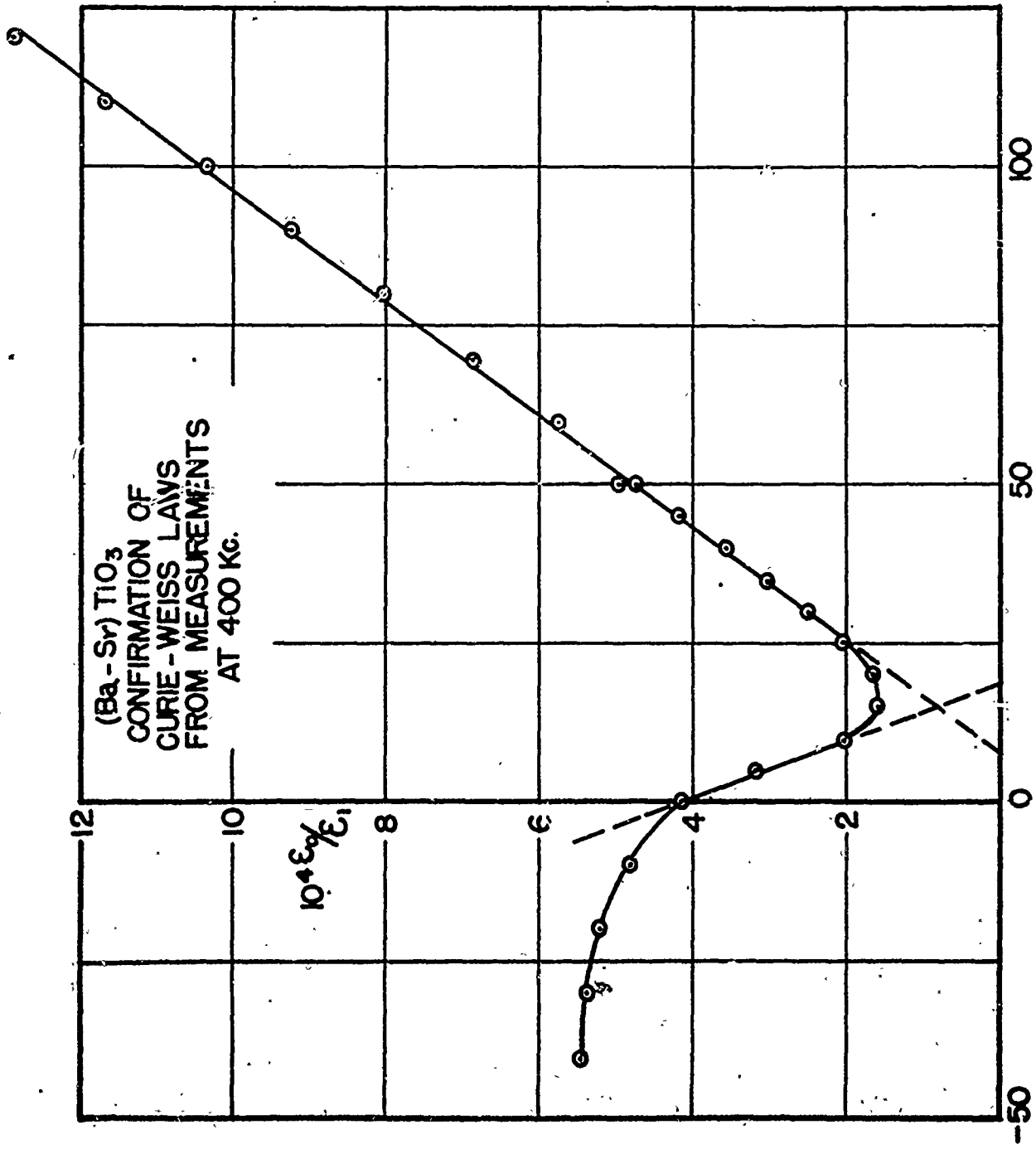


FIG. 23. SAMPLE 16 DEGREES CENTIGRADE

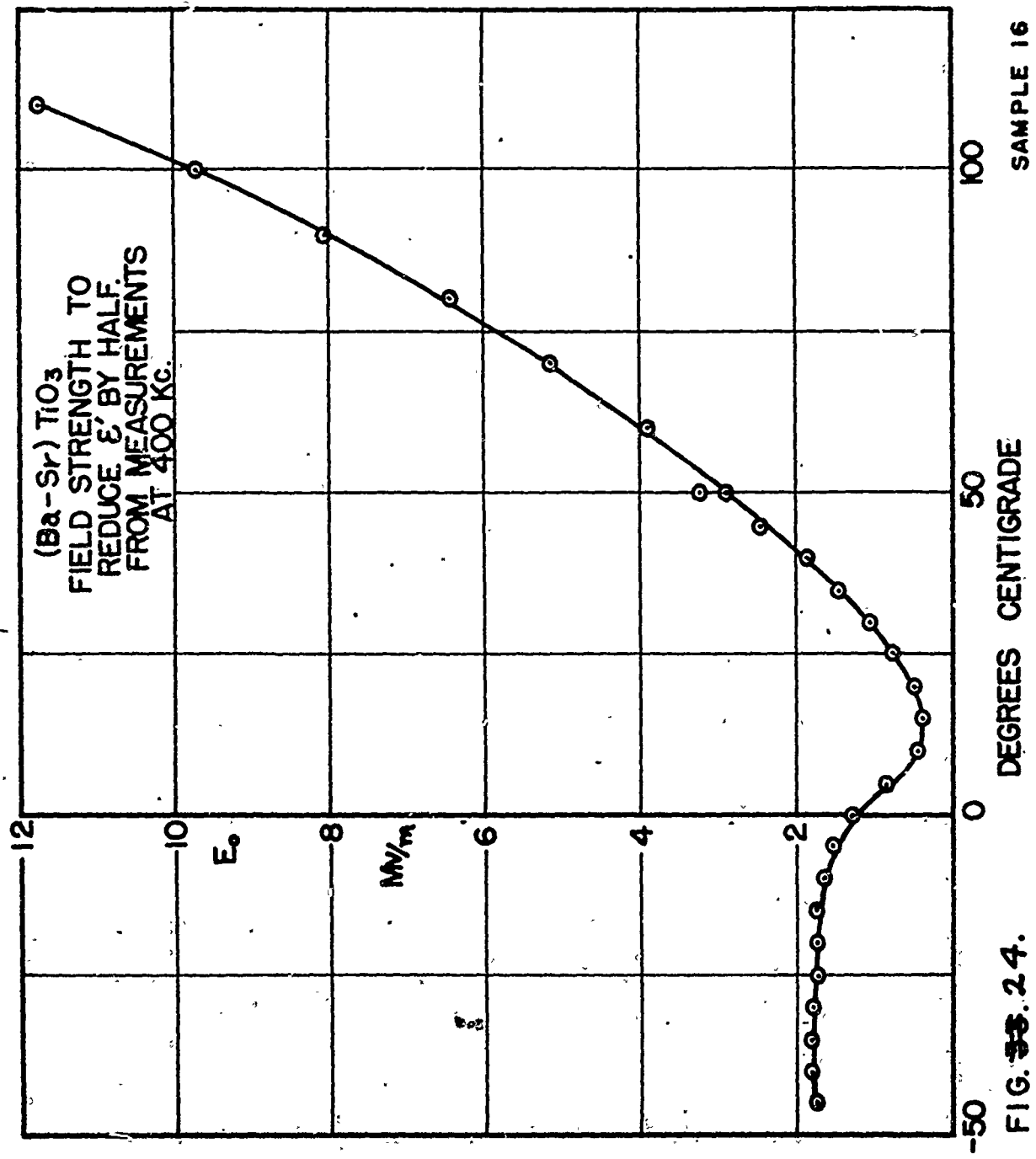


FIG. 3.2.4.

shows the field strength E_0 , which is required to reduce ϵ' to half its initial value, versus temperature. It is noted that the minimum occurs at a lower value and is broader than for pure barium titanate. A Curie-Weiss law, derived in Appendix B, is valid for E_0 above the Curie point. To check this we have shown $E_0^{2/3}$ versus temperature in fig. 25. The fact that the experimental data fall on a straight line above the Curie point indicates that the coefficient β in eq. IV-1 is a constant independent of temperature. Fig. 26 shows the increase in loss factor of the barium and strontium titanate mixture resulting from a-c bias, and indicates, as one would expect, that this phenomenon disappears above the Curie point.

3. Dielectric Constant and Loss Versus Frequency--

One of the most surprising results of our investigation was the extreme variation in dielectric constant and loss which we found in our samples of barium titanate as a function of frequency. Fig. 27, for example, shows the real component of capacitance of one of our samples versus frequency, while fig. 28 shows the corresponding imaginary or loss component of capacitance. The loss component is perhaps more instructive because it shows a peak corresponding to each resonance frequency. The situation is even more complicated than these figures indicate, however, because what appears in the figures as a simple resonance, for example at 500 Kc, is really a complex pattern with much finer detail than we have attempted

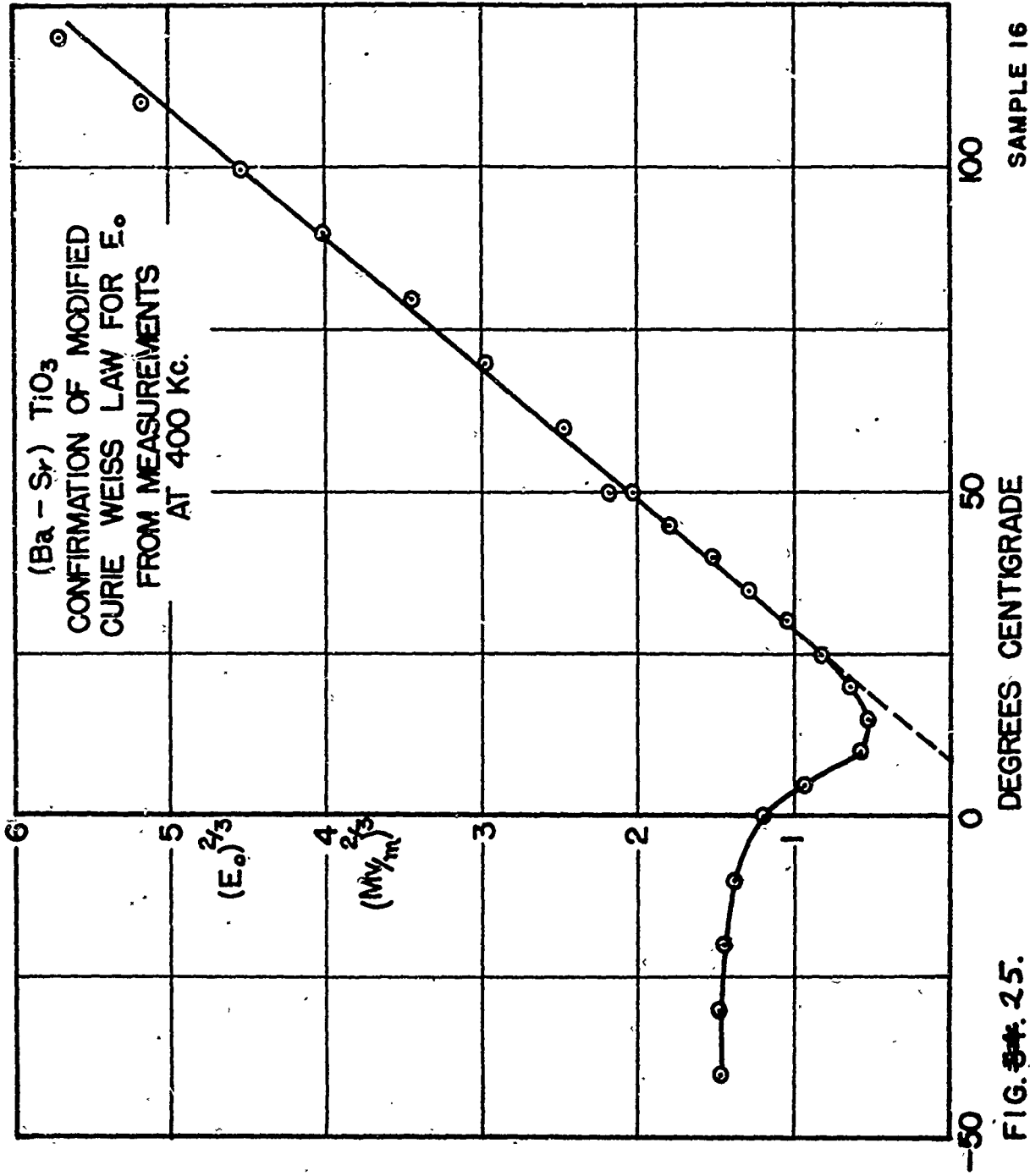


FIG. 25.

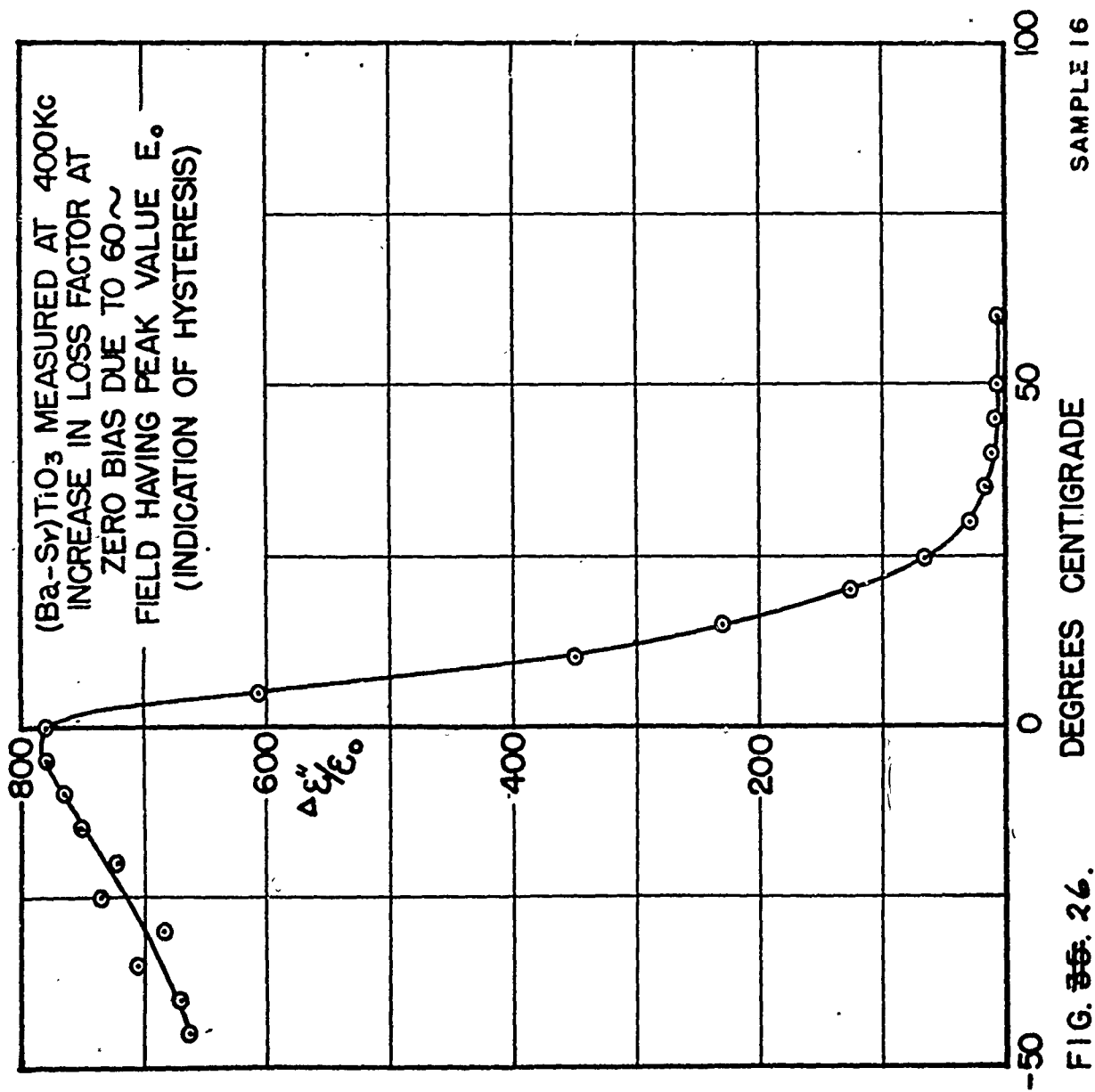
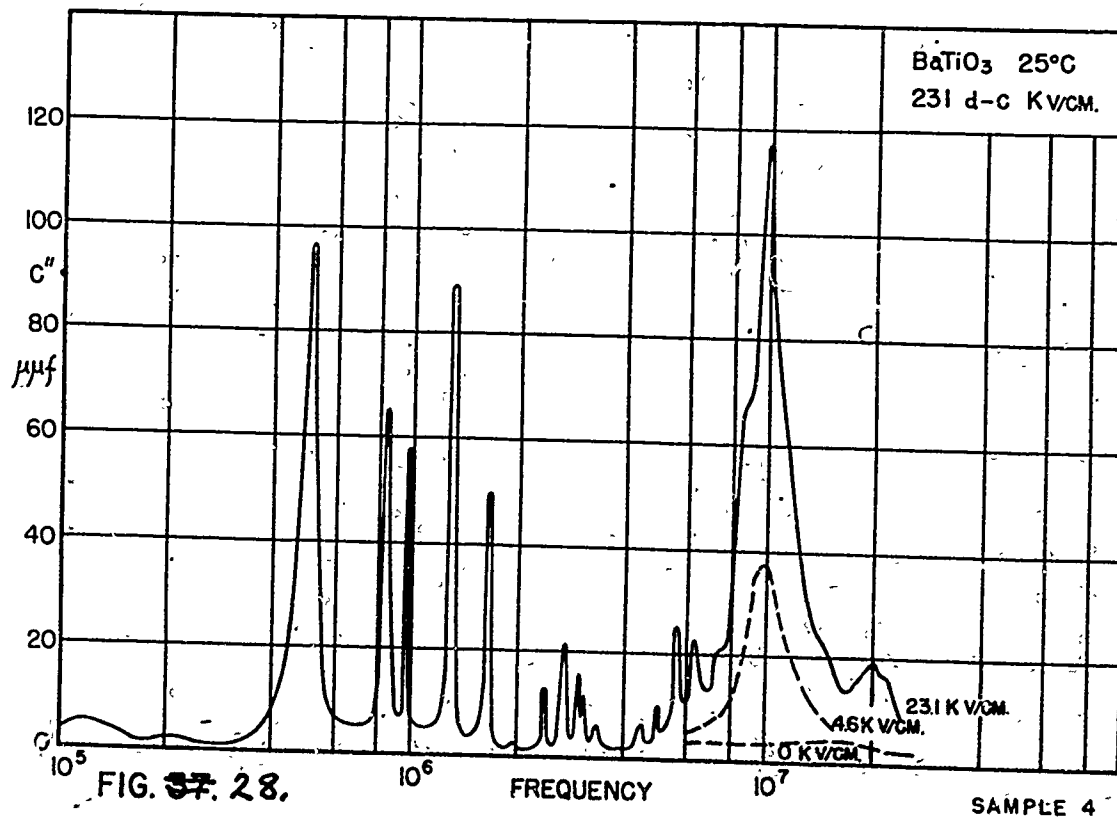
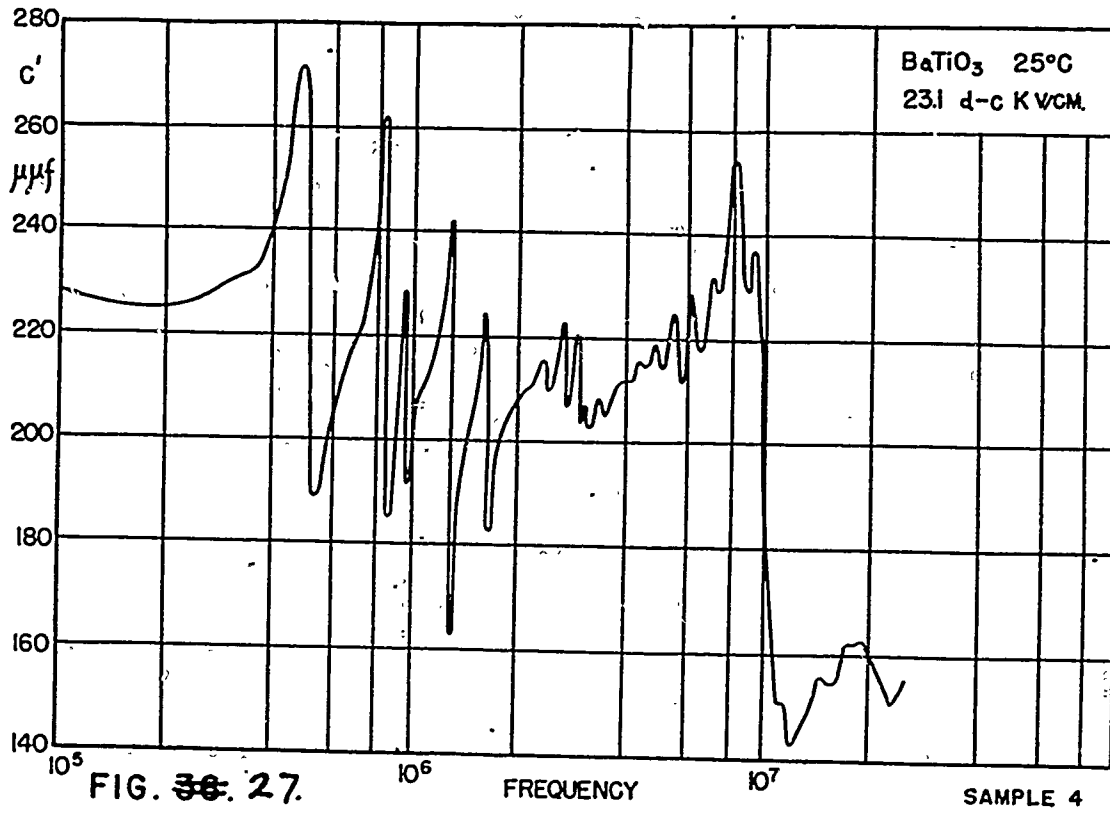


FIG. 26.



to measure. The above results were obtained with sample no. 4 which had a painted silver electrode on the back. Tests at different field strengths indicate that the resonance frequencies do not shift noticeably with field strength.

We found that these resonances could be observed only if the dielectric is polarized. In the absence of an electric field or any remanent polarization, the effect disappears completely. The variation of loss factor as a function of d-c field strength at one of the resonance frequencies is shown in fig. 11, which we have already discussed. This figure shows that the loss due to the remanent polarization, with no external field applied, can be very pronounced. As a matter of fact, the loss at a resonance frequency can be used as a very sensitive indication of remanent polarization.

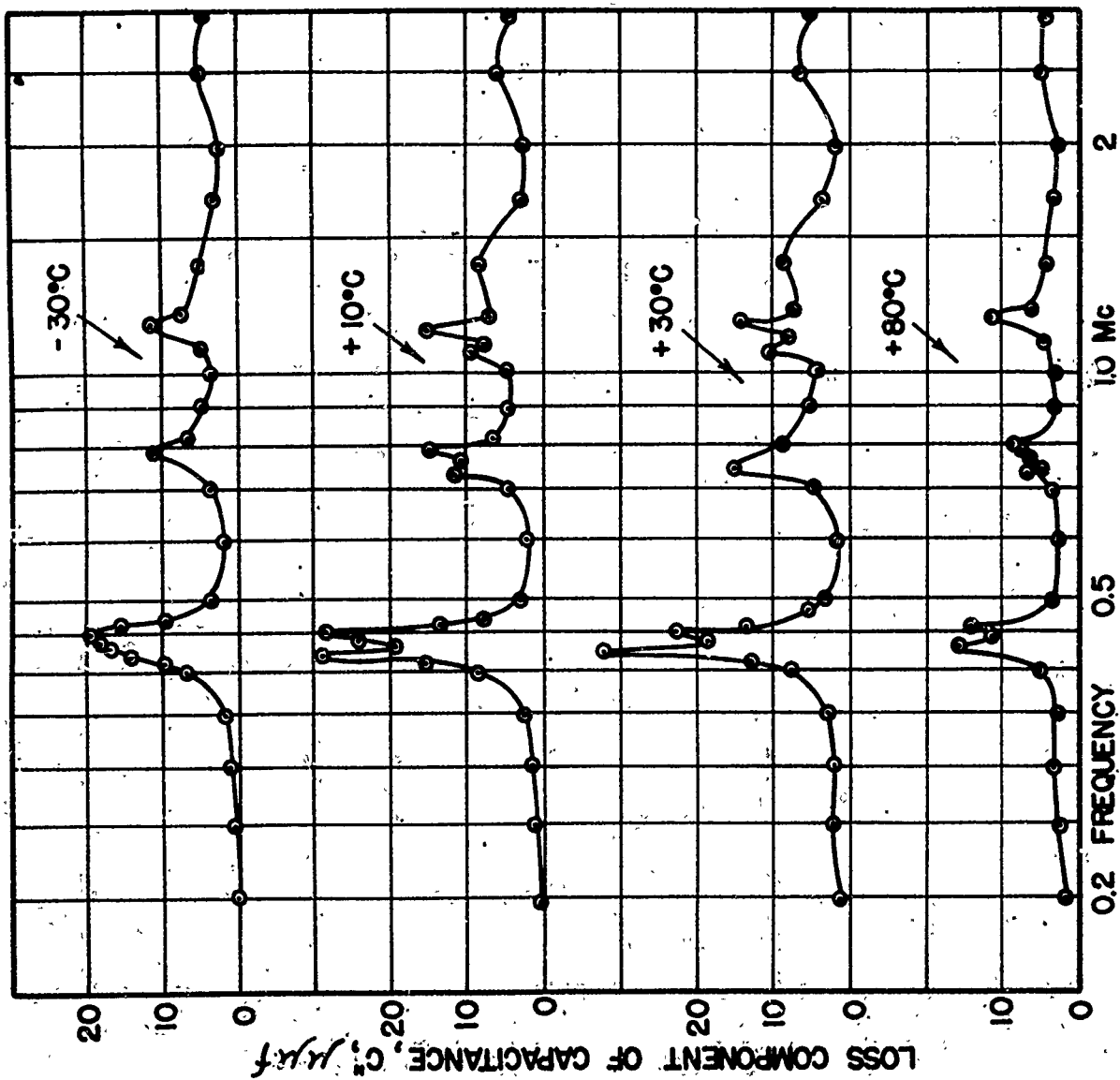
The next step was to study the effect of temperature on this resonance phenomenon. For this test sample no. 18 with a platinum foil electrode was used. The results are shown in fig. 29. The highest temperature used for this test had to be below the Curie point of barium titanate. The conductivity and possibility of breakdown at high temperature made it impossible to apply the high field strength for any length of time at higher temperatures. The resonances indicated in fig. 29 are all much more feeble than those in fig. 28. The resonance frequencies did not seem to change noticeably with temperature.

BaTiO₃
 THICKNESS .0036"
 FIRED ON PLATINUM
 FOIL .0005" THICK
 C₀ = .404 μ f
 D-C FIELD STRENGTH
 3.28 MV/cm (300V.)

TEMP. °C	C' μ f
-30	162
+10	204
+30	262
+80	268

SAMPLE 18

FIG. 38.29.



The results of a corresponding test of the barium-strontium titanate are shown in fig. 30. Here it was possible to make measurements at and above the Curie point. These measurements indicate that the resonance phenomena disappear above this point. Otherwise the results are not essentially different than those for barium titanate.

From the fact that the resonances are all so much more feeble for samples with the platinum foil electrodes, it was surmised that the resonances might be of a mechanical nature involving the whole sample in a natural vibrational mode and that the platinum might act as a damper which would reduce the Q of the mechanical resonator. The vibrations were assumed to be of a type having the direction of motion parallel to the flat surface of the disc. The resonance frequencies for vibrations of this type depend only on the radius of the disc, not on its thickness--which explains why we have observed resonances at about the same frequencies for samples of different thickness. To check this interpretation we performed the following experiment proposed by R.L. Kuhl.

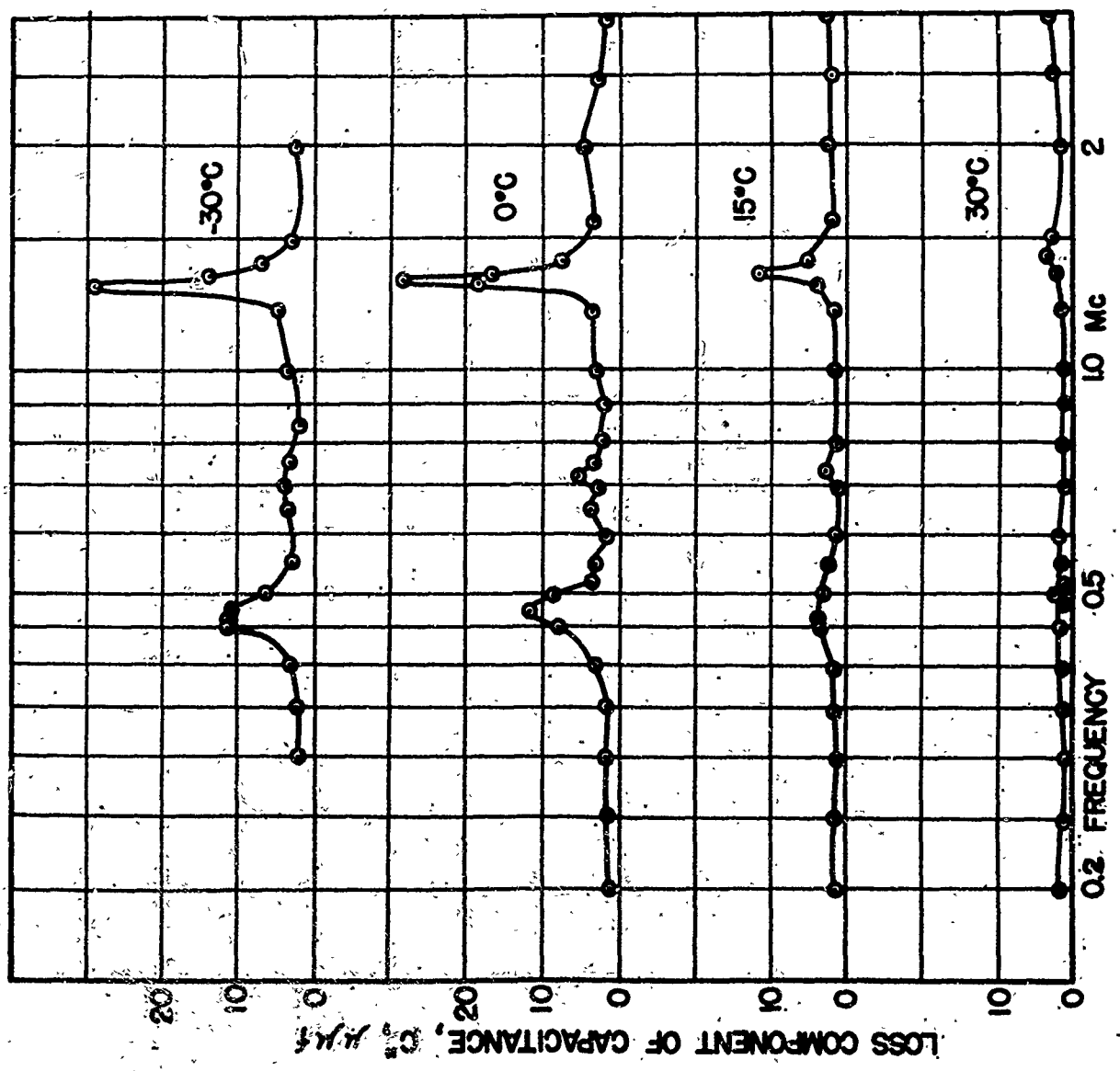
We measured the loss component of capacitance versus frequency of sample no. 9, which was originally of the same diameter as samples no. 4 and 5. The result of this test is shown in the top curve of fig. 31. Then we chipped pieces of ceramic away from the edge, thereby reducing the diameter without affecting in any way the part of the ceramic between

(Ba-Sr) TiO₃
 THICKNESS .0042"
 FIRED ON PLATINUM
 FOIL .0005" THICK
 C₀ = .282 μμf
 D-C FIELD STRENGTH
 2.81 MV/cm (300V)

TEMP. °C	C' μμf
-30	249
0	286
+15	370
+30	408

SAMPLE 16

FIG. 30.

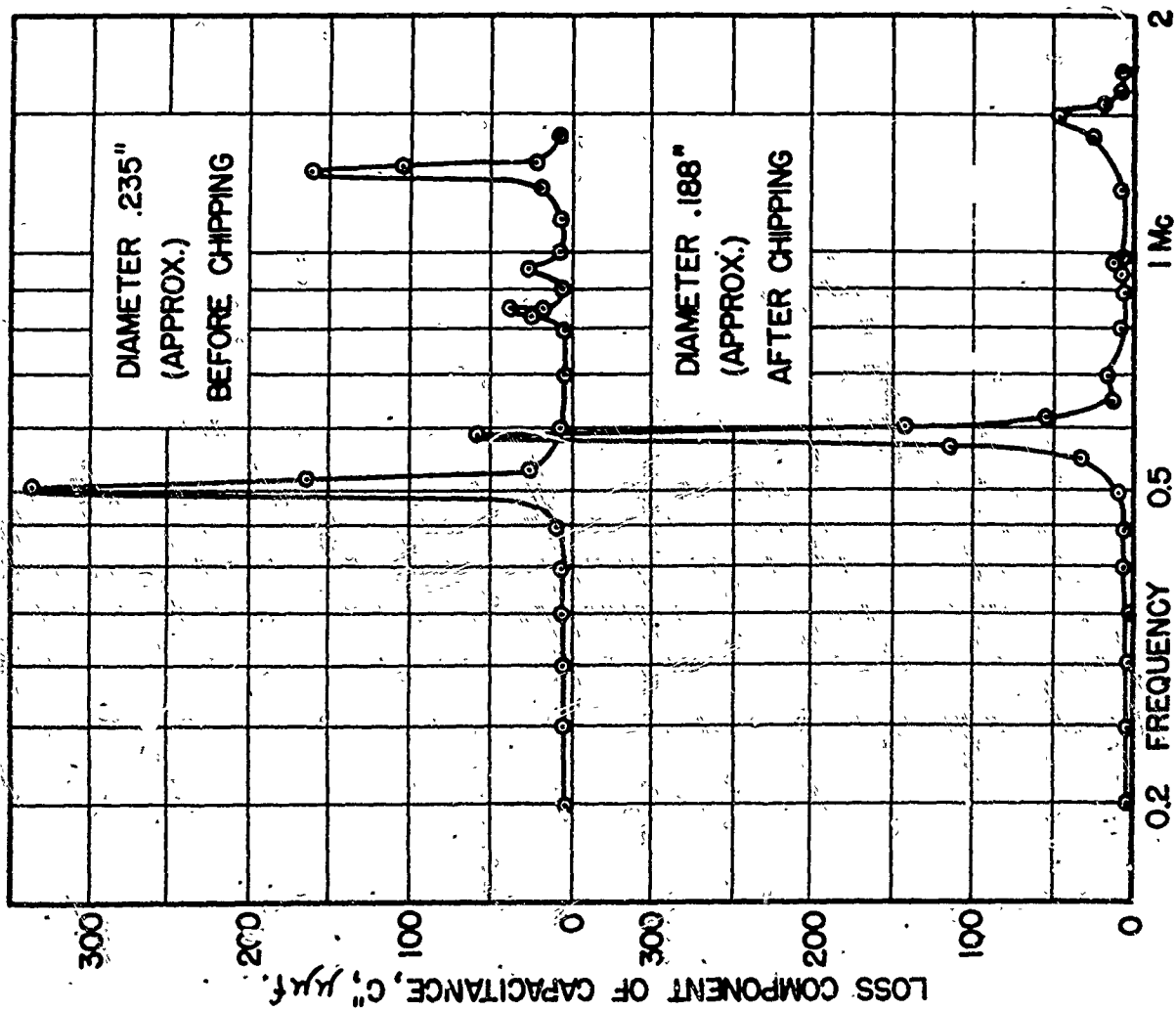


$BaTiO_3$
 THICKNESS .0080"
 SILVER PASTE ELECTRODES
 ELECTRODE THICKNESS
 .0033" TOTAL (APPROX.)
 D-C FIELD STRENGTH
 1.48 MV/m (300V.)

C' AT 300KG $\mu\mu f$
 BEFORE CHIPPING 315
 AFTER CHIPPING 306

SAMPLE 9

FIG. #31.



the electrodes. The loss component of sample no. 9 after chipping is shown by the lower curve of fig. 31. These curves indicate that the resonance frequencies have definitely changed as a result of chipping and that the resonance frequencies are roughly inversely proportional to the diameter. (The diameter has been measured with rather poor accuracy).

A further confirmation of the theory is obtained from a calculation of the natural frequencies of vibration of a circular plate. The ratio of the characteristic frequencies agrees very well with our experiment. The details of this calculation are given in Appendix C, which also shows that a reasonable value for Young's modulus can be derived from the experimental values of resonant frequency.

4. D-C Conductivity and Breakdown Strength—

The d-c conductivity and breakdown strength are additional factors which determine the usefulness of these dielectrics in circuit applications. We have had some difficulty in obtaining reliable data on these properties because very gradual changes over a period of time are involved. If a high field strength is applied continuously the resulting current, which is small to start with, apparently causes a steady deterioration in the dielectric so that the current increases with time. This is accompanied by a darkening of the dielectric, visible around the edge of the electrode. For example, sample no. 16 of barium-strontium titanate (thickness 0.0107 cm., effective

area $.052 \text{ cm.}^2$) was subjected to a field strength of 4 Mv/m at a temperature 50°C for a period of four days. Starting from an initial value of about $0.5 \mu\text{a}$, the current increased at a more or less constant rate of about $5 \mu\text{a}$ per day. After remaining with the voltage turned off for a week at room temperature (25 to 30°C) the sample was again heated to $+50^\circ\text{C}$ and the same field reapplied. The current was then only $11 \mu\text{a}$, indicating that the deterioration is not entirely permanent. This sample had previously been able to withstand field strengths up to 5 Mv/m at a temperature of 120°C for short periods of time.

A similar test on barium titanate, sample no. 5 (thickness $.0196 \text{ cm.}$, effective area $.104 \text{ cm.}^2$) at a field strength 2.5 Mv/m and a temperature 25°C indicated that the current reached a saturation value of about $0.1 \mu\text{a}$ taking about 8 hours to reach 70% of this value.

The breakdown strength of barium titanate is quoted at from 4 to 16 Mv/m and a maximum operating field strength of 8 Mv/m has been proposed.²⁸ Since the real danger from operation at high field strength is not so much a sudden breakdown as a slow deterioration, we are inclined to feel that the latter figure should be revised downward. We propose a maximum of 2.5 Mv/m for continuous operation and 4 Mv/m for the maximum instantaneous field strength. It would require life tests for a considerably longer period than we have attempted, however, to make sure that even

these proposed values of maximum field strength would be acceptable for engineering applications.

We have measured the conductivity of barium titanate at relatively weak fields allowing some time for the current to reach an equilibrium value in each case. The results are shown in fig. 32.

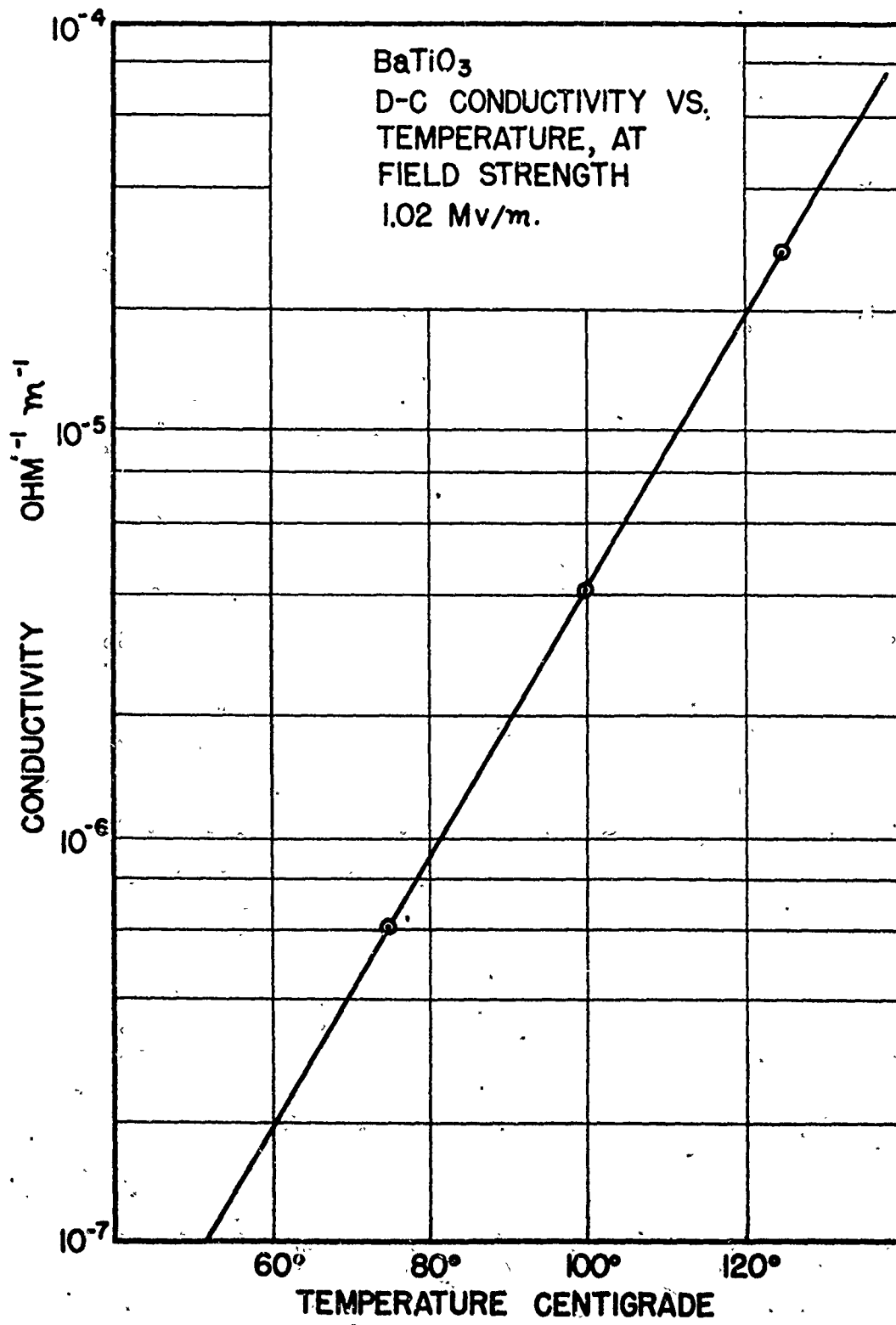


FIG. #. 32.

SAMPLE 5

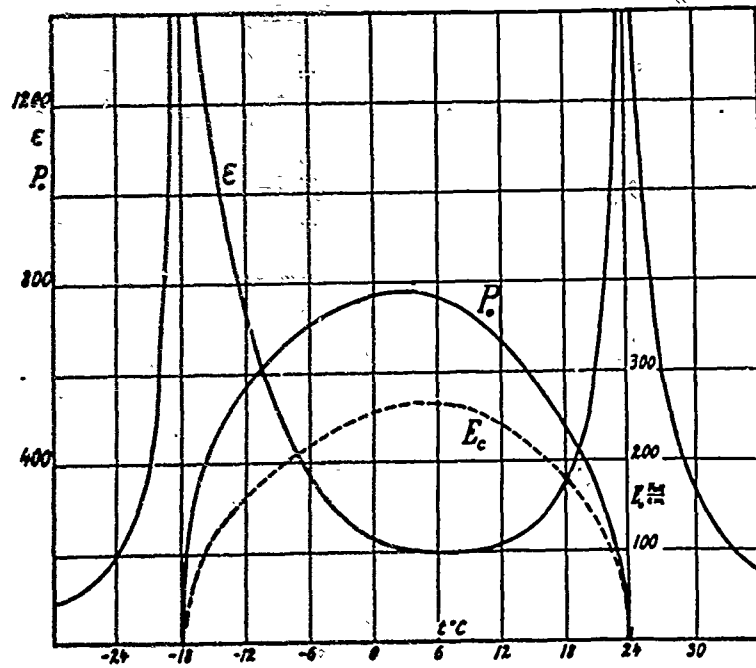
V. THEORY OF FERROELECTRIC DIELECTRICS

1. Introduction--

Until recently the only materials known to have significant nonlinear dielectric properties were certain piezoelectric crystals known as "Seignette-electrics", the prototype of this class being Rochelle salt (sel de Seignette),^{35(p.7)} These crystals are "ferroelectric" at certain temperatures in that the D versus E characteristics show hysteresis like the B versus H characteristics of iron. The titanate ceramics which we have studied are likewise ferroelectric, as we have already indicated. Therefore the significance of the results of our measurements can be fully appreciated only in comparison with the corresponding properties of Rochelle salt. Since Rochelle salt has been studied in greater detail, it is believed worth while to summarize at this point some of its pertinent dielectric properties, and to discuss some of the theories applicable to ferroelectric materials in general.

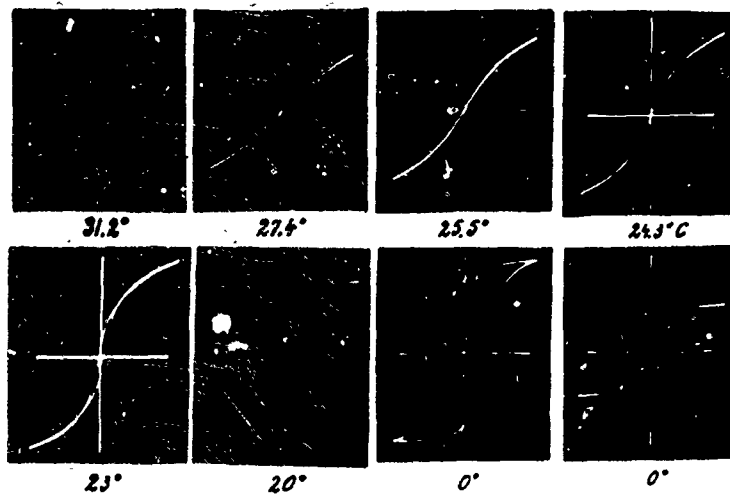
2. Some Dielectric Properties of Rochelle Salt--

Rochelle salt is characterized by an electric axis (normally designated the X -axis) in which direction anomalous dielectric properties are observed.^{35(p.510)} The dielectric constant in this direction varies enormously with temperature, field strength and strain. The dielectric constant of the free crystal at low field strengths is shown versus temperature in fig. 33.⁴¹ At temperatures between



Remanent polarization P_r , coercive force E_c and dielectric constant for small fields of Rochelle salt in the ferroelectric temperature range.

Fig. 33. (Mueller⁴¹)



Polarization curves of Rochelle salt. Upper row: for temperatures above the upper Curie point, lower row: Hysteresis loops for temperatures between the Curie points.

Fig. 34. (Mueller⁴¹)

-18°C and +23.7°C the dielectric constant of the free crystal in the frequency range 50 - 10,000 cycles/sec has a minimum of about 200, and rises at these limiting temperatures to very high values (> 1400). Between these temperatures Rochelle salt is ferroelectric, as evidenced by the hysteresis diagrams shown in the lower row in fig. 34. These diagrams were obtained by Mueller⁴¹ by the method of Sawyer and Tower.⁴²

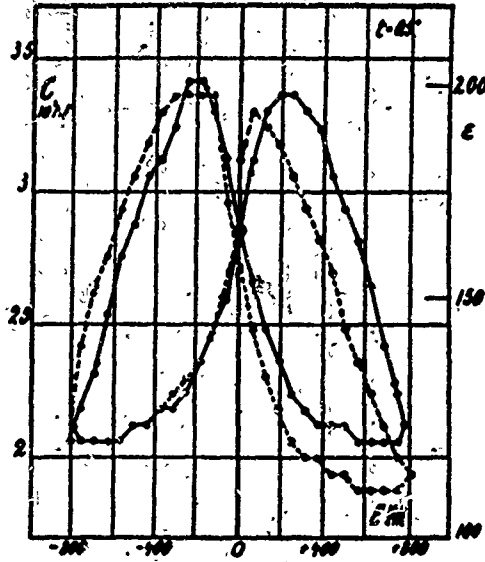
Fig. 35 shows a typical result in this range of temperature for the capacitance measured in an a-c bridge versus bias. This figure indicates hysteresis in that a different value of capacitance is measured at the same value of d-c voltage depending on whether the voltage is increasing or decreasing. The curves on the right side of the figure are apparently traversed in a clockwise direction and vice-versa on the other side.

At temperatures just below -18°C and just above +23.7°C the dielectric constant can be expressed by Curie-Weiss laws⁴¹ which are analogous to the corresponding law for the paramagnetic susceptibility of iron.⁵⁰ As a result of this analogy these temperatures are called Curie points. As an example, the Curie-Weiss law for the dielectric constant at low field strengths in the temperature range 24 to 32°C is

$$\frac{\epsilon_1}{\epsilon_0} = \frac{C}{T - T_0} \quad (V-1)$$

where

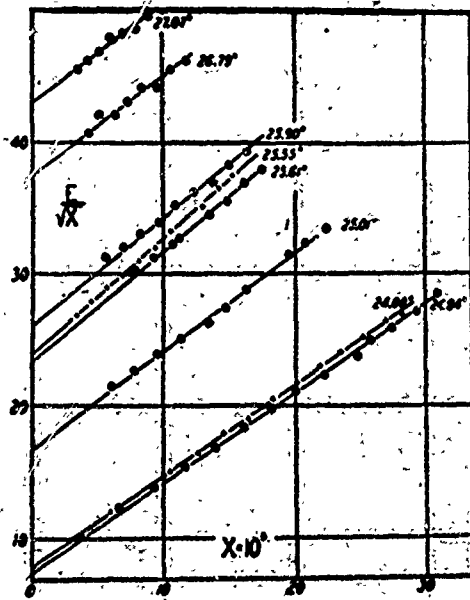
$$\begin{aligned} C &= 2240^\circ\text{K} \\ T &= \text{absolute temperature K} \\ T_0 &= 296.1^\circ\text{K} (23.0^\circ\text{C}) \\ \epsilon_0 &= \text{permittivity of free space} \end{aligned}$$



The reversible dielectric constant of Rochelle salt in the ferroelectric temperature range. The curve is the derivative of a hysteresis loop.

Fig. 35.

(Mueller⁴¹)



Verification of the law $\frac{E\epsilon - 1}{\epsilon} = M(t - t_0) + NX$, whereby $X = (n - \epsilon_2)/\epsilon_2$.

Fig. 36.

(Mueller⁴¹)

and from 32°C to 50°C this equation is valid with slightly different constants.

$$\begin{aligned} C &= 1710^{\circ}\text{K} \\ T_c &= 298.4^{\circ}\text{K} \quad (25.3^{\circ}\text{C}) \end{aligned}$$

a similar law is valid just below -18°C.

It is to be noted that the values of T_c are slightly different from the temperature (23.7°C) at which the dielectric constant reaches its maximum value. The value of T_c is generally called the Curie temperature. (to be distinguished here from the Curie "points" 23.7°C and -18°C).

Above the upper Curie point (23.7°C) the hysteresis disappears, or in other words the D vs. E characteristic follows the same curve ascending and descending. This is shown in the upper row of oscillograms in fig. 34. It is important to recognize that although hysteresis disappears, the relation of D vs. E is nevertheless still nonlinear.

In this range of temperature, Mueller's technique of measuring the incremental dielectric constant in an a-c bridge with a d-c biasing voltage is especially useful and gives reproducible results which show accurate agreement with the values predicted theoretically. The formula between field strength, dielectric constant and temperature derived by Mueller⁴⁰ is:

$$EX^{-1/2} = M(t - t_c) + NX \quad (V-2)$$

where

$$X = \frac{4\pi(\epsilon_1 - \epsilon)}{\epsilon_1 \epsilon}$$

ϵ_0 = permittivity at weak fields
 ϵ = permittivity at field strength E
 t = temperature Centigrade
 t_c = Curie temperature (23.0°C)
 M = 13.5
 N = 800
 (c.g.s. electrostatic units used in this equation)

The excellent agreement between this formula and the experimental results is shown in fig. 36.

Eq. V-2 is consistent with our eq. IV-2, which may be derived from it. However, Mueller's equation involves the Curie-Weiss law, which is not a necessary condition in the derivation of eq. IV-2. Furthermore, it is not immediately obvious from Mueller's equation that only two parameters are involved.

3. Domain Theory--

It is interesting to note that eq. V-1 would give negative values of ϵ , if extrapolated below the Curie point. However, a negative value of the static dielectric constant is never found in nature because such a dielectric would be inherently unstable. For example, an R-C circuit, with a condenser containing such a dielectric, would have transients with a positive exponential. Thus, instead of being in the unstable unpolarized state at temperatures below the Curie point, a Rochelle salt crystal is made up of a number of distinct domains each of which is spontaneously polarized in a direction either parallel or antiparallel to the X-axis.

The domain structure of Rochelle salt is well supported by experimental evidence. For example, by sprinkling

Burker's powder⁴⁵ on the surface of a heated crystal the oppositely charged regions corresponding to the domains become evident. From a study of the dust patterns, the size and shape of the domains can be ascertained. The domains tend to be in the form of laminae from 1 to 8 mm. thick in the Y direction and 1 cm. or more in extent parallel to X and Z.^{35(p.707)} Different tests on the same specimen give essentially the same pattern. Furthermore there is an electrical Barkhausen effect,⁴⁰ indicating discontinuous jumps in the process of polarization as the field is gradually increased.

The domain theory is useful in interpreting hysteresis and remanence. If the polarized domains are oriented in a random fashion, they tend to neutralize each other and no net polarization is observed externally. If, however, the domains are made to point in the same direction by applying an electric field, then when the field is removed the domains do not completely neutralize each other and a permanent state of electrification remains which is demonstrable as hysteresis or remanence.

4. Extrapolation of the Curie-Weiss Law Below the Upper Curie Point--

The nonlinear dielectric phenomena in the temperature range above the upper Curie point as stated in Mueller's eq. V-2 and confirmed by experiment can be derived, as we

shall show in Appendix B, from a relatively simple relation between the electric displacement D and the field strength E .

$$E = \alpha D + \beta D^3$$

where

$$\alpha = \frac{1}{\epsilon_1} = \frac{1}{\epsilon_0 C} (T - T_c) \quad (V-3)$$

$$\beta = \text{constant}$$

Eq. V-3 can be extrapolated slightly below the Curie point to determine values of the permittivity of a single domain, but it should be emphasized that the results so obtained do not necessarily agree accurately with observed values for an aggregate of domains. If $T < T_c$ then α is negative and the condition $D = 0$ is unstable, as we have indicated. However, there are now two other stable solutions for D when $E = 0$. These are

$$D = \pm \sqrt{\frac{-\alpha}{\beta}} \quad (V-4)$$

These solutions correspond to the spontaneous polarization with its direction either parallel or antiparallel to the X-axis. The reciprocal of the dielectric constant is

$$\frac{1}{\epsilon} = \frac{dE}{dD} = \alpha + 3\beta D^2 \quad (V-5)$$

And on substituting the above value of D one obtains

$$\frac{1}{\epsilon_1} = \alpha - 3\alpha$$

or

(V-6)

$$\epsilon_1 = \frac{-1}{2\alpha} = \frac{\epsilon_0 C}{2(T_c - T)}$$

Eq. V-6 thus expresses the Curie-Weiss law valid for temperatures slightly below the Curie point. This law is confirmed experimentally in the case of Rochelle salt and the value of C is the same as immediately above the Curie point.⁴⁰ However, the Curie temperature T_c in this case is about 24.8°C as compared to 23.0°C above the Curie point.

VI. CONCLUSIONS AND PROPOSED APPLICATIONS

1. General Conclusions--

We now consider the question of the suitability of barium titanate and barium-strontium titanate as nonlinear dielectrics for circuit applications. We have seen that barium titanate has two rather serious disadvantages at normal temperatures. In the first place, the losses are momentarily excessively high during part of the cycle of a low frequency biasing or modulating voltage. Secondly, the mechanical resonances cause severe fluctuations of the dielectric properties as a function of frequency. On the other hand, the dielectric constant is relatively constant over a wide range of temperature.

In the case of barium-strontium titanate these difficulties can be avoided by adjusting the composition so that the Curie point comes just below room temperature. Operation at a temperature just above the Curie point has the additional advantage that hysteresis is not found in this range of temperature. However, the initial dielectric constant and the field strength required to reduce it to half the initial value depend very critically on temperature in this range. Even so, the dependence of dielectric constant on temperature at a given field strength is not as critical as might be supposed, because the decrease in initial dielectric constant and the increase in the field

required to reduce it tend to compensate each other. The resulting variation of dielectric constant with field strength at different temperatures is shown in fig. 37, calculated from the data given in figs. 22 and 24.

We have shown that desirable nonlinear dielectric properties can only be found at temperatures above the Curie point. In this case the allowable temperature range is a fundamental limitation. If the temperature is too high, E_0 may be larger than the breakdown strength, in which case the dielectric constant is insensitive to the attainable electric fields. In order to compare the operating temperature ranges of different nonlinear dielectrics we arbitrarily set as an upper limit the temperature at which E_0 is equal to the maximum operating field strength, and as a lower limit, the Curie point. If the value 4 Mv/m is taken as the maximum field strength of barium-strontium titanate, the limiting temperatures are $T_{\min} = 15^\circ\text{C}$, $T_{\max} = 58.5^\circ\text{C}$. The corresponding temperature range for Rochelle salt can be calculated from Mueller's data.⁴⁰ If the maximum field strength for Rochelle salt is assumed to be 1 Mv/m the limiting temperatures are $T_{\min} = 23.7^\circ\text{C}$, $T_{\max} = 31.5^\circ\text{C}$. The value 1 Mv/m is chosen because it is the highest field strength used by Mueller.⁴⁰ According to these figures the barium-strontium titanate is a useful nonlinear dielectric over almost six times as great a range of temperature as Rochelle salt.

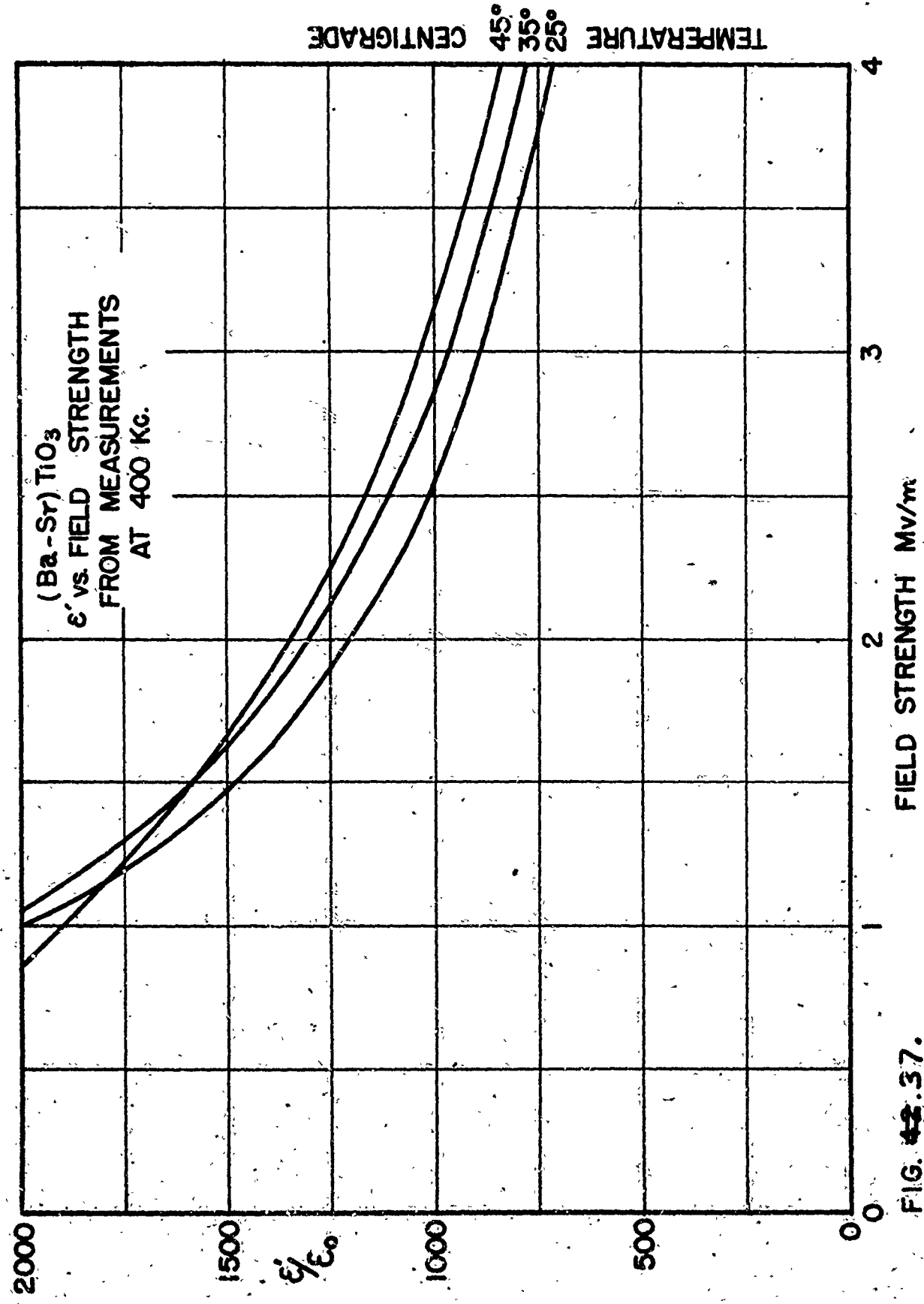


FIG. 42.37.

Furthermore Rochelle salt is piezoelectric in this range of temperature and will have electromechanical resonances, which are avoided in the ceramic.

From the experiment in which the resonance frequencies were shifted by chipping the edge of the sample, we conclude that these resonances are of a mechanical nature and that they must be caused by an interaction between the electric field and the mechanical deformation of the dielectric. In the most general sense, according to Cady,^{35(p.198)} the term "electrostriction" applies to any interaction phenomenon of this sort. According to the dictionary,⁵³ the term "piezoelectricity" is used only when electric charge can be generated as a result of pressure. Electrostriction is a common property of all materials, but, according to Cady,^{35(p.5)} only a few crystals are naturally piezoelectric. In fact no isotropic medium can be piezoelectric. However, some non-crystalline and polycrystalline substances can be made artificially piezoelectric by electrical polarization.^{35(p.233)} An "electret", for example, is piezoelectric.⁴³ Our measurements indicate that barium titanate, too, is piezoelectric at temperatures below the Curie point if it has either induced or remanent polarization. The piezoelectric effect is a disadvantage in some respects, as we have seen, but on the other hand there may be useful applications for barium titanate as a piezoelectric medium. We can not make any specific proposals, however, without quantitative data.

2. Miscellaneous Circuit Applications--

The first circuit to be considered is the oscillator shown in fig. 38. In this diagram there are two nonlinear condensers each designated C_1 and represented by a new characteristic symbol in order to distinguish them from conventional condensers. The inductances marked L_c are the usual choke coils and the condensers C_B are the usual by-pass or blocking condensers. When the circuit is oscillating properly, an a-c voltage V_1 appears across the inductance L_1 , so the a-c voltage across each condenser C_1 is $\frac{1}{2}V_1$. This voltage is small compared to the control bias V_0 which determines the effective value of C_1 in accordance with the curves shown in fig. 37.

The frequency of oscillation is determined by the inductance L_1 and the capacitance $\frac{1}{2}C_1$.

$$f = \frac{1}{2\pi \sqrt{\frac{1}{2}L_1 C_1}} \quad (\text{VI-1})$$

Thus if the capacitance can be changed by a ratio 2:1, the frequency can in this way be controlled over a range 1.4:1. The circuit shown in the figure with two equal condensers C_1 tends to reduce the even harmonics because the condensers operate in "push pull" as far as the oscillating circuit is concerned.

The use of a nonlinear Rochelle salt condenser to control the frequency of an oscillator was demonstrated at low frequency by Mueller in 1933.⁴⁰ Circuits operating on this principle could be used at higher frequencies to

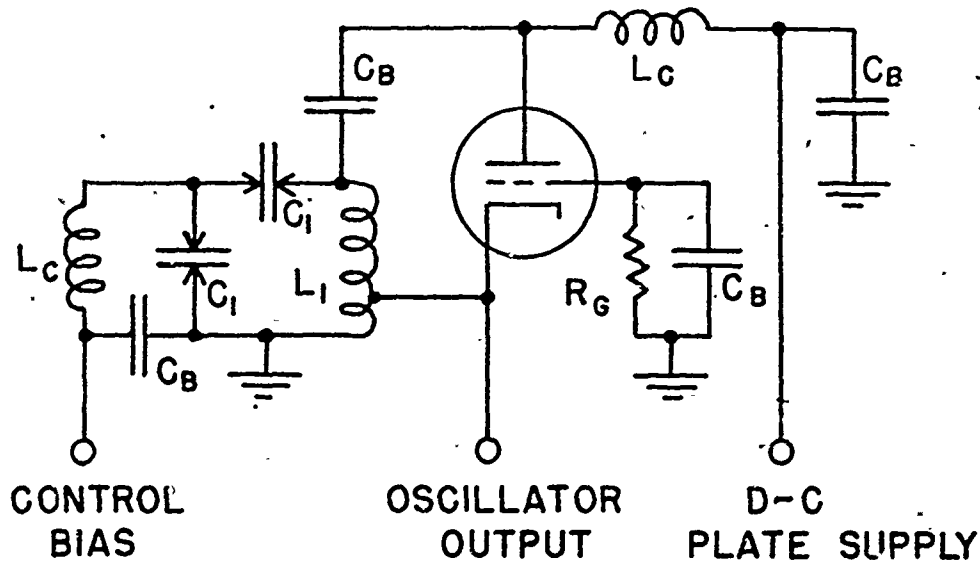


FIG. 38. FREQUENCY CONTROL BY NONLINEAR CONDENSERS.

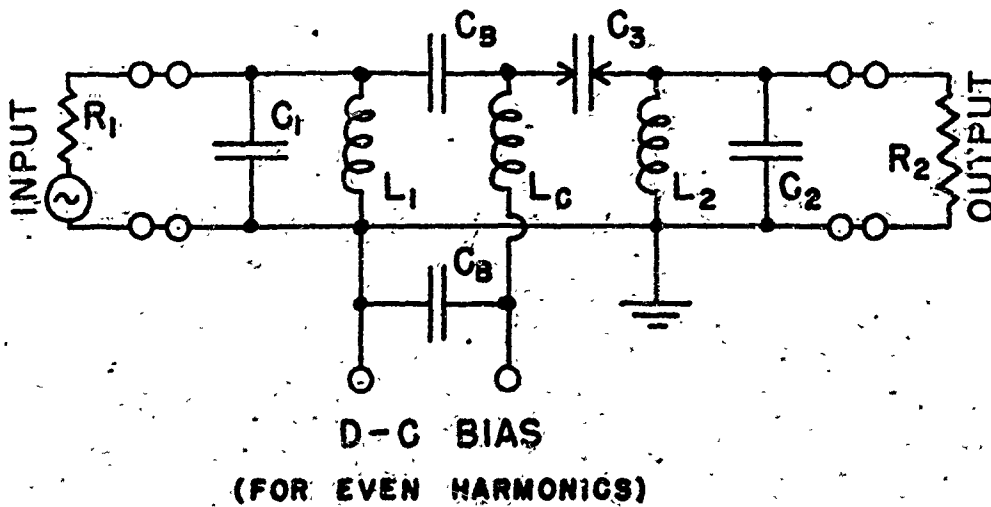


FIG. 39. NONLINEAR CONDENSER AS A HARMONIC GENERATOR.

replace the reactance tubes used for automatic frequency control and frequency modulation.⁵ Oscillators with various types of resistance-capacitance feedback using several nonlinear condensers controlled by a common bias could be operated in a similar manner over a wider range of frequency than the circuit shown in fig. 38 because the frequency of this type of oscillator is inversely proportional to the capacitance rather than to its square root. Circuits of this latter type might also find useful applications.³

The circuit shown in fig. 39 makes use of the nonlinear condenser to generate harmonics of the applied fundamental frequency. The values of L_1 and C_1 are tuned to resonance at the fundamental or input frequency, while L_2 and C_2 are tuned to the harmonic frequency. The field strength at the fundamental frequency is so high in condenser C_3 that IV-2 is not helpful in analyzing the operation of this circuit. Instead one would make use of the original relation between D and E given by eq. IV-1.

$$E = \alpha D + \beta D^3 \quad (\text{IV-1})$$

where

$$\alpha = \frac{1}{\epsilon_1}$$

$$\beta = \frac{16}{27} \frac{1}{\epsilon_1^3 E_0^2}$$

The detailed analysis of the operation of this circuit is a rather complex problem which could appropriately be solved on the differential analyzer. We have not done this,

but it is relatively easy to see that harmonics must be generated because the current and voltage cannot both be sinusoidal in a nonlinear circuit element if the amplitudes are high. It is also clear that the appropriate harmonic frequency, if generated, will be delivered efficiently to the output. Harmonic generation by means of a nonlinear condenser is very similar in principle to harmonic generation with a nonlinear inductor^{9,13} or with a nonlinear resistor.

Another circuit making use of nonlinear condensers is the amplitude modulator shown in fig. 40. In this circuit r-f power is introduced in the primary L_3 of a transformer with balanced secondary windings L_1 and L_2 . The secondaries are then connected to the output in opposition. A condenser, C_2 connected across the secondary winding L_2 , is tuned nearly to resonance while two nonlinear condensers C_1 are connected in series across L_1 . Thus if $\frac{1}{2}C_1 = C_2$, the voltages appearing across each secondary are equal and they cancel as far as the output is concerned. If C_1 changes by a small amount as a result of a change in d-c bias, or as a result of a small d-c signal voltage, the r-f voltage across winding L_1 will likewise change and will fail to cancel that across L_2 . The difference voltage appears at the output terminals. If a slowly varying or low frequency input signal is applied instead of d-c, then the circuit can operate as a balanced modulator, or if the d-c bias is shifted slightly the same circuit can operate as an unbalanced modulator in which case the envelope of the output voltage is a facsimile of the signal input.

The circuit shown in fig. 40 is just one example of the many ways of obtaining amplitude modulation with a nonlinear condenser. Our measuring circuit is another example, and can be used to demonstrate amplitude modulation by this means.

The amplitude modulator circuit has some interesting possibilities when its analogy to the magnetic amplifier^{1,20} is considered. Like the magnetic amplifier, this circuit can be used to control a relatively large amount of r-f power with a small amount of low frequency signal power, and the theoretical limit of power amplification is equal to the ratio of the r-f carrier frequency to the highest signal frequency to be amplified. It has the advantage that it can operate at higher frequencies than the magnetic amplifier. It might be useful, for example, as a modulator in telephone carrier systems where copper-oxide rectifiers⁴ are used at present. The dielectric modulator would in this case amplify the signal instead of attenuating it and would be scarcely any more complicated than the copper-oxide modulator.

The output of the amplitude modulator can be connected to a demodulator using a crystal rectifier, for example, if simple amplification is desired. This is indicated in fig. 41. This amplifier is an interesting novelty in that it uses no vacuum tubes although it does require a high frequency source of power. No practical applications for this circuit are envisaged at the present time.

3. Application as a Phase Modulator—

The modulation of frequency and amplitude has already been considered. To complete the picture, fig. 42 shows a circuit for phase modulation consisting of a ladder network with series capacitance and shunt inductance. The phase shift per section, which depends on the value of the capacitance, can be controlled by a d-c bias or by a low frequency modulating signal and the total phase shift of a network of N sections will be N times this value.

A linear relation between applied voltage and phase shift is an important object in the design of a circuit of this type. However the relation between dielectric constant and field strength in fig. 37 is far from linear. To correct for this we have chosen a particular ladder network which has the desired compensating nonlinear relation between capacitance and phase shift per section. The results which we will describe cannot be obtained with the series-L, shunt-C ladder network. At a frequency $\omega/2\pi$ the phase shift per section is given by^{18(p.194)}

$$\cos \phi = 1 - \frac{1}{2\omega^2 LC_1} = 1 - \frac{C_{1x}}{C_1} \quad (\text{VI-2})$$

where

$$C_{1x} = \frac{1}{2\omega^2 L} \quad (\text{VI-3})$$

The dimensions of the nonlinear condenser are chosen so that the capacitance is C_{1x} assuming that $\epsilon/\epsilon_0 = 1100$.

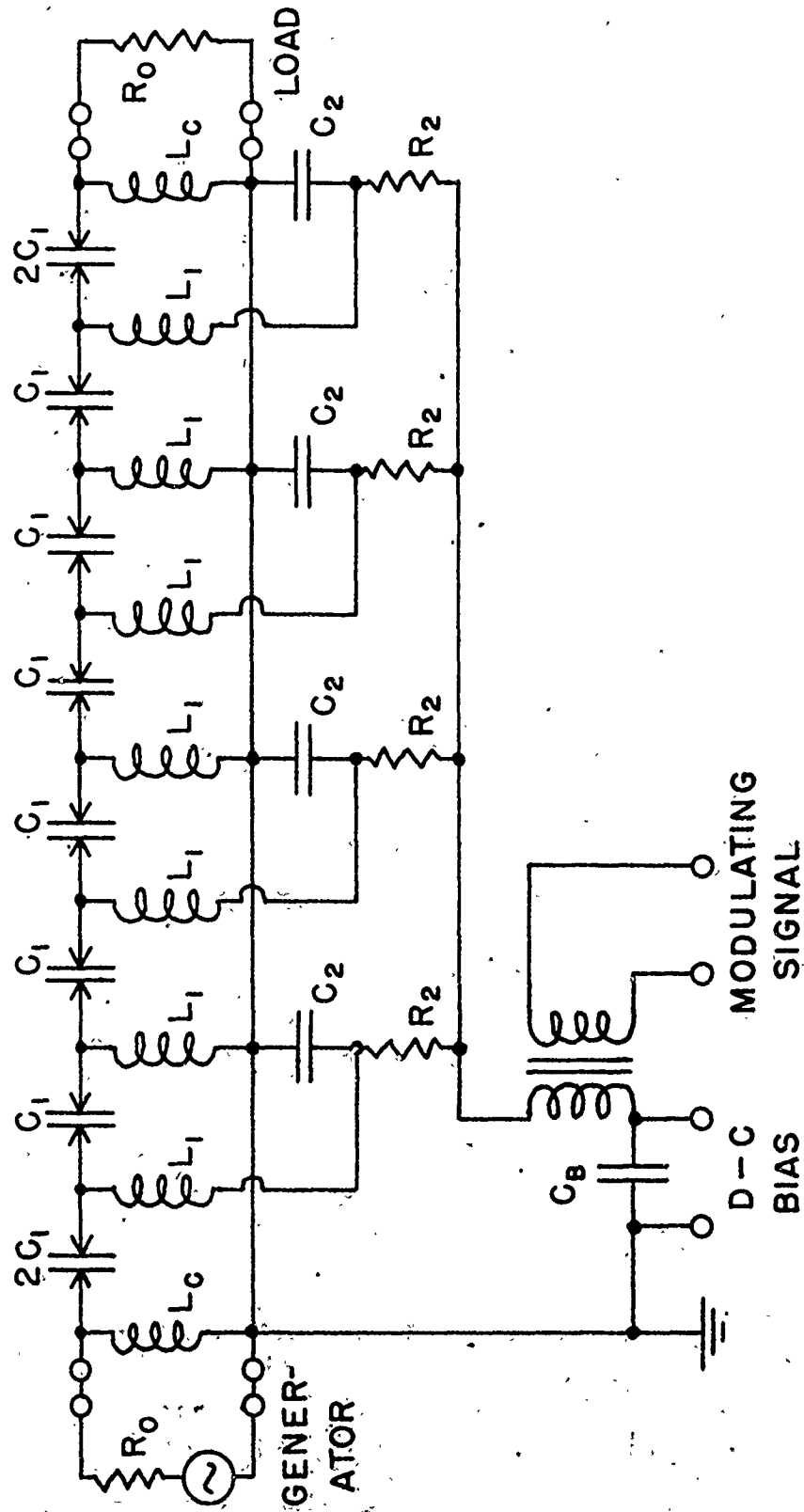


FIG. 42. ELECTRICALLY VARIABLE PHASE SHIFTER (7 SECTIONS)

In other words

$$\frac{C_{1x}}{C_1} = \frac{1100}{\epsilon'/\epsilon_0} \quad (\text{VI-4})$$

On the basis of eqs. VI-2 and VI-4 and the data given in fig. 37 we have calculated the phase shift per section of a ladder network and the results for different temperatures are shown in fig. 43. This figure indicates that the modulation characteristic is nearly a straight line and that each section can furnish phase modulation of at least ± 20 degrees. In each case the graphically calculated second harmonic distortion is less than two percent.

The characteristic impedance of the mid-series terminated network is^{18(p.194)}

$$R_t = \sqrt{\frac{L}{C_1} - \frac{1}{4\omega^2 C_1^2}} = \sqrt{\frac{L}{C_{1x}} \left[\frac{C_{1x}}{C_1} - \frac{1}{2} \left(\frac{C_{1x}}{C_1} \right)^2 \right]} \quad (\text{VI-5})$$

If $C_1 = C_{1x}$ we have

$$R_{tx} = \sqrt{\frac{L}{2C_{1x}}} \quad (\text{VI-6})$$

$$\frac{d}{dC_1} (R_t) = 0 \quad (\text{VI-7})$$

The latter result indicates that if the termination is matched to the characteristic impedance when $C_1 = C_{1x}$, i.e. $R_0 = R_{tx}$, then the reflection coefficient, $(R_0 - R_t)/(R_0 + R_t)$, will be very small even if C_1 changes slightly. It is important to prevent reflections in this network because a reflected signal can interfere with the directly transmitted

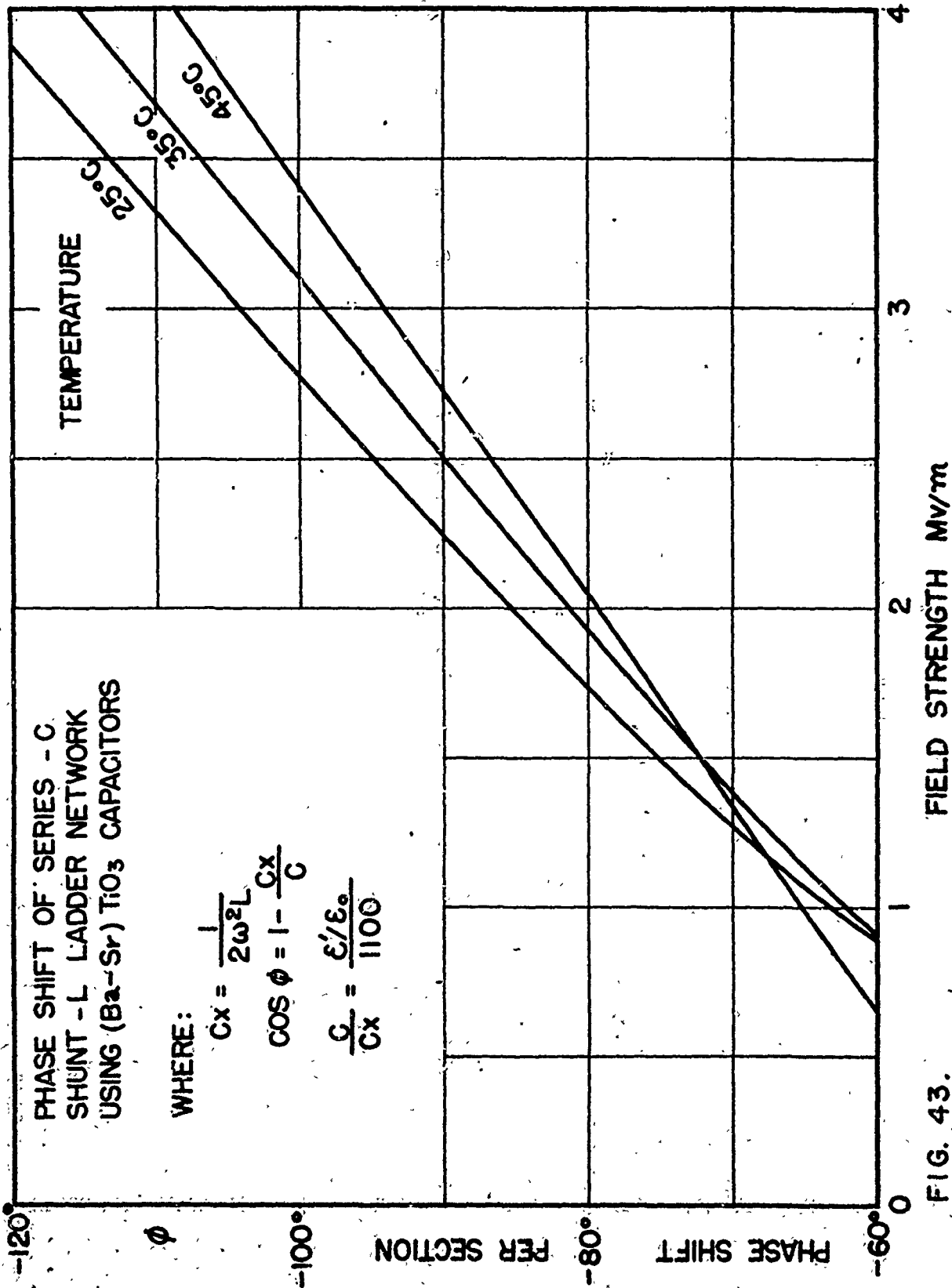


FIG. 43.

signal thereby causing spurious results. If R_0 and ω are specified, C_{1x} and L can be derived from them making use of eqs. VI-3 and VI-6.

$$L = \frac{R_0}{\omega}; \quad C_{1x} = \frac{1}{2\omega R_0} \quad (\text{VI-8})$$

It is important to bear in mind that a signal transmitted in this network suffers a delay and that the delay time per section is^{7(p.476)}

$$\tau = \frac{d\phi}{d\omega} \quad (\text{VI-9})$$

Noting that

$$\frac{d}{d\omega} \cos \phi = -\sin \phi \frac{d\phi}{d\omega} = \frac{1}{\omega^3 L C_1} \quad (\text{VI-10})$$

and putting $C_1 = C_{1x}$, we have

$$\tau_x = \frac{1}{\omega^3 L C_{1x}} = \frac{2}{\omega} \quad (\text{VI-11})$$

And the delay for N sections is N times this value.

It is clear that in order to modulate faithfully at high audio frequencies the ladder network should be so designed that the total delay is less than one-half cycle of the highest audio frequency with which it is to be modulated. If this frequency is $\omega_2/2\pi$ we have

$$\frac{2N}{\omega} \leq \frac{\pi}{\omega_2} \quad (\text{VI-12})$$

and the maximum permissible number of sections is

$$N_{\max} = \frac{\pi}{2} \cdot \frac{\omega}{\omega_2} \quad (\text{VI-13})$$

The ladder network is essentially a modulator of phase. When it forms the basis of a frequency modulation system it

is necessary to predistort the modulating signal so that the low frequencies are emphasized in inverse proportion to frequency.² This is done by the resistor and condenser R_2 and C_2 connected to every other section. This resistor and condenser also act as a filter to prevent undesired leakage of the carrier frequency. The time constant of the resistor and condenser determine a lower limit $\omega_1/2\pi$ to the modulating frequency.

$$\omega_1 = \frac{1}{R_2 C_2} \quad (\text{VI-14})$$

As a numerical example we will design a ladder network with the maximum number of sections for a carrier frequency of 500 Kc and for modulating frequencies from 50 to 20,000 cycles per second with a characteristic impedance of 1000 ohms.

$$\omega = \pi \times 10^6$$

$$\omega_1 = 2\pi \times 50$$

$$\omega_2 = 2\pi \times 20,000$$

$$R_0 = 1000$$

$$L = \frac{1000}{\pi \times 10^6} = 318 \mu\text{h.}$$

$$C_{1x} = \frac{1}{2\pi \times 10^6 \times 1000} = 159 \mu\text{f.}$$

$$N_{\text{max}} = \frac{\pi}{2} \frac{\pi \times 10^6}{2\pi \times 20,000} = 39$$

maximum phase shift:

$$\pm \frac{1}{18} \times 39 = \pm 2.17 \text{ cycles}$$

$$\text{let } C_2 = .01$$

$$\text{then } R_2 = \frac{10^6}{100\pi \times .01} = 318 \text{ K}\Omega$$

The advantages of this circuit become evident when one considers the usual methods of obtaining phase modulation in frequency-modulated transmitters. The Armstrong system of frequency-modulation, for example, makes use of phase modulation of a crystal controlled oscillator.^{2,8} This is done by combining the output of a balanced amplitude modulator with a carrier which is 90 degrees out of phase. This arrangement provides a maximum phase shift of about ± 25 degrees if the harmonic distortion is to be less than 5%. This is followed by a complicated system of frequency multipliers and heterodyne circuits in order to obtain a maximum phase deviation of about ± 100 to 200 cycles at the final output frequency.

In order to eliminate some of the frequency multiplication circuits an ingenious scheme has been worked out using a specially designed cathode ray tube¹⁵ having a circular sweep operating at the frequency of a crystal controlled oscillator. The diameter of the sweep circle is then controlled by the modulating signal. The phase modulated output is obtained from special spiral shaped electrodes on the screen. In this system the maximum phase shift is determined by the number of revolutions made by each spiral electrode. Tubes providing a phase shift of as high as ± 2.5 cycles have been described.

Another system for obtaining a large phase shift is based on pulse techniques.⁶ By this method phase shifts up to $\pm \frac{1}{4}$ cycle can be obtained with low distortion, using a carrier

frequency of 200 Kc.

In contrast with the alternative methods described above the ladder network has the advantages of complete flexibility in design and simplicity of operation. It introduces a relatively large amount of phase shift thereby greatly simplifying the design of frequency-modulation transmitters.

4. Summary of our Results--

a. We have derived a new general formula for the dielectric constant versus field strength in a nonlinear dielectric, making use of a new parameter--namely the critical field strength required to reduce the dielectric constant to half its original value at low field strength. Our measurements agree with this formula especially at temperatures above the Curie point. The critical field strength depends on temperature in the manner we have predicted in accordance with the Curie-Weiss laws.

b. We have devised a new measuring technique making it possible to determine the dielectric constant and loss factor at high frequency as a function of time during the cycle of a low-frequency biasing voltage. This type of measurement is necessary in order to predict the operation of a nonlinear condenser in a modulator circuit. We find that at temperatures above the Curie point the results of this method agree well with measurements made with d-c bias, but at temperatures below the Curie point they do not agree.

In fact the losses are found to be so much greater in the latter range of temperature with a-c bias, instead of d-c, that the general application of a nonlinear dielectric in modulator circuits is considered impractical under these conditions.

c. We have obtained extensive data on the dielectric properties of barium titanate and a mixture of barium and strontium titanates as a function of biasing field strength temperature and frequency. In addition to any theoretical value they may have, these data are especially pertinent to the design of modulator circuits.

d. In measuring the dielectric constant and loss versus frequency we have found a surprising series of resonance phenomena which occurred only during or after application of a moderately strong d-c field. Upon application of a weaker field of reversed polarity the resonances could be "erased". The resonance frequencies were found to be relatively independent of field strength and temperature except that they disappeared above the Curie point. The resonance frequencies were finally shown to correspond to the mechanical modes of vibration, a fact which proves the existence of a new electrostriction or piezoelectric phenomenon in barium titanate.

e. Our measuring circuit has served to demonstrate the application of a nonlinear condenser as an amplitude modulator.

f. We have worked out the details for the design of an original phase-modulator circuit suitable for use in a frequency-modulation transmitter. This method allows the direct modulation of phase over a range of several cycles without vacuum tubes, thus permitting a substantial simplification in the circuits now used in frequency-modulation transmitters.

APPENDIX A

Calculation of Edge Correction--

Edge corrections for various types of flat plate condensers have been worked out by Scott and Curtis.⁵² However it is not felt that their solutions are quite appropriate for the problem at hand, which involves a thin ceramic disc of thickness d with a very high dielectric constant. A small circular electrode of diameter D is fired on to the top, while the other electrode covers the entire bottom. If the electric field went straight across from the top electrode to the bottom with no fringing flux at the edge, the calculated capacitance would be

$$C_c = \epsilon \frac{\pi D^2}{4d} \quad (\text{A-1})$$

Instead, the capacitance is larger than this as a result of the fringing flux at the edge of the electrode. To account for this the upper electrode can be assigned an "effective" diameter D_e which, when substituted in the above formula gives the true capacitance.

$$C = \epsilon \frac{\pi D_e^2}{4d} \quad (\text{A-2})$$

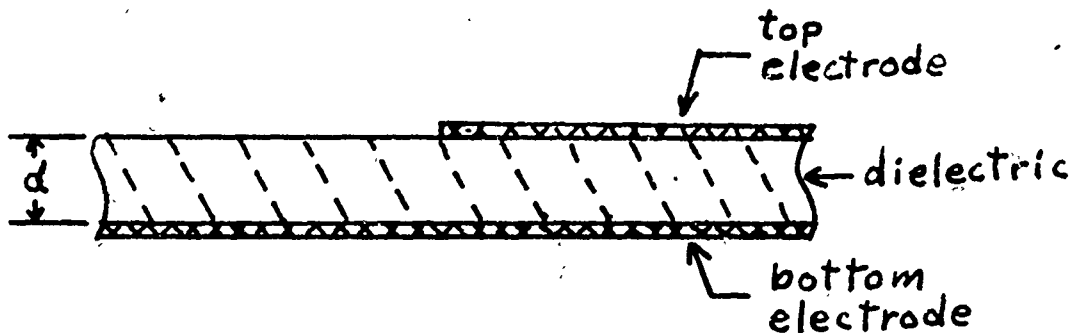
where

$$D_e = D + 2\delta \quad (\text{A-3})$$

δ is then called the edge correction.

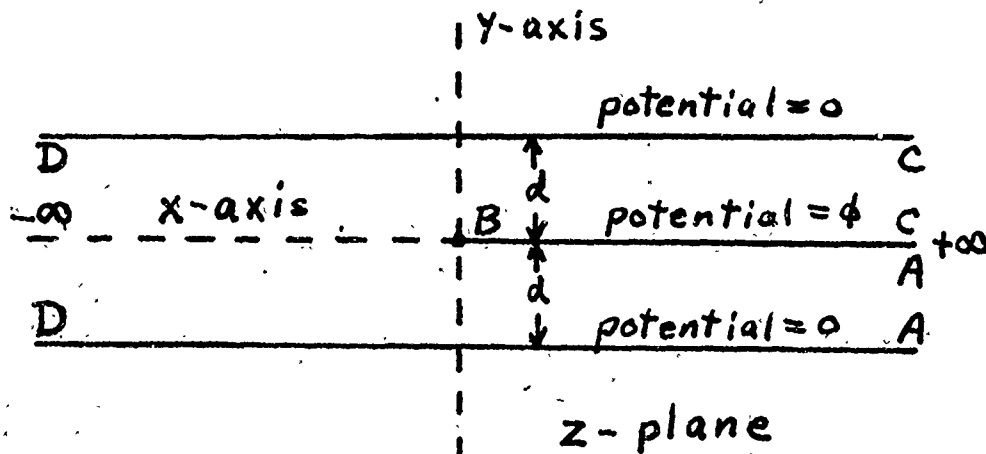
The edge correction should be about the same for a straight edge as for a curved edge, as long as the radius

of curvature $D/2$ is large compared to the thickness d . Therefore we shall calculate the edge correction for an infinitely long straight edge, a cross section of which is shown below.

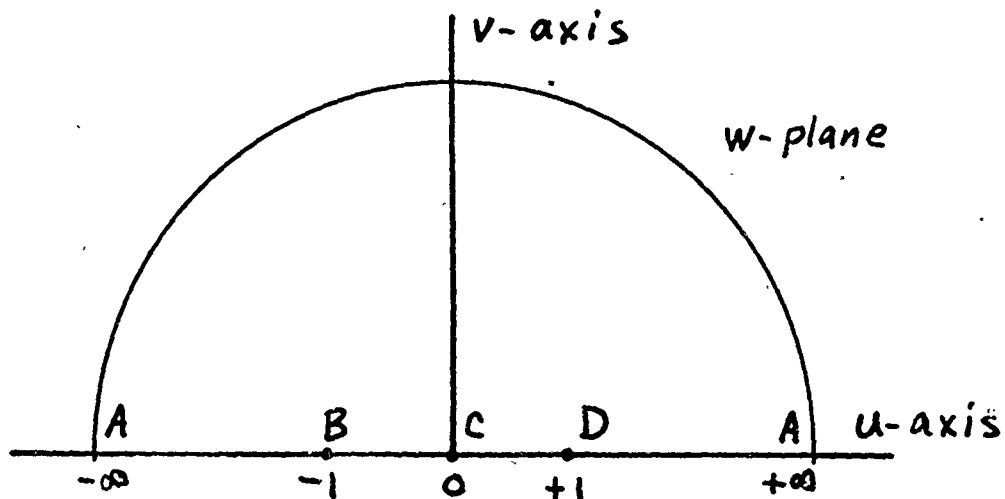


The electric field is perpendicular to the electrode surfaces, which are equipotentials. To find the boundary condition at the exposed surface of the dielectric we make use of the fact that the dielectric has a very high dielectric constant so that the electric flux tends to be confined to the dielectric and therefore is horizontal at the exposed surface.

By combining the field with its mirror image about the x -axis the solution of the problem is reduced to the following electrode configuration.



In order to solve this problem the above z-plane diagram is mapped on the upper half of the w-plane, indicated below, by means of a Schwarz-Christoffel transformation.^{51(p.125)}



The points A, B, C and D on the z-plane are to be transformed to the corresponding points on the w-plane. The differential equation for this transformation is derived in the usual manner.

$$\frac{dz}{dw} = \frac{K}{(w+1)^{-1} w^{+1} (w-1)^{+1}} = K \frac{w+1}{w(w-1)} \quad (\text{A-4})$$

where K is a scale constant determined below.

$$\int_{\infty+i0}^{\infty+id} dz = id = K \int_{\infty}^0 \frac{w+1}{w(w-1)} dw = \pi i K$$

$$\text{or } K = \frac{d}{\pi} \quad (\text{A-5})$$

The solution of eq. A-4 is

$$z = K \log \left[\frac{(w-1)^2}{-w} \right] + C \quad (\text{A-6})$$

$$= \frac{d}{\pi} \log \left[\frac{(w-1)^2}{-w} \right] + C$$

where C is the constant of integration, determined as follows.

$$z = 0, \text{ when } w = -1$$

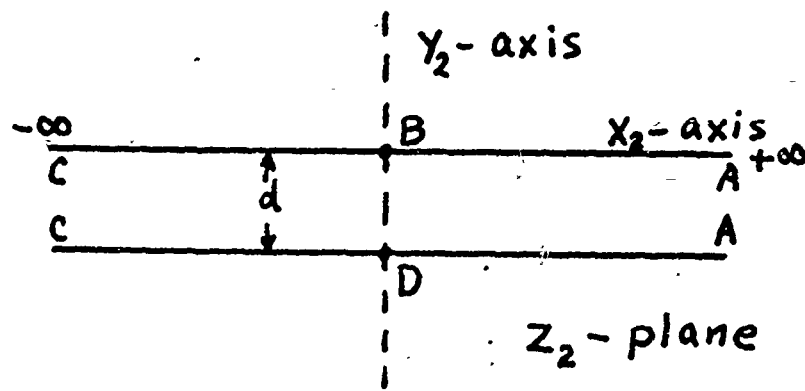
$$0 = \frac{d}{\pi} \log 4 + C \quad (\text{A-7})$$

$$C = -\frac{d}{\pi} \log 4$$

For large values of w ($w \gg 1$) eq. A-6 may be simplified to

$$z = \frac{d}{\pi} \log(-w) - \frac{d}{\pi} \log 4 \quad (\text{A-8})$$

A parallel-plane condenser can be mapped on the same w -plane.



In this case the transformation equation is

$$\frac{dz_2}{dw} = \frac{K}{w} ; z_2 = K \log(-w) + C_2 \quad (\text{A-9})$$

$$\int_{-\infty - i0}^{-\infty - id} dz_2 = -id = K \int_{-\infty}^{-\infty} \frac{dw}{w} = -\pi i K$$

$$\text{or } K = \frac{d}{\pi}$$

(A-10)

if $z_2 = 0$ when $w = -1$, then $C_2 = 0$.

$$z_2 = \frac{d}{\pi} \log (-w) \quad (\text{A-11})$$

Comparing A-11 with A-8 we see that for large values of w , z differs from z_2 by a constant value, $\frac{d}{\pi} \log 4$. Therefore it follows that this value is the edge correction.

$$\delta = d \frac{\log 4}{\pi} = .441 d \quad (\text{A-12})$$

And the final expression for the edge correction is

$$D_e = D + 2\delta = D + .882 d \quad (\text{A-13})$$

APPENDIX B

Dependence of \mathcal{E} on Field Strength in a Nonlinear Dielectric--

The electric displacement D is normally an odd function of the field strength E in any nonlinear isotropic dielectric which does not have hysteresis.

$$D = aE + bE^3 + cE^5 + \dots \quad (\text{B-1})$$

where a , b & c are appropriate constants. Alternatively E may be expressed as an odd-power series in D .

$$E = \alpha D + \beta D^3 + \gamma D^5 + \dots \quad (\text{B-2})$$

The dielectrics which we have to consider tend to become saturated at high field strengths. In other words E increases faster than D . This observation indicates that series (2) should converge more rapidly than series (1) at high field strengths (E). As a matter of fact, series (2) converges so rapidly that all our experimental results are consistent with the series approximation which retains only the first two terms.

$$E = \alpha D + \beta D^3 \quad (\text{B-3})$$

For very small values of D , the relation between D and E is linear and their ratio defines the initial permittivity ϵ_1 for low field strength.

$$E = \alpha D = \frac{1}{\epsilon_1} D$$

$$\text{or } \alpha = \frac{1}{\epsilon_1}$$

(B-4)

Substituting this value of α in eq. B-3, we have

$$E = \frac{1}{\epsilon_1} D + \beta D^3 \quad (B-5)$$

The general permittivity is defined as the slope of the D versus E characteristic

$$\epsilon = \frac{dD}{dE}, \text{ or } \frac{1}{\epsilon} = \frac{dE}{dD} \quad (B-6)$$

then

$$\frac{1}{\epsilon} = \frac{1}{\epsilon_1} + 3\beta D^2 \quad (B-7)$$

Solving eq. B-7 for D and putting the result in eq. B-5 gives

$$\frac{E}{E_0} = \frac{1}{4} \sqrt{\frac{\epsilon_1}{\epsilon} - 1} \left(\frac{\epsilon_1}{\epsilon} + 2 \right) \quad (B-8A)$$

where

$$E_0 = \frac{4}{(3\epsilon_1)^{3/2} \beta^{1/2}} = 4 \left(\frac{\alpha}{3} \right)^{3/2} \beta^{-1/2} \quad (B-8B)$$

To determine E_0 as a function of temperature we may substitute the value of ϵ_1 given by the Curie-Weiss law (eq. I-1 or V-1). Then

$$E_0 = \frac{4}{(3\epsilon_0 C)^{3/2} \beta^{1/2}} (T - T_c)^{3/2} \quad (B-9)$$

Experimentally we find that the relation between E_0 and temperature is

$$E_0 = K(T - T_c)^{3/2} \quad (B-10)$$

where K is a constant. Thus we conclude that β is independent of temperature while α has a simple zero at the Curie point.

The appropriate values of C and T_c in degrees Kelvin and K in megavolts per meter per degree^{3/2} for barium-strontium titanate and Rochelle salt and several other crystals are listed in Table II for comparison.

Table II--Curie-Weiss Law Constants

<u>Material</u>	<u>T_c</u>	<u>C</u>	<u>K</u>
(Ba-Sr)TiO ₃	281	88,000	.0112
Rochelle salt ⁴¹	296	2,240	.0405
KH ₂ PO ₄ ³⁴	115	3,600	
KH ₂ ASO ₄ ³⁴	91	2,600	
Iron ⁵⁰	1029	0.4	

APPENDIX C

Vibrational Modes of a Circular Plate--

The natural frequencies of vibration of a circular plate in which the motion is parallel to the surface have been calculated by Petrzilka⁴⁷ and reported by Schmidt.⁴⁸ Only the modes with circular symmetry have been calculated. The frequencies of compressional vibrations in this case are given by

$$f_v = \frac{\rho_v}{2\pi a} \sqrt{\frac{Y}{\rho_0 (1 - \sigma^2)}} \quad (C-1)$$

where a = radius

Y = Young's modulus

σ = Poisson's ratio

ρ_0 = density

and ρ_v is the v -th root of the following equation:

$$\rho J_0(\rho) - (1 - \sigma) J_1(\rho) = 0 \quad (C-2)$$

If the value $\sigma = 0.3$ is assumed, the roots are:

$$\rho_1 = 2.05 \qquad \rho_4 = 11.73$$

$$\rho_2 = 5.39 \qquad \rho_5 = 14.88$$

$$\rho_3 = 8.57$$

The values of the roots are relatively independent of the value of σ . For example if $\sigma = .258$, only the first two are affected.

$$\rho_1 = 2.02, \qquad \rho_2 = 5.38$$

Since the ratio of the frequency of the first overtone having radial symmetry to that of the fundamental is relatively independent of the value of σ , we will use the value $\sigma = 0.3$, which is an average value for most materials. In this case the frequency ratio is $\rho_2/\rho_1 = 2.63$. In fig. 31 (top) the ratio of the resonance frequencies is $1.26/0.50 = 2.52$. The relatively weak resonances at .84 and .95 Mc are assumed to correspond to modes of vibration that do not have radial symmetry. Considering that the resonance frequencies must be influenced somewhat by the mass of the silver electrodes, which are several thousandths of an inch thick, and the oil bath, the agreement between theory and experiment is very encouraging.

If the above interpretation is correct and one assumes the following values,

$$\sigma = 0.3$$

$$\rho_2 = 4.7$$

$$a = 0.30$$

$$f_1 = 0.50 \times 10^6$$

$$\rho_1 = 2.05,$$

then Young's modulus can be determined from eq. C-1. The result of this calculation is $Y = 9 \times 10^{11}$ dynes/cm². The value of Y calculated in this manner is relatively independent of the value chosen for σ . The result obtained above is within the range of Y for electrical porcelains listed in the International Critical Tables (average 6 to 10 x 10¹¹ dynes/cm²).

BIBLIOGRAPHYNonlinear Circuits and Engineering Applications

1. Alexanderson, E.F.W.: A Magnetic Amplifier for Radio Telephony, Proc. I.R.E., v. 4, pp. 101-129, April 1916.
2. Armstrong, E.H.: A Method of Reducing Disturbances in Radio Signaling by a System of Frequency Modulation, Proc. I.R.E., v.24, pp.689-740, May 1936.
3. Artzt, M.: Frequency Modulation of Resistance-Capacitance Oscillators, Proc. I.R.E., v. 32, pp. 409-414, July 1944.
4. Caruthers, R.S.: Copper Oxide Modulators in Carrier Telephone Systems, Trans. A.I.E.E., v. 58, pp. 253-259, June 1939.
5. Crosby, M.G.: Reactance-Tube Frequency Modulators, R.C.A. Rev., v.5, pp. 89-96, July 1940.
6. Gordon, J.F.: A New Angular-Velocity-Modulation System Employing Pulse Techniques, Proc. I.R.E., v. 34, pp. 328-334, June 1946.
7. Guillemin, E.A.: Communication Networks, John Wiley & Sons, Inc., 1935.
8. Jaffe, D.L.: Armstrong's Frequency Modulator, Proc. I.R.E. v. 26, pp. 475-481, April 1938.
9. Joly, M.: Sur des Transformateurs Statiques de Frequence, Comptes Rendus, v. 152, pp. 699-702, Mar. 1911.

10. Kuhn, L.: *Über Ein Neues Radiotelephonisches System*, Jahrb. d. Draht. Tel., v. 9, pp. 502-534, 1915.
11. Mass. Inst. of Tech., E.E. Dept. Staff: *Electric Circuits*, John Wiley & Sons, Inc., 1943.
12. McEachron, K.B.: *Thyrrite: A New Material for Lightning Arrestors*, Gen. Elec. Rev., v. 33, pp. 92-99, Feb. 1930.
13. Peterson, E., J.M. Manley & L.R. Wrathall: *Magnetic Generation of a Group of Harmonics*, Elect. Eng., v. 56, pp. 995-1001, Aug. 1937.
14. Peterson, L.C. & F.B. Llewellyn: *The Performance and Measurement of Mixers in Terms of Linear Network Theory*, Proc. I.R.E., v. 33, pp. 458-476, July 1945.
15. Shelby, R.E.: *A Cathode-Ray Frequency Modulation Generator*, Electronics, v.13, pp. 14-18, Feb. 1940.
16. Suits, C.G.: *Non-Linear Circuits for Relay Applications*, Elect. Eng., v. L, pp. 963-964, 1931.
17. Suits, C.G.: *Non-Linear Circuits Applied to Relays*, Elect. Eng., v. 52, pp. 244-246, 1933.
18. Terman, F.E.: *Radio Engineers' Handbook*, McGraw-Hill Book Co., 1943.
19. Way, K.J.: *Voltage Regulators Using Magnetic Saturation*, Electronics, vol. 10, pp. 14-16, July 1937.
20. *Reactance Amplifiers*, Electronics, v. 10, pp. 28-30, Oct. 1937.

10. Kuhn, L.: Uber Ein Neues Radiotelephonisches System, Jahrb. d. Draht. Tel., v. 9, pp. 502-534, 1915.
11. Mass. Inst. of Tech., E.E. Dept. Staff: Electric Circuits, John Wiley & Sons, Inc., 1943.
12. McEachron, K.B.: Thyrite: A New Material for Lightning Arrestors, Gen. Elec. Rev., v. 33, pp. 92-99, Feb. 1930.
13. Peterson, E., J.M. Manley & L.R. Wrathall: Magnetic Generation of a Group of Harmonics, Elect. Eng., v. 56, pp. 995-1001, Aug. 1937.
14. Peterson, L.C. & F.B. Llewellyn: The Performance and Measurement of Mixers in Terms of Linear Network Theory, Proc. I.R.E., v. 33, pp. 458-476, July 1945.
15. Shelby, R.E.: A Cathode-Ray Frequency Modulation Generator, Electronics, v.13, pp. 14-18, Feb. 1940.
16. Suits, C.G.: Non-Linear Circuits for Relay Applications, Elect. Eng., v. L, pp. 963-964, 1931.
17. Suits, C.G.: Non-Linear Circuits Applied to Relays, Elect. Eng., v. 52, pp. 244-246, 1933.
18. Terman, F.E.: Radio Engineers' Handbook, McGraw-Hill Book Co., 1943.
19. Way, K.J.: Voltage Regulators Using Magnetic Saturation, Electronics, vol. 10, pp. 14-16, July 1937.
20. Reactance Amplifiers, Electronics, v. 10, pp. 28-30, Oct. 1937.

30. Willis-Jackson and Reddish: High Permittivity of Crystalline Aggregates, *Nature*, v. 156, p. 717, Dec. 15, 1945.
31. Wul, B.M. & I.M. Goldman: Dielectric Constant of Titanates of the Metals of the Second Group, *Comptes Rendus (Doklady) de l'Acad. des Sci. de l'U.R.S.S.*, v. 46, no. 4, pp. 139-142, 1945.
32. Wul, B.M.: Dielectric Constants of Some Titanates: *Nature*, v. 156, p. 480, Oct. 20, 1945.
33. Wul, B.M. & I.M. Goldman: Dielectric Constant of Barium Titanate as a Function of Strength of an Alternating Field, *Comptes Rendus de l'Acad. des Sci. de l'U.R.S.S.*, v. 49, no. 3, pp. 177-180, 1945.

Properties of Rochelle Salt, etc.

34. Busch, G: Neue Seignette-Elektrika, *Helv. Phys. Acta.*, v. 11, pp. 269-298, 1938.
35. Cady, W.G: Piezoelectricity, McGraw-Hill Book Co., 1946.
36. Fowler, R.H: A Theory of the Rotations of Molecules in Solids and of the Dielectric Constants of Solids and Liquids, *Proc. Royal. Soc.*, v. 149, pp 1-28, 1935.
37. Kobeko, P. & I. Kurtschatov: Dielectric Properties of Rochelle Salt Crystals, *Zeits f. Phys.*, v. 66, pp. 192-205, 1930.
38. Kourtschatov, I.V: Le Champ Moléculaire dans les Diélectriques, Hermann et. Cie, Paris, 1956.

39. Mueller, H. & J.E. Forbes: Dielectric Measurements of Rochelle Salt (Abst.), Phys. Rev., v. 43, p. 756, 1934.
40. Mueller, H: Properties of Rochelle Salt, Phys. Rev., v. 47, pp. 175-191, Jan. 15, 1935.
41. Mueller, H: Dielectric Anomalies of Rochelle Salt, Ann. of N.Y. Acad. Sci., v. 40, Art. 5, pp. 321-356, Dec. 1940.
42. Sawyer, C.B. & Tower, C.H.: Rochelle Salt as a Dielectric, Phys. Rev., vol. 35, pp. 269-273, Feb. 1, 1930.

Miscellaneous

43. Adams, E.P: On Electrets, Jour. Frank. Inst., v. 204, no. 4, pp. 469-486, Oct. 1927.
44. Bates, L.F: Modern Magnetism, Camb. Univ. Press, 1939.
45. Bürker, K: Über Ein Drépulvergemisch zur Darstellung Elektrischer Staubfiguren, Ann. der Physik, ser. 4, v. 1, pp. 474-482, 1900.
46. Curie, P: Propriétés Magnetiques des Corps a Diverses Temps, Ann. de Chimie et Phys., ser. 7, v. 5, p. 289 - 1895.
47. Petrzilka, V: Längs- und Biegungsschwingungen von Turmalinplatten, Ann. der Phys., ser. 5, v. 15, pp. 881-902, 1932.
48. Pierce, G.W: Magnetostriction Oscillators, Proc. Amer. Acad. Arts & Sci., v. 63, pp. 1-47, 1928.

49. Schmidt, H: Dehnungs- und Drillungsschwingungen
Elastischer Platten, Wien-Harms, Handbuch der
Experimentallphysik, v. 17, part 1, pp. 364-373, 1934.
50. Weiss, P: L'Hypothèse du Champ Moléculaire et la
Propriété Ferromagnétique, Jour. de Phys., ser. 4,
v.6, pp. 661-690, 1907.
51. Rothe, R; F. Ollendorff & K. Pohlhausen: Theory of
Functions as Applied to Engineering Problems,
Technology Press, 1933.
52. Scott, A.H. & H.L. Curtis: R.P. 1217, Edge Correction
in the Determination of Dielectric Constant,
U.S. Bur. Stds., Jour. Res., v. 22, no. 6, pp. 747-775,
1939.
53. Webster's New International Dictionary, C. & G. Merriam Co.,
1939.

CLASSIFIED DOCUMENT RECEIPT ARMED SERVICES TECHNICAL INFORMATION AGENCY				RECEIPT SERIAL NUMBER 57-5234
DATE 3/1/57	LOAN <input checked="" type="checkbox"/>	RETENTION <input type="checkbox"/>	ACCESSION <input type="checkbox"/>	ARC CONTROL NUMBER
TO: OHR Library-741 Wash., D. C. VIA: Attn: Mrs. Wood		code 936		FROM: ASTIA REFERENCE CENTER LIBRARY OF CONGRESS WASHINGTON 25, D.C. ATTN: SERVICE SECTION
			REFERENCE: ph. req. of 2/26/57	
AD, TIP OR ATI NUMBER (OR OTHER IDENTIFICATION)			COPY NUMBER	DATE DUE
U 57528			46	4/1/57
				uncl.
sj/pjp				
<p><i>The report(s) listed below, and requested in your letter is (are) unavailable due to being on loan to another borrower. When returned, your request will be filled.</i></p>				
Receipt is acknowledged of material listed above. (If contractor, it is recognized that this material is classified and comes within the purview of the security agreement signed by this concern.)				
Sender forwards with Document. Recipient signs and returns original to sender.		DATE	SIGNATURE	

CLASSIFIED DOCUMENT RECEIPT ARMED SERVICES TECHNICAL INFORMATION AGENCY				RECEIPT SERIAL NUMBER 57-2234
DATE 3/1/57	LOAN <input checked="" type="checkbox"/>	RETENTION <input type="checkbox"/>	ACCESSION <input type="checkbox"/>	ARC CONTROL NUMBER
TO: ASIA Library-742 Wash., D. C.		FROM: ASTIA REFERENCE CENTER LIBRARY OF CONGRESS WASHINGTON 25, D. C. ATTN: SERVICE SECTION		
VIA: Attn: Mrs. Wood		REFERENCE: Ch. 105, of 2/26/57		
AD, TIP OR ATI NUMBER (OR OTHER IDENTIFICATION)			COPY NUMBER	DATE DUE
57223			26	3/1/57
				uncl.
				2/22
<p><i>The report(s) listed below and requested in your letter is (are) unavailable due to being on loan to another borrower. When returned, your request will be filled.</i></p>				
<p>Receipt is acknowledged of material listed above. (If contractor, it is recognized that this material is classified and comes within the purview of the security agreement signed by this concern.)</p>				